



THE HONG KONG
POLYTECHNIC UNIVERSITY

香港理工大學

Pao Yue-kong Library

包玉剛圖書館

Copyright Undertaking

This thesis is protected by copyright, with all rights reserved.

By reading and using the thesis, the reader understands and agrees to the following terms:

1. The reader will abide by the rules and legal ordinances governing copyright regarding the use of the thesis.
2. The reader will use the thesis for the purpose of research or private study only and not for distribution or further reproduction or any other purpose.
3. The reader agrees to indemnify and hold the University harmless from and against any loss, damage, cost, liability or expenses arising from copyright infringement or unauthorized usage.

IMPORTANT

If you have reasons to believe that any materials in this thesis are deemed not suitable to be distributed in this form, or a copyright owner having difficulty with the material being included in our database, please contact lbsys@polyu.edu.hk providing details. The Library will look into your claim and consider taking remedial action upon receipt of the written requests.

One-dimensional Sonomyography (SMG) for Skeletal Muscle Assessment and Prosthetic Control

Jing-Yi Guo

Ph.D

The Hong Kong Polytechnic University

2010

The Hong Kong Polytechnic University
Department of Health Technology and Informatics

**One-dimensional Sonomyography (SMG)
for Skeletal Muscle Assessment and
Prosthetic Control**

Jing-Yi Guo

A thesis submitted in partial fulfillment of the
requirements for the Degree of Doctor of Philosophy

May 2010

CERTIFICATE OF ORIGINALITY

I hereby declare that this thesis is my own work and that, to the best of my knowledge and belief, it reproduces no material previously published or written, nor material that has been accepted for the award of any other degree or diploma, except where due acknowledgement has been made in the text.

_____ (Signed)

Jing-Yi Guo (Name of student)

Abstract of thesis

“One-dimensional Sonomyography (SMG) for Skeletal Muscle Assessment and Prosthetic Control”

Submitted by Jing-Yi Guo

for the Degree of Doctor of Philosophy

at The Hong Kong Polytechnic University

in May 2010

As indicators of torque output and motor unit recruitment, both electromyography (EMG) and mechanomyography (MMG) have been widely used to assess muscle fatigue, muscle pathology, control over prosthetic devices, etc. On the other hand, ultrasound imaging has been suggested as a method for viewing muscular architectural changes during contractions. Sonomyography (SMG) is the signal we previously termed to describe muscle contraction using real-time muscle morphological changes extracted from ultrasound images or signals.

With the advantages of being less expensive, more compact, A-mode ultrasound was introduced to detect the dynamic thickness change of skeletal muscles during contraction, named as one-dimensional sonomyography (1D SMG). The 1D SMG signal was extracted from the ultrasound signal by automatically tracking the shift of echoes from tissue interfaces and the muscle thickness change was calculated. Compared with surface EMG, 1D SMG could discriminate activity of deep muscles from more superficial muscles. It was also found that 1D SMG signal linearly correlated with the wrist extension angle.

Moreover, the least squares support vector machine (LS-SVM) and artificial neural networks (ANN) were used to predict dynamic wrist angles from 1D SMG signals. Synchronized wrist angle and SMG signals from the extensor carpi radialis muscles of nine normal subjects were recorded during the process of wrist extension and flexion at rates of 15, 22.5, and 30 cycles/min, respectively. An LS-SVM model together with back-propagation (BP) and radial basis function (RBF) ANN was trained using the data sets collected at the rate of 22.5 cycles/min for each subject. It was concluded that the wrist angle could be precisely estimated from the thickness changes of the extensor carpi radialis using LS-SVM or ANN models.

In this thesis, the potential of 1D SMG in prosthetic control was also investigated. The performances of SMG and surface EMG (SEMG) signal in tracking the guided patterns of wrist extension were evaluated and compared. The subjects (n=16) were instructed to perform the wrist extension under the guidance of displayed sinusoidal, square and triangular waveforms at the movement rates of 20, 30, 50 cycles/min. It was showed that the RMS errors of SMG tracking were significantly smaller than those of SEMG. Significant differences in RMS tracking error of SMG among the three movement rates ($p < 0.01$) for all the guiding waveforms were also observed using one-way analysis of variance (ANOVA). The results suggest that SMG signal has great potential to be an alternative method to SEMG to evaluate muscle function and control prostheses.

We further compared subjects' performance using 1D SMG and surface EMG in a series of discrete tracking tasks, both with and without a concurrent auditory attention task. The performances of subjects (n=10) were evaluated under isometric contraction and wrist extension using the extensor carpi radiali muscle. Using SMG generated significantly lower numbers of "E" wrongly canceled than using EMG for both

isometric contraction and wrist extension ($p < 0.001$) controls. It also demonstrated that there was no significant difference of performances of canceling “E” between the single and dual tasks by using any of the control signals ($p = 1.0$). The SMG control provided more consistent performances under the single and dual tasks in comparison with EMG control.

In addition, the feasibility of using 1D SMG signal for controlling a powered prosthesis was investigated by evaluating the performances of subjects ($n = 16$) in tracking guided motion patterns of wrist extension. The RMS tracking error between the guiding waveform and the signal representing the degree of the prosthetic hand’s open-close level, which was measured by an electronic goniometer, was calculated to evaluate the control performance. The results suggest that SMG signal, based on further improvement, has potentials to be an alternative method for prosthetic control.

Finally, an amputee subject was recruited to perform the tasks of tracking the guided patterns of wrist extension, discrete tracking task and controlling a powered prosthesis. The performance of the subject using 1D SMG and EMG signals were evaluated to see whether 1D SMG signal could really used by the amputee. The feasibility of using 1D SMG by the amputee was demonstrated.

To sum up, we have successfully demonstrated that SMG (related to muscle architectural properties) can provide complementary information about muscle function in comparison with EMG (related to muscle bioelectrical properties), which has been commonly used for muscle activity assessment and prosthetic control.

Keywords: Skeletal muscles, Ultrasound, Sonomyography, SMG, Electromyography, EMG, Mechanomyography, MMG, Wrist angle prediction, Support vector machine, Artificial neural network, Cognition, Muscle, Prosthetic control.

PUBLICATIONS ARISING FROM THE THESIS

Journal Paper

1. **J.-Y. Guo**, Y.-P. Zheng, L. Kenney, A Bowen, D Howard, J Canderle, and H.-B. Xie. Evaluation of sonomyography (SMG) compared with electromyography (EMG) for control purpose, IEEE Transactions on Biomedical Engineering, submitted 2010.
2. **J.-Y. Guo**, Y.-P. Zheng, H.-B. Xie, and X. Chen. Continuous monitoring electromyography (EMG), mechanomyography (MMG), sonomyography (SMG) and torque during ramp vs. step isometric contraction, Medical Engineering & Physics, in press, 2010. 10.1016/j.medengphy.2010.07.004.
3. **J.-Y. Guo**, Y.-P. Zheng, H.-B. Xie, and X. Chen. Muscle force predictions from mechanomyography (MMG) and electromyography (EMG) using support vector machine: improving MMG-based muscle force estimation by discrete wavelet transform, Journal of Mechanics in Medicine and Biology, submitted 2010.
4. X. Chen, Y.-P. Zheng, and **J.-Y. Guo**. Ultrasound as a control signal for powered prosthesis hand: a pilot study of sonomyography control, Ultrasound in Medicine and Biology, ,Ultrasound in Medicine and Biology, Vol. 36(7), pp1076-1088, 2010.
5. **J.-Y Guo**, Y.-P. Zheng, Q.-H. Huang, X. Chen, J.-F. He, and H. Chan. Performances of one-dimensional sonomyography and surface electromyography in tracking guided patterns of wrist extension, Ultrasound in Medicine and Biology, Vol. 35 (6), pp 894-902, 2009.
6. H.-B. Xie, Y.-P. Zheng, and **J.-Y. Guo**. Classification of mechanomyogram signal using wavelet packet transform and singular value decomposition for multifunction prosthesis control, Physiological Measurement, Vol. 30 (5), pp 441-457, 2009.
7. H.-B. Xie, Y.-P. Zheng, **J.-Y. Guo**, X. Chen, and J. Shi. Estimation of wrist angle from sonomyography using support vector machine and artificial neural network models, Medical Engineering & Physics, Vol. 31 (3), pp 384-391, 2009.
8. **J.-Y. Guo**, Y.-P. Zheng, Q.-H. Huang, and X. Chen. Dynamic monitoring of forearm muscles using 1D sonomyography (SMG) system, Journal of Rehabilitation Research and development, Vol. 45 (1), pp187-196, 2008.

Conference Proceedings

1. **J.-Y. Guo**, Y.-P. Zheng, L. P. Kenney, and H.-B. Xie. Evaluation of sonomyography (SMG) for control compared with electromyography (EMG) in a discrete target tracking task, 31st Annual International Conference of the IEEE Engineering in Medicine and Biology Society, Minnesota, USA, pp 1549--1552, September, 2009.

2. **J.-Y. Guo**, X. Chen, and Y.-P. Zheng. Use of muscle thickness change to control powered prosthesis: a pilot study, 31st Annual International Conference of the IEEE Engineering in Medicine and Biology Society, Minnesota, USA, pp 193--196, September, 2009.
3. **J.-Y. Guo**, Y.-P. Zheng, and L. P. Kenney. Comparison between sonomyography and electromyography in terms of accuracy and cognitive requirement, WACBE World Congress on Bioengineering, Hong Kong, China, p 127, July, 2009.
4. **J.-Y. Guo**, Y.-P. Zheng, Q.-H. Huang, X. Chen, and J.-F. He. Comparison of sonomyography and electromyography of forearm muscles in the guided wrist extension, 5th International Workshop on Wearable and Implantable Body Sensor Networks (BSN 2008) In conjunction with 5th International Summer School and Symposium on Medical Devices and Biosensors (ISSS-MDBS 2008), Hong Kong, China, pp 235--238, June, 2008.
5. **J.-Y. Guo**, Y.-P. Zheng, Q.-H. Huang, and X. Chen. Monitoring of forearm muscle contraction using 1D sonomyography (SMG), The 2nd Biomedical Engineering Conference, Hanoi, Vietnam, July, 2007.
6. **J.-Y. Guo**, Y.-P. Zheng, Q.-H. Huang, and X. Chen. Development of 1D sonomyography system to dynamically monitor dimensional change of forearm muscles during wrist extension and flexion, The Fifth International Conference on the Ultrasonic Measurement and Imaging of Tissue Elasticity, Snowbird, Utah, USA, p 55, October 2006.
7. **J.-Y. Guo**, Y.-P. Zheng, Q.-H. Huang, X. Chen, and J. Shi. Controlling prosthesis using 1 D sonomyography signal generated from forearm muscles, BME 2006 Biomedical Engineering Conference "Education, Research and Industry in Biomedical Engineering", Kowloon, Hong Kong, China, pp165--167, September, 2006.

ACKNOWLEDGEMENTS

Given this precious opportunity, I would like to express my sincere appreciation to people whose dedication and efforts made this thesis possible.

First and foremost, I would like to express my deepest and most sincere appreciation to Prof. Yong-Ping Zheng, my supervisor, for being my advisor, mentor and launching my academic career. His rigorous scholarship, kindness and patience gave me a deep impression. I always got plentiful suggestions, feedbacks and ideas by discussing with him about my research work. His working attitude has deeply affected me and pushed me to keep working hard. He has provided me with encouragement, timely support and opportunities of working with exceptionally experienced and talented colleagues, which has greatly inspired my growth as a student, a researcher and a scientist want to be. I thank him for patiently guiding me, pointing out the problems with me, instilling the real value of research, providing academic and professional suggestions, and sharing the wisdom in both research and life with me.

I would like to thank Prof. Ming Zhang, Dr. Michael Ying, Dr. Parco Ming-Fai SIU, Dr. Thomas Ming-Hung LEE and Dr. Mo Yang for assessing my proposal, confirmation report, providing valuable suggestions and pointing out problems existing in my work and presentations.

I gratefully acknowledge Dr Hong-Bo Xie for his advice, discussion and crucial contribution, which have triggered my great interest in the area of bio-signal processing. I thank Dr Xin Chen, Dr Qing-Hua Huang, Mr Zheng-Ming Huang for their great help in software, hardware guidance and support. Great thanks are given to Ms. Sally Ding for her reviewing, editing my papers, thesis, and her encouragement during my study, and Mr. James Cheung for his instruction on device of workshop. To Dr Qing Wang, Dr

Min-Hua Lu, Dr Yong-Jin Zhou, Dr. Jun Shi, Mr Cong-Zhi Wang and Mr Jun-Feng He, I would like to thank them for helping me in technical assistance, especially at the early stage of my study and being the model for hard workers in the lab.

I am also grateful to many colleagues and students, who learned along with me, for maintaining a stimulating and flexible working environment, most notably Mr Like Wang, Mr. Yanping Huang, Dr. Queeny Yuen, Dr. Carrie Ling, Ms. Jiawei Li, Ms. Shu-Zhe Wang, Mr. Louis Lee, Mr., Man, Miss Yen, Mr. Wen-Tao Liu, Mr Jin-Jiang Yu.

I would like to thank my beloved family for their persistent supports over all these years, especially my dear Mom, Mrs Qu Meimei, whom I always take as the model since I was a little girl. Her positive attitude towards life and warm smile always cheer me up. In addition, this thesis is also in memory of my grandma now in heaven.

Finally, I would like to acknowledge the financial support from The Hong Kong Polytechnic University (J-BB69) and Research Grant Council of Hong Kong (PolyU 5331/06E).

ACADEMIC AWARD

Hong Kong Medical and Healthcare Device Industries Association Student Research
Award, 1st runner-up, Nov. 2009

TABLE OF CONTENTS

CERTIFICATE OF ORIGINALITY	III
ABSTRACT OF THESIS	IV
PUBLICATIONS ARISING FROM THE THESIS	VII
ACKNOWLEDGEMENTS	IX
ACADEMIC AWARD	XI
TABLE OF CONTENTS	XII
LIST OF ABBREVIATIONS	XV
LIST OF FIGURES	XVII
LIST OF TABLES	XXV
CHAPTER 1 INTRODUCTION	1
1.1 BACKGROUND AND SIGNIFICANCE	1
1.2 OBJECTIVES OF THIS STUDY	3
1.3 OUTLINE OF THE DISSERTATION	4
CHAPTER 2 LITERATURE REVIEW	6
2.1 SKELETAL MUSCLE PHYSIOLOGY.....	6
2.1.1 <i>Anatomy of Skeletal Muscle</i>	6
2.1.2 <i>Motor Units</i>	7
2.1.3 <i>Skeletal Muscle Fibre Type</i>	8
2.1.4 <i>Muscle Motor Control Strategy: Size Principle</i>	9
2.1.5 <i>Morphological Parameters</i>	10
2.1.5.1 <i>Pennation Angle and Fascicle Length</i>	10
2.1.5.2 <i>Cross-sectional Areas</i>	12
2.1.6 <i>Muscle Contraction Pattern</i>	12
2.1.7 <i>Muscle Dysfunction</i>	13
2.2 TECHNOLOGY FOR MUSCLE ASSESSMENT AND PROSTHETIC CONTROL	15
2.2.1 <i>Electromyography</i>	15
2.2.2 <i>Mechanomyography</i>	18
2.2.3 <i>Sonomyography</i>	20
2.2.4 <i>Other Physiological Signals</i>	22
2.3 MODELS USED TO PREDICT JOINT ANGLE	23
2.3.1 <i>Artificial Neural Network</i>	23
2.3.2 <i>Support Vector Machine</i>	24
2.4 SUMMARY	25
CHAPTER 3 METHODS	28
3.1 SKELETAL MUSCLE MEASUREMENT SYSTEM.....	28
3.1.1 <i>System Description</i>	28
3.2 SKELETAL MUSCLE EVALUATION BY 1D SMG	30
3.2.1 <i>Subjects</i>	30
3.2.2 <i>Monitoring of Forearm Muscles Using 1D SMG</i>	30
3.2.2.1 <i>Measurement of Wrist Angle, 1D SMG and Surface EMG</i>	30
3.2.2.2 <i>Cross-Correlation Algorithm to Calculate the Muscle Thickness Change (1D SMG)</i>	33
3.2.2.3 <i>Statistical Analysis</i>	36
3.2.3 <i>1D SMG Based Wrist Angle Prediction</i>	36
3.2.3.1 <i>Wrist Angle Prediction Models</i>	36
3.2.3.2 <i>Data Analysis</i>	39
3.3 COMPARISONS OF 1D SMG AND SURFACE EMG FOR PROSTHETIC CONTROL	41
3.3.1 <i>Performances of 1D SMG and Surface EMG in Tracking Guided Patterns of Wrist Extension</i>	41

3.3.1.1 Subjects.....	41
3.3.1.2 Experimental Protocol.....	41
3.3.1.3 RMS Tracking Error	46
3.3.2 <i>Comparison of 1D SMG and Surface EMG in Visuomotor “E” Cancellation Test</i>	46
3.3.2.1 Subjects.....	46
3.3.2.2 SMG-EMG Compound Sensor	47
3.3.2.3 Protocol in the Visuomotor “E” Cancellation Test	49
3.3.2.4 Selection of Sampling Rate and Number of Epoch of EMG.....	54
3.3.2.5 Data Analysis.....	55
3.3.3 <i>Prosthesis Control by 1D SMG and Surface EMG</i>	55
3.3.3.1 Subjects.....	55
3.3.3.2 Experimental Setup.....	56
3.3.3.3 Experimental Protocol.....	59
3.4 CASE STUDY ON AMPUTEE.....	61
3.4.1 <i>Subject</i>	61
3.4.2 <i>Experimental Protocol</i>	61
3.4.2.1 Performances of 1D SMG and Surface EMG in Tracking Guided Patterns of Wrist Extension.....	61
3.4.2.2 Comparison of 1D SMG and Surface EMG in Visuomotor “E” Cancellation Test	62
3.4.2.3 Prosthesis Control by 1D SMG and Surface EMG	63
CHAPTER 4 RESULTS.....	64
4.1 MUSCLE THICKNESS CHANGE DETECTED BY 1D SMG	64
4.1.1 <i>The Relationship between Muscle Deformation (SMG) and Wrist Angle</i>	64
4.2 SMG-BASED WRIST ANGLE ESTIMATION	69
4.2.1 <i>RMSD and CC of SVM, BP and RBF ANN</i>	69
4.3 PERFORMANCE OF 1D SMG AND SURFACE EMG IN TRACKING GUIDED PATTERNS OF WRIST EXTENSION	72
4.3.1 <i>Comparison in RMS Tracking Error between 1D SMG and Surface EMG among Various Guiding Waveforms</i>	72
4.3.2 <i>RMS Tracking Error of 1D SMG/surface EMG for Three Guiding Waveforms under Different Movement Rates</i>	75
4.4 COMPARISON OF 1D SMG AND SURFACE EMG IN VISUOMOTOR “E” CANCELLATION TEST.....	76
4.5 COMPARISON OF 1D SMG AND SURFACE EMG IN PROSTHETIC CONTROL	80
4.6 THE PERFORMANCE OF AMPUTEE USING 1D SMG AND SURFACE EMG SIGNALS FOR CONTROL PURPOSE	90
4.6.1 <i>Performances of 1D SMG and Surface EMG in Tracking Guided Patterns of Wrist Extension</i>	90
4.6.2 <i>Comparison of 1D SMG and Surface EMG in Visuomotor “E” Cancellation Test</i>	92
4.6.3 <i>Prosthesis Control by 1D SMG and Surface EMG</i>	93
CHAPTER 5 DISCUSSION.....	96
5.1 SKELETAL MUSCLE EVALUATED BY 1D SMG	96
5.1.1 <i>The Relationship between 1D SMG and Wrist Angle</i>	96
5.1.2 <i>1D SMG Based Wrist Angle Estimation</i>	98
5.2 COMPARISONS OF 1D SMG AND SURFACE EMG FOR PROSTHETIC CONTROL	100
5.2.1 <i>1D SMG in Tracking Guided Patterns of Wrist Extension</i>	100
5.2.2 <i>1D SMG in Visuomotor “E” Cancellation Test</i>	102
5.2.3 <i>Evaluation of 1D SMG for Prosthetic Control</i>	105
5.2.4 <i>Amputee’s Performance using 1D SMG to Control</i>	110
5.2.4.1 Performances of 1D SMG and Surface EMG in Tracking Guided Patterns of Wrist Extension.....	110
5.2.4.2 Comparison of 1D SMG and Surface EMG in Visuomotor “E” Cancellation Test	110
5.2.4.3 Control Prosthesis by 1D SMG and Surface EMG	111
5.2.5 <i>Summary</i>	114
CHAPTER 6 CONCLUSIONS AND FUTURE STUDIES.....	115
6.1 CONCLUSIONS	115
6.2 FURTHER STUDIES.....	119
REFERENCES.....	123
APPENDIX.....	155

I. INFORMATION SHEET	155
實驗指引	156
II CONSENT FORM	157
同意書	158

LIST OF ABBREVIATIONS

2D	Two-dimensional
ANN	Artificial neural network
BMI	Brain-machine interface
BP	Back-propagation
CC	Correlation coefficient
CSA	Cross sectional area
CT	Computerised axial tomography
DOF	Degree of freedom
ECoG	Electrocorticography
EEG	Electroencephalogram
EMG	Electromyography
FES	Functional electrical stimulation
HMI	Human-machine interface
ICC	Intraclass correlation coefficient
MDF	Median frequency
MEG	Magnetoencephalography
MK	Myokinematic
MMG	Mechanomyography
MRI	Magnetic resonance imaging
MU	Motor unit
MUAP	Motor unit action potential
MVC	Maximal voluntary contraction
1D	One-dimensional
RBF	Radial basis function
RF	Rectus femoris
RMS	Root mean square

RMSD	Root mean square difference
SMG	Sonomyography
STDEV	Standard deviations
SVM	Support vector machine
TEA	Test of everyday attention
TMR	Targeted muscle reinnervation
UMME	Ultrasound measurement of motion and elasticity

LIST OF FIGURES

Fig. 2. 1 Structure of a skeletal muscle (from http://training.seer.cancer.gov/)....	7
Fig. 2. 2 Structure of motor unit (from http://ecampus.wsc.edu/).	8
Fig. 2. 3 Pennation angle and fascicle length of vastus lateralis muscle (Fukunaga et al., 1997).	11
Fig. 2. 4 CT scan obtained from an untrained healthy subject. The knee extensor muscle: A-adductors, G-gracilis, H-hamsstrings, Q-quadriceps, S-sartorius (Maughan et al., 1983).....	12
Fig. 3. 1 The diagram of data collection system.....	29
Fig. 3. 2 The Placement of the 1D SMG transducer, surface EMG electrodes and electronic goniometer on the forearm. Ultrasound coupling gel was applied between the ultrasound transducer and skin.....	32
Fig. 3. 3 The demonstration of using the cross correlation algorithm to find the position change of ultrasound echoes due to the thickness changes of skeletal muscle during movement (a) The signal within the red window (x(i)) was chosen as the reference signal at the fist frame. (b) In the second frame, the red window was searching 500 data points right and left (search range =500) from the position in the first frame and calculating a cross-correlation value once moving a data point. Finally, the echo with the maximal cross correlation value	

was selected and the corresponding position was regarded as the current position of the selected signal $y(i)$ 34

Fig. 3. 4 The software interface used to simultaneously collect 1D SMG and, surface EMG signals; (a) The sinusoidal waveform with a rate of 20 cycles/min was used to guide the wrist extension movement. The subject used 1D SMG signal to track the sinusoidal pattern; (b) Surface EMG was also collected for reference; (c) The SMG signal was measured by detecting the distance change between the A-mode ultrasound echoes reflected from the fat-muscle and muscle-bone interfaces, which were selected by the two tracking windows. A cross-correlation algorithm was employed to track the movements of the echoes during the wrist extension. The SMG signal was calculated using the change of the time interval between the echoes and displayed along with the guiding waveform for tracking; (d) 1D SMG signal was tracking the square waveform at a rate of 30 cycles/min; (e) 1D SMG signal was tracking the triangular waveform at a rate of 50 cycles/min. 43

Fig. 3. 5 The software interface used to collect the surface EMG and A-mode ultrasound signals. (a) Surface EMG signal was collected; (b) The sinusoidal waveform with a rate of 20 cycles/min was used to guide the wrist extension movement; SEMG RMS was calculated to track the sinusoidal pattern; (c) A-mode ultrasound signal was also collected for reference; (d) Surface EMG RMS was tracking the square waveform at a rate of 30 cycles/min; (e) Surface EMG RMS was tracking the triangular waveform at a rate of 50 cycles/min. 45

Fig. 3. 6 (a) The ultrasound-EMG compound sensor (1D ultrasound transducer, SEMG electrodes) placed on the extensor carpi radialis muscle of the subject during the wrist extension. A goniometer was placed across the wrist joint; (b) The length between the centres of the EMG sensors was 4.3 cm; (c) The diameter of A-mode ultrasound sensor was 0.7cm.48

Fig. 3. 7 The ultrasound-EMG compound sensor placed on the belly of the extensor carpi radialis muscle when the subject was performing the force control task. The force of the hand was detected using a custom-made force sensor.....49

Fig. 3. 8 The diagram of the experimental protocol. Each motor control test was divided into calibration, practice and test. During the calibration, the system recorded the maximal and minimal values of each signal during movements. Then, the subject could go to practice stage to exam the result of calibration. If satisfied with the calibration result, they could begin the test; otherwise, they had to go back to calibration part to reset the maximal and minimal values. There were repeated trials in a test session of 90s.51

Fig. 3. 9 (a) The software interface used to collect 1D SMG signal. The muscle deformation signal (i.e. SMG) extracted from A-mode ultrasound was displayed for controlling the cursor to cancel the letters. The muscle deformation was measured according to the echo movement reflected from the muscle-bone interface. Window was selected to include the ultrasound echoes. (b) The EMG signal collected from the extensor carpi radialis muscle and EMG RMS was

used to control the cursor. (c) The force collected from force sensor or angle detected by electrical goniometer was used to control the cursor. 53

Fig. 3. 10 An illustration of the SMG prosthesis control experiment. 57

Fig. 3. 11 An illustration of the software interface used to simultaneously collect 1D SMG and goniometer signal and to control prosthesis. (a) The top window illustrates the sinusoidal waveform used to guide the wrist extension movement along with the goniometer signal which represents the prosthesis open-close level. The bottom window shows the ultrasound signal with the selected reference echo used for tracking the muscle thickness change; (b) A typical sinusoid waveform with a rate of 10 cycles/min; (c) A typical square waveform with a rate of 10 cycles/min. 59

Fig. 3. 12 A pedal foot switch was utilized for the amputee with bilateral wrist amputation to make decision during visuomotor “E” cancellation test..... 63

Fig. 4. 1 The muscle deformation and the wrist extension angle of a typical trial with three cycles of wrist extension of subject C at the rate of 30 cycles/min.... 65

Fig. 4. 2 The relationship between the percentage of muscle deformation and wrist extension angle of the trial shown in Fig. 4. 1. The linear regression was used to represent the correlation between the two signals. 65

Fig. 4. 3 The ratios between the muscle deformation and the wrist angle for the nine subjects (1-9) under different extension rates. The error bar represents the

standard deviation of the results of the three trials for each subject at each rate. The last bar (mean) represents the overall mean and standard deviation of the results of the nine subjects. 66

Fig. 4. 4 The EMG RMS and the wrist extension angle of a typical trial with three cycles of wrist extension of subject C at the extension rate of 30 cycles/min. 68

Fig. 4. 5 The relationship between the EMG RMS and the wrist extension angle of the trial shown in Fig. 4. 4. The two signals were also found to be linearly correlated. 68

Fig. 4. 6 Comparison of the predicted and measured wrist angles at the extension rate of 15 cycles/min by LS-SVM, BP ANN and RBF ANN. 69

Fig. 4. 7 Comparison of the predicted and measured wrist angles under the extension rate of 30 cycles/min by LS-SVM, BP ANN and RBF ANN. 70

Fig. 4. 8 The mean and standard deviation of prediction RMSD of the nine subjects at extension rates of 15, 30 cycles/min, by LS-SVM, BP ANN and RBF ANN. 71

Fig. 4. 9 The mean and standard deviation of prediction CC of the nine subjects at 15, 30 cycles/min extension rate by LS-SVM, BP ANN and RBF ANN. 71

Fig. 4. 10 The RMS tracking error (%) of 1D SMG and surface EMG for the different guiding waveforms. The error bar represents the standard deviation of the results obtained at three different movement rates..... 73

Fig. 4. 11 The tracking errors of SMG for the three guiding waveforms under different movement rates. The error bar represents the standard deviation of the results of the sixteen subjects. 75

Fig. 4. 12 The RMS tracking error of surface EMG under the three different wrist extension rates for various guiding waveforms. The error bar represents the standard deviation of the results obtained from the sixteen subjects. 76

Fig. 4. 13 Correlations between the numbers of “E” correctly cancelled in 90s under the single and dual tasks when (a) SMG and (b) EMG were used as control signals, respectively..... 79

Fig. 4. 14 The overall mean RMS tracking error of SMG and surface EMG for each subject for all the movement rates and waveforms. The error bar represents the standard deviation from the mean. 81

Fig. 4. 15 Plots of muscle deformation (SMG) and angle curves as function of time in one trial. The left Y-axis indicates the SMG signal, while the right Y-axis represents the prosthesis angle normalized to the maximal angle at full opening position..... 83

Fig. 4. 16 The input-output relationship of the prosthetic control system where the input was the SMG signal, and the output was the prosthesis opening position represented by goniometer angle. Linear regression was applied to indicate their relationship. 84

Fig. 4. 17 The R^2 values of linear regression for each subject under three movement rates. The error bar represents the standard deviation from the mean of the three trials. For all the subjects, higher movement rate resulted in lower R^2 value..... 85

Fig. 4. 18 The relationship between R^2 value and movement rate. The error bar represents the standard deviation from the mean of the nine subjects..... 86

Fig. 4. 19 The tracking result of a typical trial under the movement rate of 4 cycles/min. Good consistency is shown between the target and the prosthesis response. (A) Tracking result of sinusoid target; (B) Tracking result of square target, RMSTE indicates the RMS tracking error..... 88

Fig. 4. 20 The overall mean RMS tracking error of each subject for all the movement rates. The error bar represents the standard deviation from the mean. 89

Fig. 4. 21 The RMS tracking error of for the two target tracks under three different movement rates. The error bar represents the standard deviation from the mean of the nine subjects. An increasing trend of RMS tracking error for

both sinusoid and square targets was observed with the increase of the movement rate..... 89

Fig. 4. 22 The RMS tracking error (%) between 1D SMG/surface EMG and the guiding waveforms. The error bar represents the standard deviation of the results of two different movement rates..... 91

Fig. 4. 23 The tracking errors of SMG for different guiding waveforms under the two movement rates. The error bar represents the standard deviation of the three repeated trials..... 92

Fig. 4. 24 The overall mean RMS tracking error of using 1D SMG and surface EMG for control by the amputee for the two guiding waveforms. The error bar represents the standard deviation from two different movement rates. 94

Fig. 4. 25 The overall mean RMS tracking errors of using 1D SMG to control prosthesis by the amputee under the two extension rates. The error bar represents the standard deviation from three repeated trials. 95

LIST OF TABLES

Table 2. 1 List of properties of type I and type II muscle fibres (http://en.wikipedia.org/wiki/Skeletal_muscle).....	9
Table 4. 1 The mean and standard deviations (STDEV) of the ratio between muscle deformation and wrist extension angle among the nine subjects. The results were calculated from the data obtained under three different rates of wrist extension.	67
Table 4. 2 The RMS tracking error (%) between 1D SMG/surface EMG and the guiding waveforms at the three movement rates (Mean \pm S.D.) and the mean RMS tracking error averaged over the three movement rates for sinusoid, square, and triangle guiding waveforms.....	74
Table 4. 3 The number of “E” correctly cancelled or that of letters wrongly cancelled in a period of 90 sec using different signals and under conditions of wrist movement and isometric contraction for both single and dual tasks. The number of bleeps counted by the subjects during the dual task test was also included.....	77
Table 4. 4 The RMS percentage tracking errors of 1D SMG and surface EMG between the prosthesis angle and the guiding waveform at the three movement rates (Mean \pm S.D.) and the mean RMS tracking error averaged over the three movement rates for sinusoid and square guiding waveforms.....	81

Table 4. 5 The RMS tracking error (%) between 1D SMG/surface EMG and the guiding waveforms at the two movement rates (Mean \pm S.D.) and the mean RMS tracking error averaged over the two movement rates for the three guiding waveforms. 90

Table 4. 6 The number of “E” correctly cancelled and that of letters wrongly cancelled using 1D SMG and surface EMG signals for both single and dual tasks. The number of bleeps counted during the dual task test was also included..... 93

Table 4. 7 The RMS tracking errors in percentage of 1D SMG and surface EMG between the prosthesis angle and the guiding waveforms at the two movement rates (Mean \pm S.D.) and the mean RMS tracking error averaged over the two movement rates for sinusoid and square guiding waveforms..... 94

CHAPTER 1 INTRODUCTION**1.1 Background and Significance**

Ultrasonography as an effective method has been employed to evaluate the morphological changes in muscle thickness or displacement (Nogueira et al., 2009; Suzana et al., 2008; Matsubayashi et al., 2008; Bojsen-Moller et al., 2003; Springer and Gill, 2007; Mannion et al., 2008; Lee et al., 2007; Lee et al., 2009), muscle fibre (Okita et al., 2009; Ichinose et al., 1997; Maganaris, 2001), pennation angle (Kawakami et al., 1993; Mahlfeld et al., 2004), and cross-sectional areas (Kanehisa et al., 1995; Narici et al., 1996). The ultrasound parameters have also been suggested to characterize muscular pain, injuries and dysfunction (Botteron et al., 2009; Diaz et al., 2008; Chester et al., 2008; Bernathova et al., 2008; Sikdar et al., 2008). Moreover, ultrasound has been used along with EMG to provide more comprehensive information on the activities and properties of skeletal muscles (Andrade et al., 2009; Hides et al., 1994; Ishikawa et al., 2006; Hodges et al., 2003; Ferreira et al., 2004).

In a previous study, Zheng et al., (2006) used sonomyography (SMG) to describe the real time signal about the muscle thickness change detected with B-mode ultrasound images during its contraction. A system was developed to record and analyze ultrasound images, force, joint angle and surface EMG simultaneously. The system has been successfully used for the analysis of muscle fatigue and it was found that the muscle thickness increased during the fatigue process (Shi et al., 2007). The correlation between EMG and SMG of muscles during isometric contraction has also been investigated (Shi et al., 2007).

The real-time change of muscle thickness detected using ultrasound, namely SMG, could be used for monitoring the muscle morphological changes and has the potential for prosthetic control (Xie et al., 2009b; Zheng et al., 2006). In contrast to these studies, which used 2 dimensional (2D) SMG, our most recent studies have shown that the muscle thickness change can also be measured with A-mode (one-dimensional or 1D) SMG. Compared to 2D SMG, 1D SMG provides a more portable, compact, inexpensive, and practical solution to detect muscle thickness changes (Guo et al., 2008, 2009). A-mode ultrasound transducers appear to be easily attached to the skin during dynamic activities of muscles and can be made to be sufficiently small to potentially be embedded in prosthetic sockets. In this study, we used A-mode ultrasound signal collected using a system equipped with a single element ultrasound transducer, named as 1D SMG, to detect the thickness changes of forearm muscles. The relationships between the surface EMG and wrist angle and between the 1D SMG and wrist angle were quantitatively studied. The results were used to assess the potential of 1D SMG signals as a non-invasive method for the detection of skeletal muscle activities in vivo.

After successfully detecting the dynamic thickness change of skeletal muscles during contraction using 1D SMG, the performance of using 1D SMG was compared with that of surface EMG in tracking guided patterns of wrist extension and in series of discrete tracking tasks. We then investigated the potential of using 1D SMG for controlling a single degree of freedom (DOF) prosthesis in real-time. The control performance was evaluated by tracking guided patterns of wrist extension. The comparison of performance of 1D SMG and EMG were tested on both healthy and amputee subjects. The study demonstrated that SMG signal could be potentially used for the control of powered prosthesis.

1.2 Objectives of This Study

The overall aim of this study is to assess the skeletal muscle function and control the prosthesis using 1D SMG signals.

The specific objectives of this study are:

1. To investigate the relationship between 1D SMG signals and wrist angle during the movement of wrist extension and explore whether the SMG signal is a reliable non-invasive method for detecting skeletal muscle activities in vivo;
2. To examine the feasibility of 1D SMG-based wrist angle prediction using support vector machine (SVM) and artificial neural network (ANN);
3. To compare the performances of subjects using 1D SMG and surface EMG signal in tracking the waveforms being displayed during the guided movement of wrist extension in terms of tracking accuracy;
4. To compare the performances of subjects using 1D SMG and surface EMG signal in terms of accuracy and cognitive requirements in series of discrete tracking task; and
5. To control a prosthesis with function of open and close using 1D SMG signal in real time.

1.3 Outline of the Dissertation

Following the introduction chapter, Chapter 2 presents a literature review on the fundamentals physiology of skeletal muscle and the technology utilized for muscular assessment and prosthetic control.

In Chapter 3, the methods used in this study are introduced. The experimental protocols are presented in detail. 1D SMG was used to monitor the wrist angle changes during wrist extension and the 1D SMG based wrist angle prediction was realized by using SVM and ANN. In addition, the performances of subjects using 1D SMG were evaluated in both the wrist extension tracking task and series of discrete tracking task. Finally, 1D SMG signal was utilized to control a single DOF prosthesis with open and close function and the related data processing and data analysis methods are included.

In Chapter 4, the results of the corresponding studies in Chapter 3 are reported, including the linear relationship between 1D SMG and wrist extension angle; the accuracy of SMG-based wrist angle estimation; the performances of the subjects using SMG in wrist extension tracking task, series of discrete tracking task and in a real prosthesis control task.

Chapter 5 presents discussion on the experimental set-ups and the results. The discussion about the experiments described in Chapters 3 and 4 are divided into two parts according to their purposes, i.e. skeletal muscle evaluation and prosthetic control. The results of this study are compared with the results of related previous studies and the explanations for our findings are given.

Chapter 6 summarizes the findings of this study and the potentials of using 1D SMG as an alternative signal to EMG in skeletal muscle assessment and prosthetic control. Suggestions on future research directions are highlighted.

CHAPTER 2 LITERATURE REVIEW

This chapter presents a review of literature on skeletal muscle physiology and its assessment methods including EMG, mechanomyography (MMG) and SMG. There are two major parts. The first part (Section 2.1) addresses the anatomy of skeletal muscle, motor units and fibre type. The second part (Sections 2.2) presents the currently available technology used for skeletal muscle assessment and prosthetic control.

2.1 Skeletal Muscle Physiology**2.1.1 Anatomy of Skeletal Muscle**

A skeletal muscle is regarded as an organ of the muscular system, consisting of nerve, blood, vascular or connective tissue besides skeletal muscle tissue. As shown in Fig. 2. 1, an individual skeletal muscle is made up of many muscle fibres bundled together and wrapped in a connective tissue covering. Each muscle is surrounded by a connective tissue sheath, which is called the epimysium. Each compartment contains a bundle of muscle fibres, which is called fasciculus and is surrounded by a layer of connective tissue called permysium. Within the fasciculus, each individual muscle cell, called muscle fibres, is surrounded by connective tissue called endomysium. Each skeletal muscle fibre is a single cylindrical muscle cell (Macintosh et al., 2006). A tendon is a tough band of fibrous connective tissue that connects muscle to bone, or muscle to muscle and is designed to withstand tension. There is an abundant supply of blood vessels and nerves in skeletal muscle. The structure described above is directly related to the primary function of skeletal muscle, contraction (David et al., 2004).

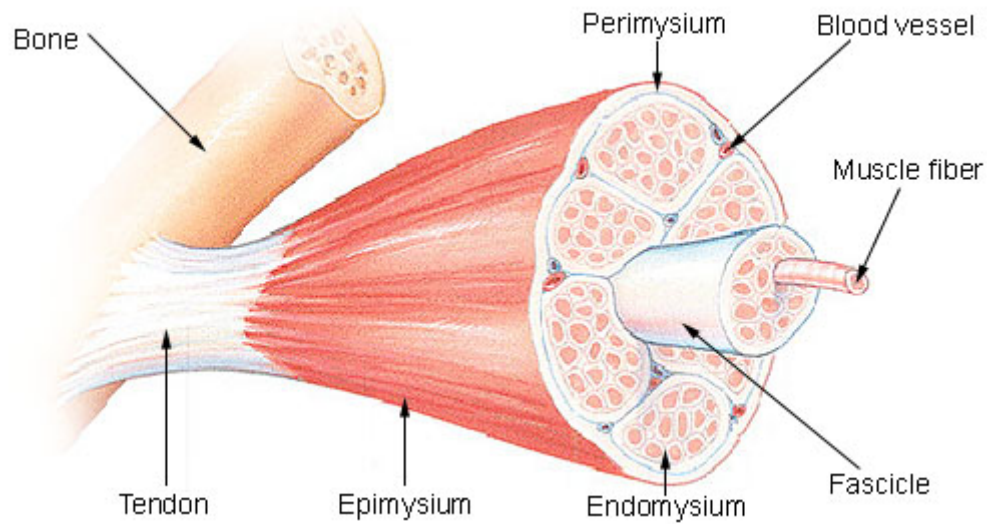


Fig. 2. 1 Structure of a skeletal muscle (from <http://training.seer.cancer.gov/>).

2.1.2 Motor Units

The smallest part of a muscle, which can be controlled, is called motor unit (MU). It includes a single motor neuron and all of the corresponding muscle fibres that it innervates (Fig. 2. 2). A great number of motor units often work together to coordinate the contraction of a single muscle. One muscle has a certain number of motor units, each of which is controlled by a separate nerve ending.

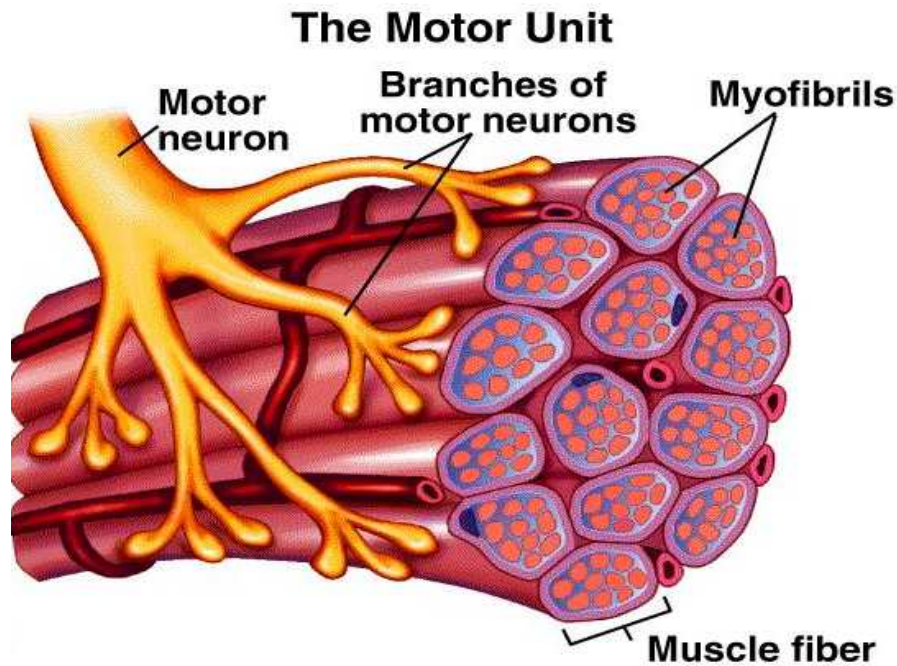


Fig. 2. 2 Structure of motor unit (from <http://ecampus.wsc.edu/>).

When it is activated by an action potential from the neuron, a muscle fibre depolarizes as the signal propagates along its surface and the fibre twitches. An electrode located near this field can detect the electric field induced by the depolarization. The electrode can be either a surface one or the one that can be inserted into the muscle. The resulting signal is called the muscle fibre action potential. The combination of muscle fibre action potentials from all the muscle fibres is the motor unit action potential (MUAP) and the sum of electrical activity generated by each active motor unit is EMG signal (De Luca 1979).

2.1.3 Skeletal Muscle Fibre Type

It is well known that the skeletal muscle fibres could be categorized into type I (slow twitch fibre) and type II (fast twitch fibre) according to their metabolic and electrophysiological properties. Fast twitch fibres can be further classified into type IIa,

type IIx and type IIb fibres. The distribution of muscle fibre types varies in different human skeletal muscles, for example, fast and slow twitch fibres are almost evenly distributed in deep biceps brachii while there are faster twitch fibres in rectus femoris muscles (Johnson et al., 1973). The different composition of muscle fibre types influences how muscles respond to training or physical activity. Table 2. 1 describes the most obvious differences among various muscle fibre types.

Table 2. 1 List of properties of type I and type II muscle fibres (http://en.wikipedia.org/wiki/Skeletal_muscle).

<i>Fibre Type</i>	<i>Type I fibres</i>	<i>Type IIa fibres</i>	<i>Type IIx fibres</i>	<i>Type IIb fibres</i>
<i>Contraction time</i>	Slow	Moderately Fast	Fast	Very fast
<i>Size of motor neuron</i>	Small	Medium	Large	Very large
<i>Resistance to fatigue</i>	High	Fairly high	Intermediate	Low
<i>Activity Used for</i>	Aerobic	Long-term anaerobic	Short-term anaerobic	Short-term anaerobic
<i>Maximum duration of use</i>	Hours	<30 minutes	<5 minutes	<1 minute
<i>Power produced</i>	Low	Medium	High	Very high

2.1.4 Muscle Motor Control Strategy: Size Principle

According to the size principle, motor units are recruited in the order of their recruitment thresholds and firing rates which results in a continuum of voluntary force (Henneman 1981). Motor-neurons with slow conduction velocity and small action current are recruited first, depending on the calibre of the axons. Correspondingly, slower units (fatigue resistant) are recruited before faster (fatigue susceptible) ones. The motor units from different regions of the same muscle may also separately involve in

different movement patterns (Cope and Pinter, 1995).

As the index of torque and the indicator of the firing rates of recruited motor units during muscle contraction (Orizio, 1993; Jaskolska et al., 2006), EMG and MMG signals can each provide information on various aspects of muscle function. Recently, many studies have been performed using EMG and MMG to identify the motor control strategies involved in force/torque production during isometric ramp increasing or step contraction, in which the force/torque is alternately linearly increased or steadily maintained (Bilodeau et al., 1997). Investigating the differences between various muscle contraction protocols may guide exercise testing and training (Bader et al., 1999). The amplitude and frequency of EMG and MMG were examined with torque during ramp increasing or step contraction (Akataki et al., 2001; Ryan et al., 2008a; Akasaka et al., 1997; Beck et al., 2005, 2004). For example, EMG has been used to illustrate the different characteristics of ramp increasing vs step contractions (Bilodeau et al., 1991; Lariviere et al., 2001; Nadeau et al., 1993; Sanchez et al., 1993), and the relationship between MMG and force/torque has also been compared (Ryan et al., 2008b).

2.1.5 Morphological Parameters

2.1.5.1 Pennation Angle and Fascicle Length

Pennation angle is defined as the angle between fascicles and aponeurosis. Aponeuroses are membranes separating muscles from each other. The propagation velocity of action potentials is correlated with the fibre length (Arendt-Nielsen et al., 1992). Fukunaga et al., (1997) used ultrasound images to detect the pennation angle and fascicle length of vastus lateralis muscle (Fig. 2. 3).

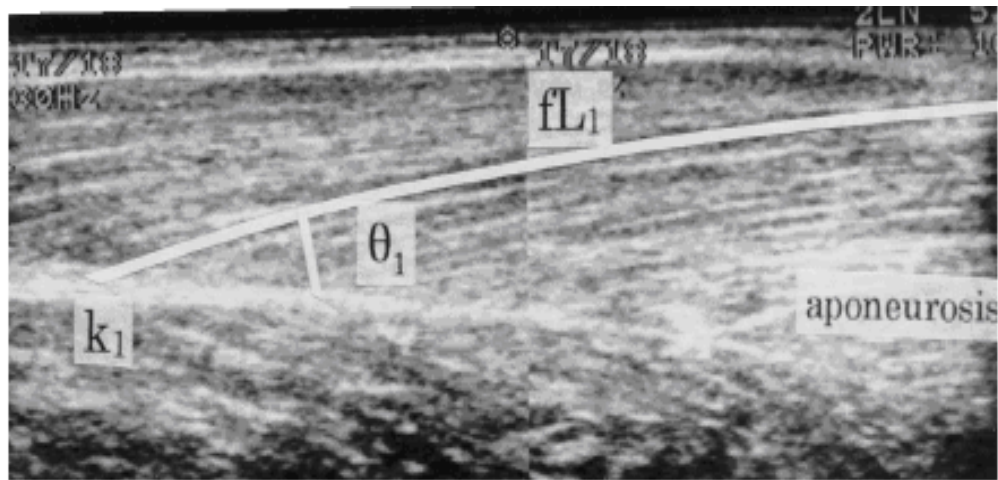


Fig. 2. 3 Pennation angle and fascicle length of vastus lateralis muscle (Fukunaga et al., 1997).

2.1.5.2 Cross-sectional Areas

The cross-sectional area (CSA) of a muscle is the sum of the CSA of all the fibres. The maximal force that a muscle can generate is closely correlated with its CSA (Morris 1948; Ikai et al., 1970). Maughan et al., (1983) studied the relationship between the CSA and the maximal voluntary isometric strength of knee extensor muscles. As shown in Fig. 2. 4, computerised axial tomography (CT) scanning was used to produce a cross-sectional image of the leg at the mid-thigh level (the half way between the greater trochanter and the upper border of the patella). The researchers reported that a significant positive correlation exists between the CSA of the knee extensor muscles and the maximal voluntary isometric force.

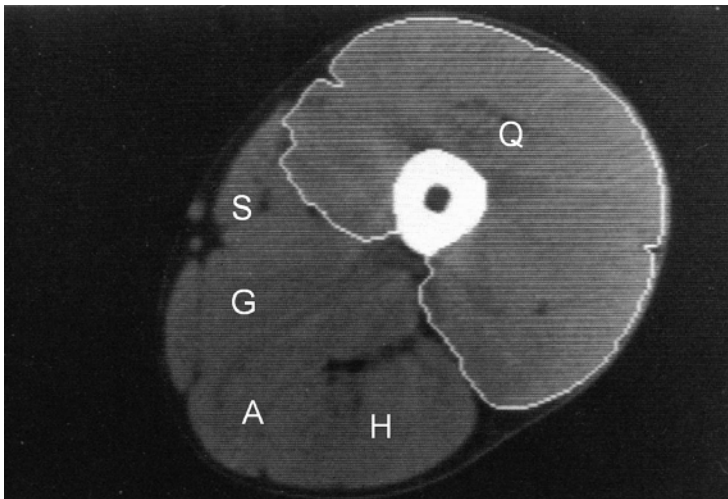


Fig. 2. 4 CT scan obtained from an untrained healthy subject. The knee extensor muscle: A-adductors, G-gracilis, H-hamsstrings, Q-quadriceps, S-sartorius (Maughan et al., 1983).

2.1.6 Muscle Contraction Pattern

The function of skeletal muscle is to generate force or to produce movement. During the normal activities, the locomotor muscles produce the force by various contractions, such

as isometric, isokinetic, isotonic, concentric and eccentric contractions (Lindstedt et al., 2002). The maximal voluntary contraction (MVC) was defined as the highest value of torque recorded during the entire isometric contraction (Hakkinen and Hakkinen, 1991). During isometric contraction, the muscle is held at a constant length. Two common isometric contractions are step and ramp. During the step contraction, the subject is required to produce a stable sub-maximal MVC torque while during the ramp increasing and decreasing, the subject is instructed to produce torques increasing from 0 to his/her MVC (or some percentage of MVC) and then decreasing back to zero linearly. Isokinetic contraction is used to describe exercises performed through the range of motion of a joint at a constant velocity. In an isotonic contraction, tension remains unchanged and the skeletal muscle's length changes. Contractions that permit the muscle to shorten are referred to as concentric contractions. Even though the muscle may be fully activated, it is forced to lengthen due to the high external load. This is referred to as an eccentric contraction (Macintosh et al., 2006).

2.1.7 Muscle Dysfunction

Dysfunction of skeletal muscles, for instance, myotonic dystrophy (Nitz et al., 1999), amyotrophy or even the lost of body part, will not only result in physical handicap but also cause social deprivation. Amputation is the removal of a body extremity in accident or to prevent the disease process in the affected limb (<http://en.wikipedia.org/wiki/Amputation>). Amputations at the wrist and forearm (below the elbow) remain one of the oldest surgical procedures. Details of the operation vary slightly depending on what part is to be removed. All amputations consist of a two-fold surgical procedure: 1) to remove diseased tissue so that the wound will heal cleanly, and 2) to construct a stump that will allow the attachment of a prosthesis or artificial

replacement part. The diseased part is removed, and the bone is smoothed. A flap is constructed of muscle, connective tissue, and skin to cover the raw end of the bone. Often, a rigid dressing or cast is applied about two weeks (Baumgartner 2001). The prosthetic designs and the patient emotional, physical, and vocational background must be considered carefully. The design of the hand prosthesis to substitute the natural one has become an important research area and drawn increasing attentions in recent years.

2.2 Technology for Muscle Assessment and Prosthetic Control

2.2.1 Electromyography

Electromyography (EMG), the electrical signal collected by the electrodes during muscle contractions, represents the neuromuscular and bioelectrical properties of skeletal muscles and demonstrates the physiological process for the muscle contraction. There are two types of EMG: needle and surface EMG. Needle EMG is collected from a needle containing two fine-wire electrodes which are inserted into the muscle by a trained professional. It is used to reflect the information of certain muscle fibres' MUP and therefore can be used to detect the neuromuscular disorders and diseases (<http://en.wikipedia.org/wiki/Electromyography>). On the other hand, surface EMG signal, collected from the electrodes attached to skin surface, is a complex signal, which is the summation of individual MUAP trains, generated by irregular discharges of active MUs during the muscle activation. Compared with the needle EMG, it provides the information of the overall muscle function rather than a single muscle fibre. In addition, surface EMG is non-invasive and non-painful to the patient. Therefore, surface EMG is widely used in both clinical diagnosis and research.

EMG is a direct reflection of muscle activities and various analyses have been carried out to investigate the relationship between the features of EMG patterns and muscle forces (Liu et al., 1999), joint angles (Sepulveda et al., 1993), joint moments (Wang and Buchanan, 2002), and joint torques and trajectory (Hahn, 2007; Koike and Kawato, 1995). Moreover, it has been widely used for the evaluation of muscle functions in the areas of biomechanics and kinesiology (Benoit and Dowling, 2006; Paavolainen et al., 2006), muscle pathology (Labarre, 2006), muscle fatigue (Masuda et al., 1999;

MacIsaac et al., 2006), and prosthetic device control (Kermani et al., 1995; Kuiken et al., 2004).

During the past decade, lots of efforts have been made to develop different algorithms to process EMG signals, such as time-frequency representation (Engelhart et al., 1999; Karlsson and Gerdle, 2001), wavelet analysis (Englehart et al., 2001; Al-Assaf 2006), fractal method (Talebinejad et al., 2009). In addition, various signal processing techniques have been reported for EMG control strategy, including classification of EMG using artificial network (Karlik et al., 2003) and fuzzy logic (Chan et al., 2000), pattern recognition for multi-channel EMG (Ajiboye and Weir, 2005), and decomposition of EMG signals using Bayesian method (wheeler et al., 2006). All these efforts aim to provide efficient EMG signal features which represent the skeletal muscle physiological characteristics and to improve the multifunctional performances of EMG control along with the reduction of control complexity for users.

Powered prostheses have been used for decades to provide an artificial extension of amputees (Muzumdar 2004). They can be used to replace parts of human body lost or to supplement defective body parts. A typical powered prosthesis is comprised of mechanical and electrical components, capable of extracting features or patterns from the electrophysiological signal (such as signals from muscle and brain) and mapping them into movement functions of the mechanical actuators.

By far the most commonly used upper-limb externally powered prosthetic devices is the myoelectric prosthesis, controlled by the EMG signal. In a myoelectric prosthesis EMG is detected from the remaining musculature of the residual limb and, the processed signal is used for control of the prosthesis motor(s). By using such devices, amputees

regain a degree of upper limb function. Although controlled studies suggest that expert users of current prostheses can perform a wide range of tasks with the devices, the reported rejection rates (Biddiss and Chau, 2007) and the high incidence of overuse injuries in the contralateral arm of unilateral amputees (Gambrell, 2008), both suggest that the additional functionality is often not fully exploited in every day life.

An effective and reliable prosthesis should have multiple DOFs, provide the user with the ability to perform task with a high degree of accuracy, yet be intuitive and simple to control (Shenoy et al., 2008; Cipriani et al., 2008). Learning to use the prosthesis should require little training and, once proficient, the user should be able to take advantage of the additional functionality in everyday situations with little cognitive effort (Cipriani et al., 2008). Researchers have made efforts to achieve these goals using various approaches. For example, Miller et al., (2008) utilized the targeted muscle reinnervation (TMR) method to increase the number of controllable DOFs. In another study, vibrotactile or electrotactile simulation was employed to provide biofeedback (Cipriani et al., 2008). To simplify the multiple DOFs control problem, a number of computing approaches have been proposed to recognize various movement patterns from one or more EMG channels (for example Kelly et al., 1990; Hincapie and Kirsch, 2009; Karlik et al., 2003; Englehart et al., 2001; Englehart and Hudgins, 2003).

However, researchers still face from the challenges of some inherent limitations of EMG control. For example, it is difficult to provide a natural control of the prosthesis with multiple DOFs based on multi-channel EMG signals. Intensive conscious effort is needed to control the prosthesis and fatigue easily occurs after long time utilization (Cipriani et al., 2008). Although many efforts have been made for the classification of multi-channel EMG signals, most of the current commercially available hand prostheses

still use two-channel EMG inputs to provide one or two DOF(s). In addition, EMG is an inherently random, non-stationary and non-linear signal whose measurement from socket-located transducers is susceptible to interference from socket movement and sweat-related skin impedance changes (Besio and Prasad, 2006; Alemu et al., 2003). It is also difficult, using surface EMG, to discriminate activity of deep muscles from activity of more superficial muscles due to muscle cross talk (De Luca, 2002), limiting the potential for multi-DOF control. Furthermore, the characteristics of the EMG signals associated with performing a particular task vary considerably between individuals (Balogh et al., 1999). Of most importance, various investigators have suggested that multi-DOF EMG-based prostheses require a very high level of concentration to control (Cipriani et al., 2008; Loeb, 2009).

Alternative signals have been searched for better assessment of muscle functions, including MMG (Orizio 1993), SMG (Zheng et al., 2006), electroencephalographic (EEG) (Chang et al., 2003; Svoboda et al., 2002), myokinematic (MK) (Kenney et al., 1999), and magnetic resonance imaging (MRI) (Kinugas et al., 2006). They are introduced in the following sections.

2.2.2 Mechanomyography

Mechanomyography (MMG) is the sound generated by a muscle during its contraction and has been used as a measure of muscle mechanical changes during contractions (Orizio et al., 2003). As the “mechanical counterpart” of the MU electrical activity measured by EMG, MMG is a recording of mechanical oscillation that is detected from the body surface overlying the muscle (Gordon and Holbourn, 1948; Beck et al., 2004). It has been advised that the lateral oscillations detected by MMG could be decomposed

to three parts: (1) a gross lateral movement at the beginning of a muscle contraction (2) smaller subsequent lateral oscillations produced at the resonant frequency of the muscle, (3) dimensional changes of the muscle fibre (Beck et al., 2004; Orizio, 1993).

The features of MMG signals have been used to reflect the kinematic and physiological characters during postural control (Kouzaki and Fukunaga, 2008), concentric muscle contractions (Ebersole et al., 1999), and cycle ergometry (Housh et al., 2000; Perry et al., 2001), to detect various muscular disorders, including cerebral palsy (Akataki et al., 1996), myotonic dystrophy (Orizio et al., 1997), low back pain (Yoshitake et al., 2001), and muscle fatigue (Mamaghani et al., 2002), etc. Furthermore, studies have been conducted with EMG and MMG simultaneously to exam the skeletal muscle characteristics. For example, EMG and MMG were used to investigate the difference in agonist and antagonist muscles between old and young women (Jaskolska et al., 2006); and to estimate the influence of torque changes during relaxation from MVC of elbow flexors at different joint angles (Jaskolska et al., 2003). Additionally, complementary information was provided by collecting EMG and MMG during concentric, isometric and eccentric contractions at different MVC (Madeleine et al., 2001).

As an alternative to EMG, MMG signal, representing the mechanical vibrations that result from muscle contraction, has shown promise for the control of powered prostheses (Silva et al., 2005). Researchers suggested that MMG signal had the potential to be an alternative control input for powered prosthesis more than two decades ago (Barry et al., 1984; Barry et al., 1986). Another research group recently designed and implemented a novel self-contained MMG-driven prosthesis for below-elbow amputees (Silva et al., 2005). However, despite significant advances, the signal transduction challenges remain. MMG signals are prone to being contaminated by low frequency

noise during muscle contraction. This is believed to result from the low frequency movement at the beginning or the end of an isometric contraction and throughout dynamic contractions. In addition, the high frequency components could be contaminated by nearby vibrating muscle fibres or other physical vibrations (Torres et al., 2005; Silva et al., 2003; Xie et al., 2009a; Silva and Chau, 2003). MMG could also be affected by many other factors, such as muscle temperature (Orizo, 1993), skinfold thickness (Jaskolska et al., 2004). These factors together with the challenges in sensor attachment and low-frequency noise elimination would affect the stability and reliability of the MMG signal, thus limit its applications in prosthesis control.

2.2.3 Sonomyography

Due to its advantages of being stable, easy to use, non-ionizing and able to record activities from deep muscles without cross talks from adjacent ones (Hodges et al., 2003), ultrasonography is a widely used method to measure the morphological changes of skeletal muscles. It has been used to detect the changes of muscle thickness or displacement (Nogueira et al., 2009; Suzana et al., 2008; Matsubayashi et al., 2008; Bojsen-Moller et al., 2003; Springer and Gill, 2007; Mannion et al., 2008; Muller et al., 2000; Farella et al., 2003; Sallinen et al., 2008), pennation angle (Kawakami et al., 1993; Mahlfeld et al., 2004), cross-sectional areas (Kanehisa et al., 1995; Narici et al., 1996; Reeves et al., 2004), and muscle fascicle length (Fukunaga et al., 2001; Ichinose et al., 1997; Griffiths, 1987). The ultrasound parameters were also suggested to be able to characterize muscular pain, injuries and dysfunction (Botteron et al., 2009; Diaz et al., 2008; Chester et al., 2008; Bernathova et al., 2008; Sikdar et al., 2008). However, most of these measurements were in static and quasi-static conditions.

Since skeletal muscle architecture is closely correlated with its function (Lieber and Friden, 2000), ultrasound has been used together with EMG to provide more comprehensive information about the muscle activities and properties (Andrade et al., 2009; Hides et al., 1994; Ishikawa et al., 2006; Hodges et al., 2003; Ferreira et al., 2004; Whittaker et al., 2007). It has been reported that the relationship between EMG and the muscle morphological changes extracted from ultrasound is almost linear in lower range of forces, but not in higher range of forces for tibialis anterior (Hodges et al., 2003), biceps brachii (Hodges et al., 2003; Shi et al., 2008), transversus abdominis (Hodges et al., 2003; McMeeken et al., 2004), masseter muscle (Georgiakaki et al., 2007), etc.

In a previous study, Zheng et al. (2006) used sonomyography (SMG) to describe the real time signal about the muscle thickness change detected using B-mode ultrasound images during its dynamic contraction. A system was developed to record and analyze ultrasound images, force, joint angle and surface EMG simultaneously. The system has been successfully used for the analysis of muscle fatigue and it was found that the muscle thickness increased during the fatigue process (Shi et al., 2007). The correlation between EMG and SMG of muscles during isometric contraction has also been investigated (Shi et al., 2007). It was proposed that the real-time muscle morphological change detected by ultrasound, i.e., SMG, would have potential for prosthetic control (Zheng et al., 2006), assessment of isometric muscle contraction (Shi et al., 2008, 2007; Zhou et al., 2008) and isotonic contraction (Xie et al., 2009). It has been demonstrated in these studies that SMG appears to have a close relationship with the change of the corresponding joint angle and most importantly it could be potentially used for the control of powered prosthesis.

However, the ultrasound imaging system employed is not suitable for the control purpose, as the system is too expensive and the ultrasound probe is too large for practical use. On the other hand, A-mode ultrasound with a more portable and compact transducer should be a less expensive and more practical alternative to detect muscle thickness changes during its contraction. A-mode ultrasound transducers may be easily attached to the skin during dynamic activities of muscles and can be small enough to be embedded in prosthetic sockets.

2.2.4 Other Physiological Signals

Some other alternative approaches have also been investigated to generate signals for control purposes, including surface electroencephalogram (EEG) (Heasman et al., 2002; Brunner et al., 2010; Shyu et al., 2010), collected using embedded neurochip implants (Nicolelis 2001; Taylor et al., 2002; Schalk et al., 2010); muscle dimensional change (Almstrom and Kadefors 1972; Kenney et al., 1999; Bu et al., 2008; Wininger et al., 2008), etc. These methods each have their own advantages and shortcomings and researchers in this field are still working hard to achieve signals for a better prosthetic control, so as to reduce the cognitive effort required from users, to provide direct feedback when performing movement, and to increase the number of DOFs.

Brain activity is an electrophysiological signal that can be potentially used for the prosthetic control. This control approach is often termed as brain-machine interface (BMI), human-machine interface (HMI), or neuroprosthesis in literature (Nicolelis 2001). EEG and magnetoencephalography (MEG) are two non-invasive methods to measure the electrical activity in brain (Kauhanen et al., 2006; Mellinger et al., 2007; Waldert et al., 2008). However, both methods can only provide relatively low

information rate, which is not sufficient to control a dexterous prosthesis (Tonet et al., 2008). Electrocorticography (ECoG) signal is invasively collected from the exposed surface of the brain, and has much higher spatial resolution than EEG, because there is no signal attenuation from skull (Wilson et al., 2006; Pistohl et al., 2008). The cortical neural signal is the most direct recording of the brain activity, and has great potential to provide dexterous control (Mussa-Ivaldi and Miller 2003; Lebedev and Nicolelis 2006). Since the original demonstration that electrical activity generated by ensembles of cortical neurons can be employed directly to control a robotic manipulator (Chapin et al., 1999), researches on neuroprosthetic developments have experienced an impressive growth (Wessberg et al., 2000; Taylor et al., 2002; Chapin 2004; Hochberg et al., 2006). Various linear and nonlinear algorithms were suggested to extract movement information from ensembles of neurons (Schwartz et al., 2001). However, it is an invasive technique and there still exist many conceptual and technological obstacles before developing neuroprosthetic devices for clinical applications.

Other signals that have shown potentials for prosthetic control include the dynamic pressure and shape changes at specific sites on amputees' residual muscles for multi-finger prosthesis (Abboudi et al., 1999; Curcie et al., 2001) and the myokinematic (MK) signal i.e., the measurement of muscle dimensional change from a socket-located displacement transducer (Kenney et al., 1999). Attachment of the sensors is also a challenge for these signals in prosthetic control.

2.3 Models Used to Predict Joint Angle

2.3.1 Artificial Neural Network

Artificial neural network (ANN) is the most popular method used to map the relationship in previous studies. Sepulveda et al. (1993) first made use of a three-layer feed-forward neural network model with the back-propagation (BP) algorithm in a supervised manner to map transformations between EMG and joint angle and joint moment. Similar approaches with different improvements have been adopted by researchers for studying the relationships between EMG and muscle force (Liu et al., 1999), arm movement (Koike and Kawato 1995), and elbow joint torque (Luh et al., 1999). Some other ANN architectures have also been proposed for the muscle system investigation in neurophysiology and biomechanics, such as Levenberg–Marquardt algorithm (Hahn 2007), time-delayed ANN (Au and Krisch 2000), and BP through time algorithm (Dipietro et al., 2003).

2.3.2 Support Vector Machine

Support vector machine (SVM), also a machine-learning algorithm, was developed by Vapnik (1982). The SVM implements the structural risk minimization (SRM) principle rather than the empirical risk minimization principle implemented by most traditional ANN models. It seeks to minimize the upper bound of the generalization error rather than minimizing the training error (Burges 1998; Smola and Scholkopf 2004). SVM achieve an optimum network structure by striking a correct balance between the empirical error and the Vapnik Chervonenkis (VC)-confidence interval which is the function of the number of training samples and the capacity of a learning machine, etc (Vapnik 1982), resulting in better generalization performance in comparison with neural network models. Although SVM was developed for pattern recognition problems (Burges 1998), it has been applied to EMG-related neuromuscular disease diagnosis (Guler and Kocer 2005; Xie et al., 2003), sonography-based decision making in the

diagnosis of breast cancer (Huang and Chen 2005), and in many other fields (Mohandes et al., 2004; Shin et al., 2005; Tay and Cao 2001; Vonga et al., 2006; Yu and Liong 2007). In most of these cases, the performance of SVM modelling either matched or was significantly better than that of ANN approaches.

2.4 Summary

This chapter has mainly reviewed the previous studies for the skeletal muscle assessment and prosthetic control. SMG signal refers to the ultrasound signal recording the skeletal muscle morphological changes in real time which differs from most of the previous studies using static or quasi-static ultrasound parameters. In comparison with EMG and MMG, SMG has the advantages of being stable, and able to record activities from deep muscles without cross talks from adjacent ones. In addition, SMG is inexpensive and therefore relatively easy accessible when compared with other imaging methods, such as CT and MRI. Furthermore, 1D SMG provides a more portable, compact, inexpensive, and practical solution to detect muscle thickness changes than 2D SMG. A-mode ultrasound transducers can be easily attached to the skin during dynamic activities of muscles and can be sufficiently small to potentially be embedded in prosthetic sockets. Therefore, 1D SMG signal has great potential to be used in skeletal muscle assessment and prosthetic control.

In previous studies, the relationship between EMG and force (or the related joint angle) has been systematically investigated and it was found that the relationship is nonlinear and affected by many factors, such as the length of the muscle (Onishi et al., 1999) and the type of muscle studied. On the other hand, the muscle thickness change detected using B-mode ultrasound images during its contraction has been proposed to control

prosthesis (Zheng et al., 2006) and used for the analysis of muscle fatigue (Shi et al., 2007). However, no studies have been reported to investigate the relationship between 1D SMG and the external physiological signals, such as force, and joint angle.

EMG based force/joint angle predictions have been mostly made by ANN on animal or human models (Liu et al., 1999, Mobasser et al., 2005, Hou et al., 2007). ANN has been widely used to map the nonlinear relationships between EMG, muscle force, and torque. Another machine-learning algorithm, SVM, has also been used for the diagnosis of EMG-related neuromuscular diseases (Güler and Kocer 2005, Xie et al 2003) and for pattern recognition (Lucas et al 2008, Yan et al 2008). Some other ANN architectures have also been proposed for the muscle system investigation in neurophysiology and biomechanics, such as Levenberg–Marquardt algorithm (Hahn 2007), time-delayed ANN (Au and Kirsch 2000), and BP through time algorithm (Dipietro et al., 2003). In contrast to the tremendous amount of research on torque predictions using EMG, there are fewer similar studies using SMG, in spite of its great potentials in representing muscle outputs.

An effective prosthesis should be intuitive and simple, requiring little effort to control. Different muscle activity signals, such as EMG and SMG, may have quite distinct relationships to the muscle activities. Therefore, it is possible to suggest that, for different signals, the different relationships between the neural activity and measured signal may have an effect on both the control accuracy and the degree of attention required. Few studies have been reported to comprehensively investigate the differences between two muscle signals for control purposes (Canderle et al., 2004). Therefore, in this thesis, we attempted to compare the performances of 1-D SMG signal and surface EMG signal in terms of accuracy and cognitive requirements. We hypothesized that

using the 1-D SMG signal measured from the extensor carpi radialis muscle would result in a better performance on both tracking guided patterns of wrist extension and series of discrete tracking tasks when compared with surface EMG measured from the same muscle, based on our findings in earlier studies (Zheng, et al., 2006; Shi et al., 2007; 2008). Furthermore, we hypothesized that using SMG signals may require less attentional effort than using EMG signals when performing the tracking tasks.

Previous studies demonstrated that SMG signal could be potentially used for the control of powered prosthesis. However, the ultrasound imaging system is not suitable for the purpose of control, as the system is too expensive and the ultrasound probe is too large for practical use. Recently, a system was developed to collect and analyze A-mode ultrasound, force, joint angle, and surface EMG (sEMG) simultaneously (Huang et al. 2007). Therefore, we attempted to investigate the potential of using 1-D SMG for controlling prosthetic hand with one DOF. The SMG signal extracted from A-mode ultrasound signal was used to control the powered prosthesis in real-time.

CHAPTER 3 METHODS

This chapter systematically introduces the methodology of this study including the skeletal muscle measurement system, experimental protocols and data statistical analysis. The main experiments are listed as follows.

1. Monitoring of forearm muscles using 1D SMG;
2. 1D SMG based wrist angle prediction;
3. Performance of 1D SMG and surface EMG in tracking guided patterns of wrist extension;
4. Comparison of 1D SMG and surface EMG in visuomotor “E” cancellation test;
5. Control prosthesis by 1D SMG and surface EMG;
6. Case study on amputee.

3.1 Skeletal Muscle Measurement System

3.1.1 System Description

As shown in Fig. 3. 1, an ultrasound pulser/receiver (model 5052 UA, GE Panametrics, Inc. West Chester, OH, USA) was used to drive a 10 MHz single element ultrasound transducer (model V129, GE Panametrics, Inc., West Chester, OH, USA), and amplify the received signals. The A-mode ultrasound signal was digitized by a high speed A/D converter card using a sampling rate of 100 MHz (Gage CS82G, Gage Applied Technologies, Inc, Canada). The angle signal during the wrist extension was measured by an electronic goniometer (XM110, Penny & Giles Biometrics, Inc. UK). The surface EMG signal was captured from the EMG bipolar Ag-AgCl electrodes (Noraxon U.S.A. Inc.,USA) and pre-amplified with a gain of 100 using a circuit located near the electrodes. The signal was further amplified with another factor of 10 by the custom-

designed EMG amplifier and filtered by a 10-400 Hz band-pass analog filter within the EMG amplifier. The surface EMG and wrist angle signals were digitized by a 12 bits data acquisition card (NI-DAQ 6024E, National Instruments Corporation, Austin, TX, USA) with a sampling rate of 4 KHz. The surface EMG sampling was synchronized with the collection of ultrasound signals. Each frame of A-mode ultrasound signal contained 8K reflected ultrasound echo data, equivalent to a depth of approximately 6 cm, accompanied by an EMG epoch of 64 ms and a value of wrist angle. The frame rate of A-mode ultrasound was approximately 17Hz, which was also applied to the data rates of SMG. The A-mode ultrasound signal was saved frame by frame along with the surface EMG and wrist angle signals for subsequent analysis in a PC with 2.8GHz Pentium IV microprocessor and 512 MB RAM.

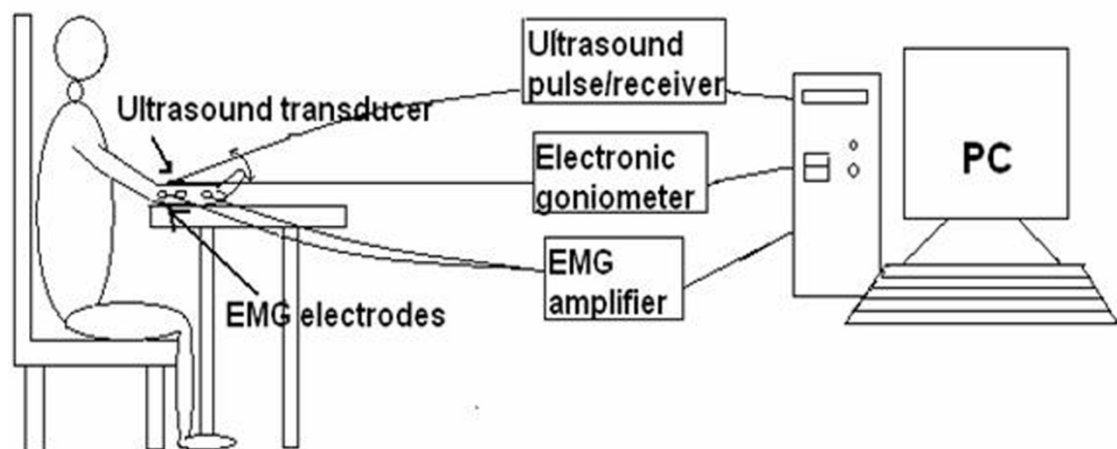


Fig. 3. 1 The diagram of data collection system.

The A-mode ultrasound, surface EMG and wrist angle signals were collected, stored and analyzed by the software for ultrasound measurement of motion and elasticity (UMME, <http://www.sonomyography.org>) developed using Visual C++. The time delay between different data collection systems was calibrated using a method similar to that described by Huang et al., (2005, 2007). As the transducer moved cyclically up and

down in a water tank, the two signals representing A-mode ultrasound, and simulated EMG respectively were collected and stored. The time delay between the data sets was calculated using a cross-correlation algorithm. The details can be found in our earlier study (Huang et al., 2007).

3.2 Skeletal Muscle Evaluation by 1D SMG

3.2.1 Subjects

Nine healthy subjects (7 male and 2 female) aged from 24 to 35 years were recruited in the experiment. The human subject ethical approval was obtained from the ethics committee of the Hong Kong Polytechnic University and informed consents were obtained from all subjects prior to the experiment. All the participants were right-hand-dominant without any known neuromuscular disorders.

3.2.2 Monitoring of Forearm Muscles Using 1D SMG

3.2.2.1 Measurement of Wrist Angle, 1D SMG and Surface EMG

The 10 MHz single element ultrasound transducer (diameter=5 mm) was selected because this frequency could satisfy the required resolution and the scanning depth in this study. It was inserted into a custom-made holder (diameter 26 mm) which was made of silicone gel in order to attach the transducer to the skin. Before the experiment, a portable B- mode ultrasound scanner (180 Plus, Sonosite Inc., Washington, USA) was used to identify where the extensor carpi radialis was and the subject was asked to perform several wrist extensions, through which the most prominent bulge of the

extensor carpi radialis belly was found. The single element ultrasound transducer was then positioned on the skin of the identified prominent bulge of the extensor carpi radialis belly and fixed by double-sided adhesive tape to measure the muscle's thickness change (Fig. 3. 2). Ultrasound gel was filled between the transducer and the skin to aid acoustic coupling. The EMG bipolar Ag-AgCl electrodes were also attached to the skin surface of the extensor carpi radialis belly near the ultrasound transducer and with a distance of approximately 1 cm to avoid the potential effects from the ultrasound coupling gel (DeLuca, 1997). The distance between the two electrodes was 20 mm and their orientation was parallel to the extensor carpi radialis muscle fibres. An additional electrode for providing the reference electrical signal was placed near the head of ulna. The electronic goniometer was placed at the middle of posterior hand to measure the wrist angle during wrist extension.

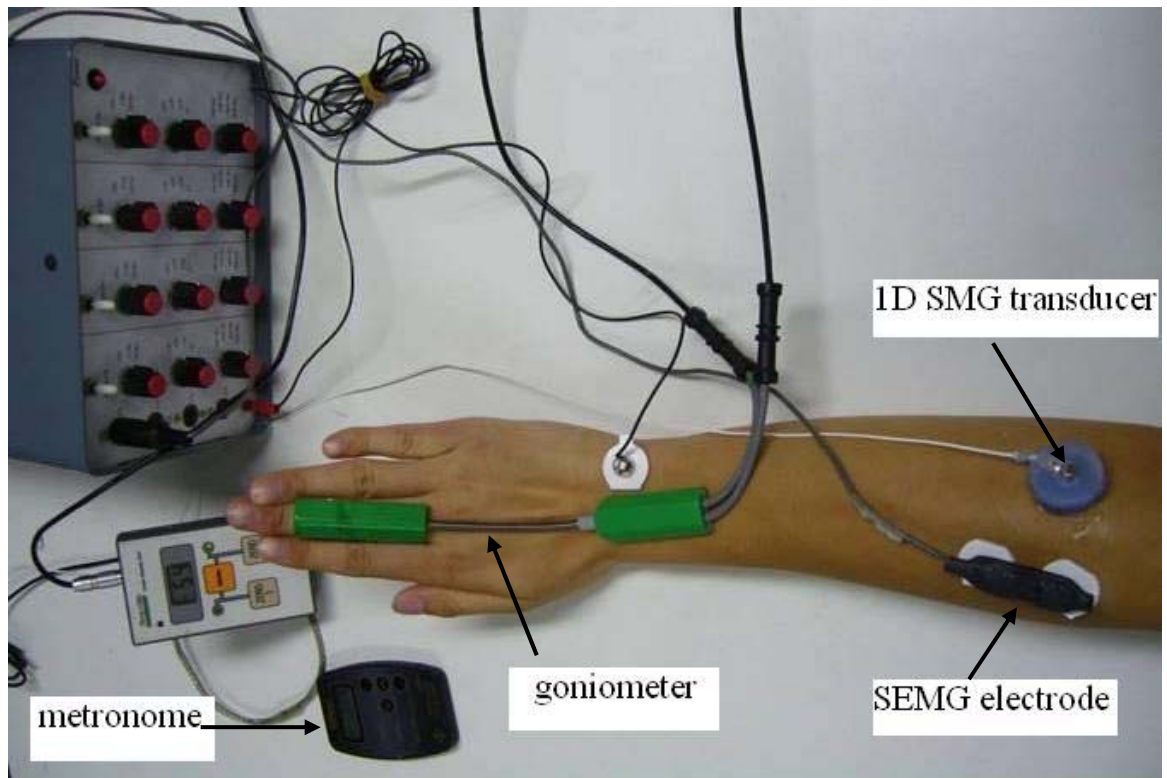


Fig. 3. 2 The Placement of the 1D SMG transducer, surface EMG electrodes and electronic goniometer on the forearm. Ultrasound coupling gel was applied between the ultrasound transducer and skin.

The right forearms of the subjects were chosen for testing, which were the dominant ones for all subjects. The subject was seated on a comfortable chair with his/her forearm resting on the table. After skin preparation with alcohol swabs and several warm-up contractions, the subject was asked to perform wrist extension guided by a metronome (MT-40, Wittner, Germany) at three extension rates of 15, 22.5, 30 cycles/min, respectively. For each extension rate, three repeated tests were performed with a rest of 3 minutes between two adjacent trials and there were three wrist extension cycles in each trial. During the experiment, the subjects were given continuous encouragement to try their best to reach their largest wrist extension angle and most of the subjects could achieve the largest wrist extension angle of 80 to 90 degrees.

3.2.2.2 Cross-Correlation Algorithm to Calculate the Muscle Thickness Change (1D SMG)

A cross-correlation algorithm was employed to track the displacements of upper and lower boundaries of extensor carpi radialis muscle during the wrist extension. The muscle deformation signal, i.e. SMG, was extracted from the A-mode ultrasound using this algorithm (Fig. 3. 3). The equation used to calculate the normalized one-dimensional cross-correlation is as follow:

$$R_{xy} = \frac{\sum_{i=0}^{N-1} [x(i) - \bar{X}][y(i) - \bar{Y}]}{\sqrt{\sum_{i=0}^{N-1} [x(i) - \bar{X}]^2 \sum_{j=0}^{N-1} [y[j] - \bar{Y}]^2}} \quad (3-1)$$

where \bar{X} and \bar{Y} are the means $x(i)$ of $y(i)$ and, respectively. It requires a reference signal from an initial frame and would search for the signal most similar to the reference signal for estimating the object position in the updated frame.

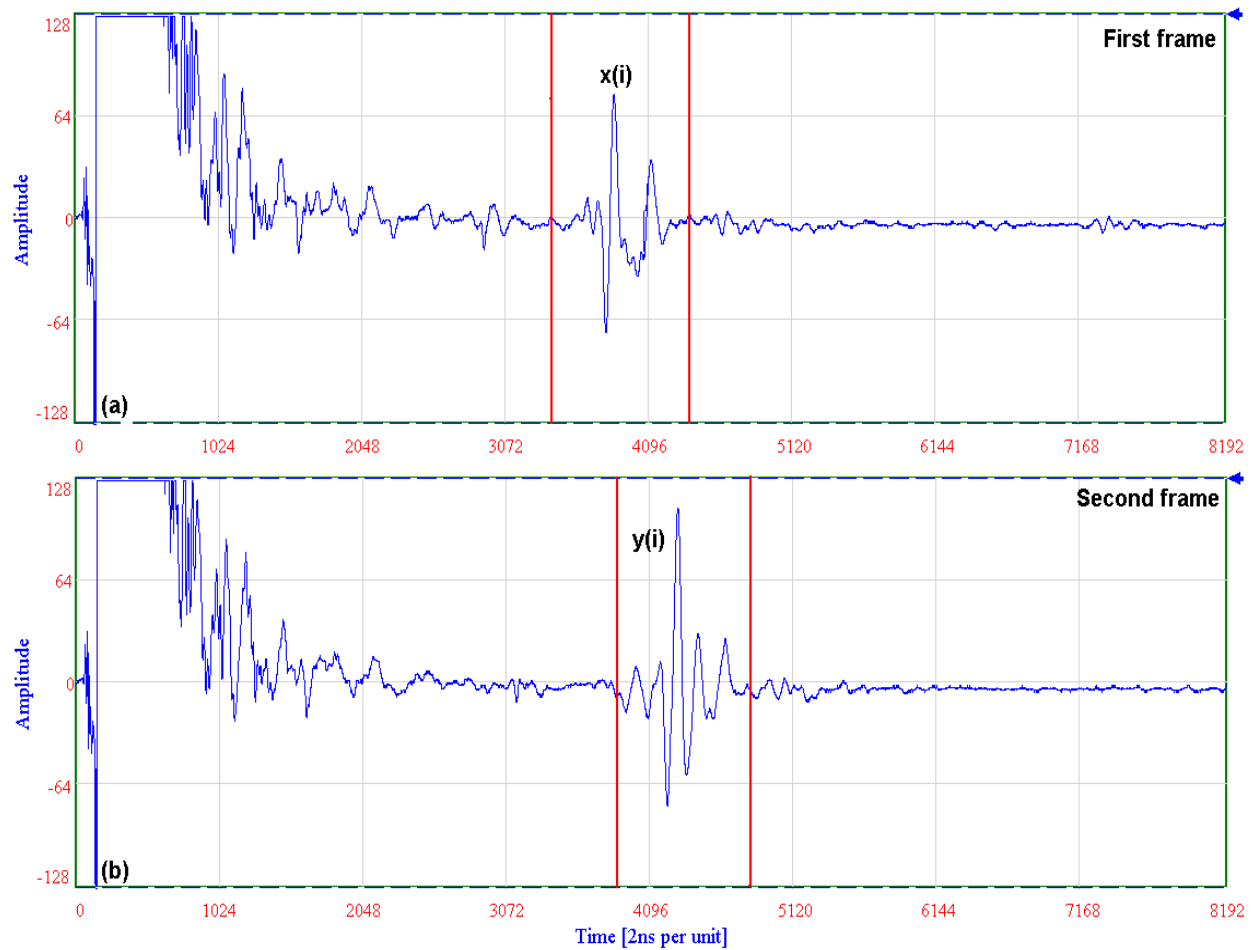


Fig. 3. 3 The demonstration of using the cross correlation algorithm to find the position change of ultrasound echoes due to the thickness changes of skeletal muscle during movement (a) The signal within the red window ($x(i)$) was chosen as the reference signal at the first frame. (b) In the second frame, the red window was searching 500 data points right and left (search range =500) from the position in the first frame and calculating a cross-correlation value once moving a data point. Finally, the echo with the maximal cross correlation value was selected and the corresponding position was regarded as the current position of the selected signal $y(i)$.

In this study, the A-mode ultrasound echoes reflected from the fat-muscle and muscle-bone interfaces were our interested signals. When the muscle was contracting, its dimensional changes induced the variations of distance between these two interfaces,

which in turn caused the A-mode ultrasound echoes to shift for a certain distance. The A-mode ultrasound signals were selected by two tracking windows and the correlation tracking algorithm was implemented to track the movement of the selected echoes frame by frame automatically. The width of the tracking window was selected manually to include enough features of the echo for a reliable tracking. On the other hand, the tracking window should not be too large, for example including the neighbouring echoes, thus increasing the calculation time, which may affect the real-time control. This manual selection of the tracking window slightly affected the value of the muscle deformation (with a high intraclass correlation coefficient (ICC) value) and its effect on the percentage change could be negligible. However, the automatic selection should be utilized in the real clinic application to reduce this effect caused by manual operation. The distance between the fat-muscle and muscle-bone interfaces was calculated for each frame. The percentage deformation of the muscle was defined as

$$D = \frac{(d - d_0)}{d_0} \times 100\% \quad (3-2)$$

Where d_0 is the initial distance between the two echoes and d is the distance when the muscle was contracting.

Since the distance between the fat-muscle interface and the ultrasound transducer, i.e. the thickness of the fat layer, did not change during the movement, the displacement of the echo from muscle-bone interface was calculated and regarded as the muscle thickness change. The correlation based method for tracking displacements of upper and lower boundaries of extensor carpi radialis muscle during wrist extension could be affected by decorrelation resulting from tissue motion in all three spatial directions. Three-dimensional ultrasound scanning will definitely increase the tracking accuracy. However, the complexity and expense of the system will be accordingly increased. In

the current experiment situation, data collected by the one dimensional ultrasound systems was with a high intraclass correlation coefficient (ICC) and therefore could be used for control purpose. Further study should be performed to reduce the effect caused by tissue motion in three spatial directions.

3.2.2.3 Statistical Analysis

To investigate the reliability of using A-mode ultrasound signal to describe the movement of wrist, the relationship between 1D SMG and wrist angle signal was studied by a linear regression. One-way ANOVA was used to analyze the angle-deformation ratios among trials with different extension rates. Intraclass correlation coefficient (ICC) was calculated using SPSS (SPSS Inc., Chicago, IL, USA) for the repeated trials under each rate. Statistical significance was set at the 5% probability level.

3.2.3 1D SMG Based Wrist Angle Prediction

3.2.3.1 Wrist Angle Prediction Models

Artificial neural networks

BP network is a feed-forward network with an error BP algorithm, one of the simplest ANN implementations. It has an input layer of source nodes, one or more layers of hidden neurons and an output layer. The BP training algorithm involves two phases. During the forward phase, the neural nodes' output is specified, and the input signal is propagated through the network layer by layer. This phase finishes with the

computation of an error signal between the desired response (measured muscle activation) and the actual output (predicted muscle activation) produced by the network. During the backward phase, the error signal is propagated through the network in the backward direction. It is during this phase that adjustments are applied to the free parameters of the network so as to minimize the error in a statistical sense. In spite of many applications of BP ANN (Hornik et al., 1989), it suffers from a main drawback of low convergence speed (Haykin 1999). For detailed tutorials on the mathematical descriptions, the readers can refer to previous publications (Hornik et al., 1989; Haykin 1999; Kasabov 1996).

Radial basis function (RBF) network is a member of the feed-forward neural network, which has both unsupervised and supervised training phases (Kasabov 1996; Powell 1992). It was developed aiming at the defects of BP network with an improved convergence rate and better initial weights determination (Haykin 1999). In the unsupervised phase, the input data are clustered and cluster details are sent to the hidden neurons, where RBF of the inputs is computed by making use of the center and the standard deviation of the clusters. The learning between hidden layer and output layer is of supervised learning type where ordinary least squares technique is used. As a consequence, the weights of the connections between the kernel layer (also called hidden layer) and the output layer are determined. Thus, it comprises a hybrid of unsupervised and supervised learning.

Support vector machine

Modeling by SVM has been effectively and widely used for torque and angle predictions (Song et al., 2006, Shi et al., 2007, Xie et al., 2009) and pattern recognition (Cui et al., 2007, Maaoui et al., 2008). In general, an SVM uses a training data set to

build a model between input and output and then uses test data to predict a target. Readers can refer to literature for detailed descriptions of SVM (Vapnik 1982, Burges 1998). Here we give a simple description of the SVM used in this thesis. For example, we used a labeled training sample:

$$S = \{(x_i, y_i)\}_i^N \quad (3-3)$$

Where x_i is the input data, y_i is the output data, and N is the number of the total training data points.

The SVM can reach a better generalized performance, compared with ANN models, and is based on results from statistical learning theory proposed by Vapnik (1995). The SVM transfers input data x_i into a high dimensional feature space by contracting a nonlinear mapping:

$$y(x) = w^T \varphi(x) + b \quad (3-4)$$

where $\varphi(x)$ is a nonlinear function, and w and b are the weight vector and bias term, respectively.

The following optimization problem is considered:

$$J = \frac{1}{2} w^T w + \frac{1}{2} \gamma \sum_{k=1}^N e_k^2 \quad (3-5)$$

where γ is the regularization parameter for determining the trade-off between minimizing training errors and minimizing model complexity, and e_k is the random error.

With these constraints:

$$y_i = w^T \varphi(x_i) + b + e_i \quad (3-6)$$

The Lagrangian equation is defined as follows:

$$L = J - \sum_{k=1}^N \alpha_k \{w^T \varphi(x_k) + b + e_k - y_k\} \quad (3-7)$$

Where α_k is a multiplier.

Kernels have the form:

$$K(x_k, y_j) = \Phi(x_k)\Phi(y_j) \quad (3-8)$$

Then, the least-squares SVM (LS-SVM) is as follows:

$$y(x) = \sum_{k=1}^N \alpha_k K(x, x_k) + b \quad (3-9)$$

where α and b are the solutions of (3-7) .

The kernel function can be chosen by Mercer's theory (Smola and Scholkopf, 2004).

We used a Gaussian kernel as the kernel function in this study.

3.2.3.2 Data Analysis

The LS-SVM, BP and RBF ANN models of each subject were designed and implemented using Matlab software (Version 6.5, MathWorks, Inc., MA, USA). The SMG features and the actual wrist angle measured by the goniometer were employed to construct input–output pairs to train the models. The dimension of input vector was five, which was formed by the current and past four SMG values. The dimension of input vector was five, which was formed by the current and past four SMG values. If the vector was too large, more training time will be required, if the vector was too small, their will be not enough features to train the model. A similar feature vector constitution method had been used in several previous EMG-based kinematic models (Liu et al., 1999; Suryanarayanan et al., 1995). Data for each subject obtained at the extension rate of 22.5 cycles/min was selected to train the models to determine the relations between the SMG and wrist angles. The data from the remaining trials with extension rates of 15

cycles/min and 30 cycles/min were used for cross-validation tests.

The BP network used in this study had 20 nodes in hidden layer and one node in the output layer. The maximal training epoch was 10,000. The learning rate was set to be 0.1 and the momentum term was 0.7. The hidden nodes used the sigmoid transfer function and the output node used the linear transfer function. The RBF network architecture used in this study was a single hidden layer with Gaussian RBF. The maximal number of hidden unit was set based on the number of the training sample and the spread parameter of RBF, which determined the smoothness of the function approximation. It was selected to be 40 in this study.

Evaluation of the wrist angle predictions from the SMG signals was made by calculating the root mean square difference (RMSD) and the correlation coefficients (CC) of the measured wrist angles and estimated values. The value of RMSD and CC was obtained as follows:

$$RMSD = \sqrt{\frac{\sum_i (\theta(i) - \theta(i)')^2}{\sum_i (\theta(i))^2}} \quad (3-10)$$

where $\theta(i)$ is the measured wrist angle, and the $\theta(i)'$ is the estimated wrist angle.

$$CC = \frac{\sum_{n=1}^N (X(n) - \bar{X}(n)) * (Y(n) - \bar{Y}(n))}{\sqrt{\sum_{n=1}^N (X(n) - \bar{X}(n))^2 * \sum_{n=1}^N (Y(n) - \bar{Y}(n))^2}} \quad (3-11)$$

where $X(n)$ is the actual wrist angle recorded during test. $Y(n)$ is the wrist angle predicted. $\bar{X}(n)$ and $\bar{Y}(n)$ are the means of $X(n)$ and $Y(n)$, respectively.

The prediction result was assessed by both RMSD and CC. Predictions were considered excellent if the coefficient of cross-correlation was greater than 0.9 and the RMSD error was smaller than 15% (Liu et al., 1999). Two-way repeated measure ANOVA with Least Significant Difference (LSD) pair-wise comparisons were used to demonstrate the effects of different movement rates [15 cycles/min vs 30 cycles/min], models [LS-SVM vs BP ANN vs RBF ANN] on the CC and RMSD. All the data were analyzed using SPSS (Version 15.0, SPSS Inc. Chicago, IL, USA) and statistical significance was set at 5% probability level.

3.3 Comparisons of 1D SMG and Surface EMG for Prosthetic Control

3.3.1 Performances of 1D SMG and Surface EMG in Tracking Guided Patterns of Wrist Extension

3.3.1.1 Subjects

Sixteen healthy adults, including eight males (mean \pm SD age= 26.3 \pm 3.4 years; body weight = 70.3 \pm 11.9 kg; height = 172.9 \pm 8.5 cm) and eight females (mean \pm SD age =23.5 \pm 1.2 years; body weight = 50.4 \pm 4.1 kg; height = 160.3 \pm 1.7 cm), volunteered to participate in this study.

3.3.1.2 Experimental Protocol

Before the experiment, all the subjects were trained for two or three trials to make sure they were familiar with the experimental protocol. None of subjects had been trained before. Both 1D SMG and surface EMG signals were tested for their accuracy in following the displayed waveform patterns. The subject was seated comfortably on an

adjustable chair with his/her trunk fixed by a strap onto the back of the chair to prevent posture change during the test and the right forearm resting on the table with pronation. The elbow was flexed at approximately 140 degree between the upper arm and forearm. The angle between the upper arm and trunk was approximately 30 degrees. The healthy subject was instructed to perform wrist extension under the guidance of displayed sinusoidal (Fig. 3. 4a), square (Fig. 3. 4d) and triangular waveforms (Fig. 3. 4e) respectively. The order of the experiments was randomly selected for each subject by lucky draw. For the SMG test, the subject was required to perform several wrist extensions before each experiment in order to determine the amplitude of the muscle deformation signal extracted from A-mode ultrasound (i.e. 1D SMG), and the amplitudes of the guiding waveforms were adjusted based on the obtained muscle deformation range. During the experiments, the subjects were encouraged to try their best to produce real-time muscle deformation signal, i.e. SMG, the same as the waveform being displayed on the screen by adjusting the range of their wrist movement in response to the visual feedback from the guiding waveforms. If the muscle deformation signal generated did not follow the guiding waveform well, the subjects could adjust the strength of their muscles in order to match the two waveforms better. The wrist extension rates were set to be 20, 30, 50 cycles/min for each guiding waveform. Therefore, each subject totally performed nine tasks of wrist extension for the three different movement patterns (sinusoidal, square and triangular waveforms) for SMG tests (Fig. 3. 4).

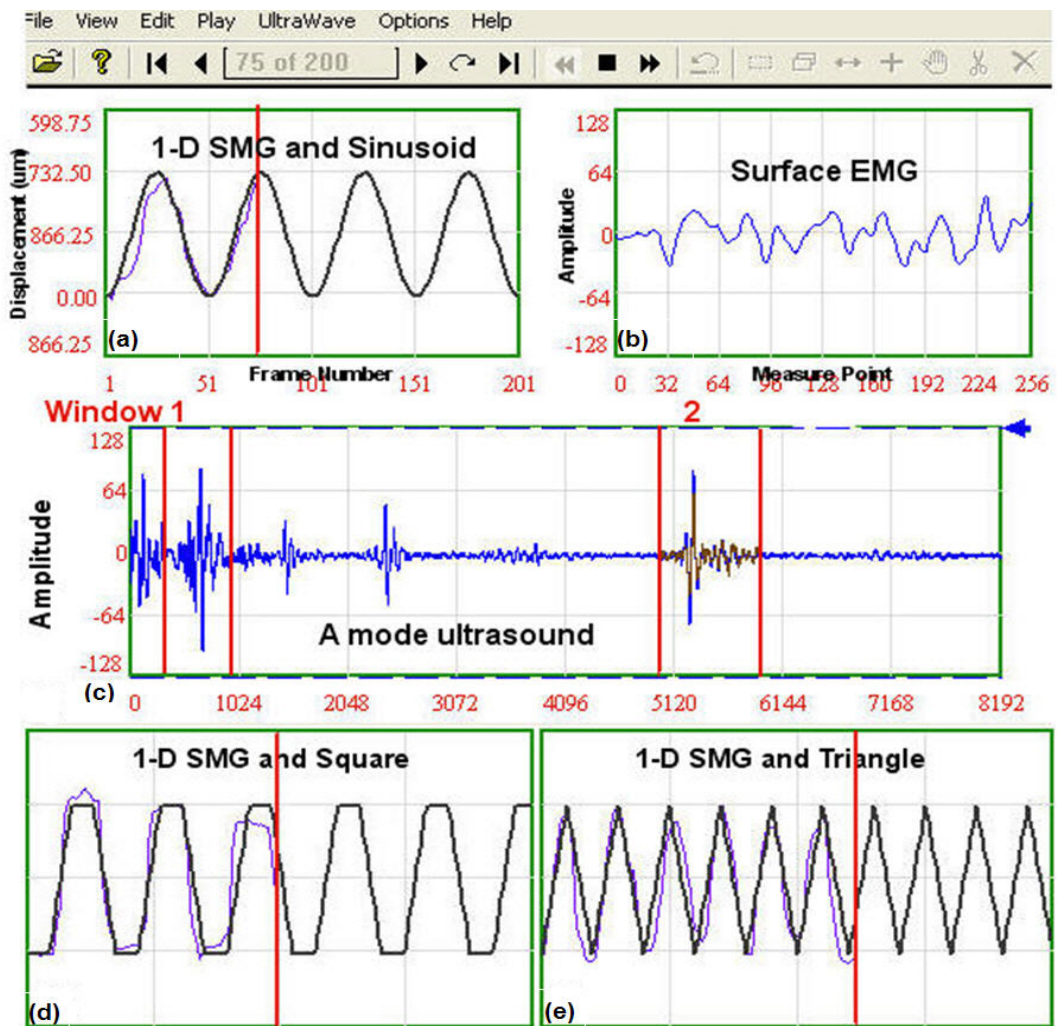


Fig. 3. 4 The software interface used to simultaneously collect 1D SMG and, surface EMG signals; (a) The sinusoidal waveform with a rate of 20 cycles/min was used to guide the wrist extension movement. The subject used 1D SMG signal to track the sinusoidal pattern; (b) Surface EMG was also collected for reference; (c) The SMG signal was measured by detecting the distance change between the A-mode ultrasound echoes reflected from the fat-muscle and muscle-bone interfaces, which were selected by the two tracking windows. A cross-correlation algorithm was employed to track the movements of the echoes during the wrist extension. The SMG signal was calculated using the change of the time interval between the echoes and displayed along with the guiding waveform for tracking; (d) 1D SMG signal was tracking the square waveform at a rate of 30 cycles/min; (e) 1D SMG signal was tracking the triangular waveform at a rate of 50 cycles/min.

The subjects were also instructed to perform another set of wrist extension tasks, using the RMS of their surface EMG signals to follow the reference waveforms. Similar testing protocol was adopted as that in the SMG test. To make the results comparable, during the EMG test, the A-mode ultrasound signals were collected and analyzed in real-time but the SMG signal was not displayed, as shown in Fig. 3. 5. The subjects could adjust the range of wrist movement according to the real-time display of their EMG RMS signals to better fit the reference signal. Totally nine tasks of wrist extension for surface EMG test under the same three wrist extension rates (20, 30, 50 cycles/min) for the three different waveforms were performed by each subject. Fig. 3. 5 shows the interface of the software to collect the data of EMG RMS and the three types of guiding waveforms.

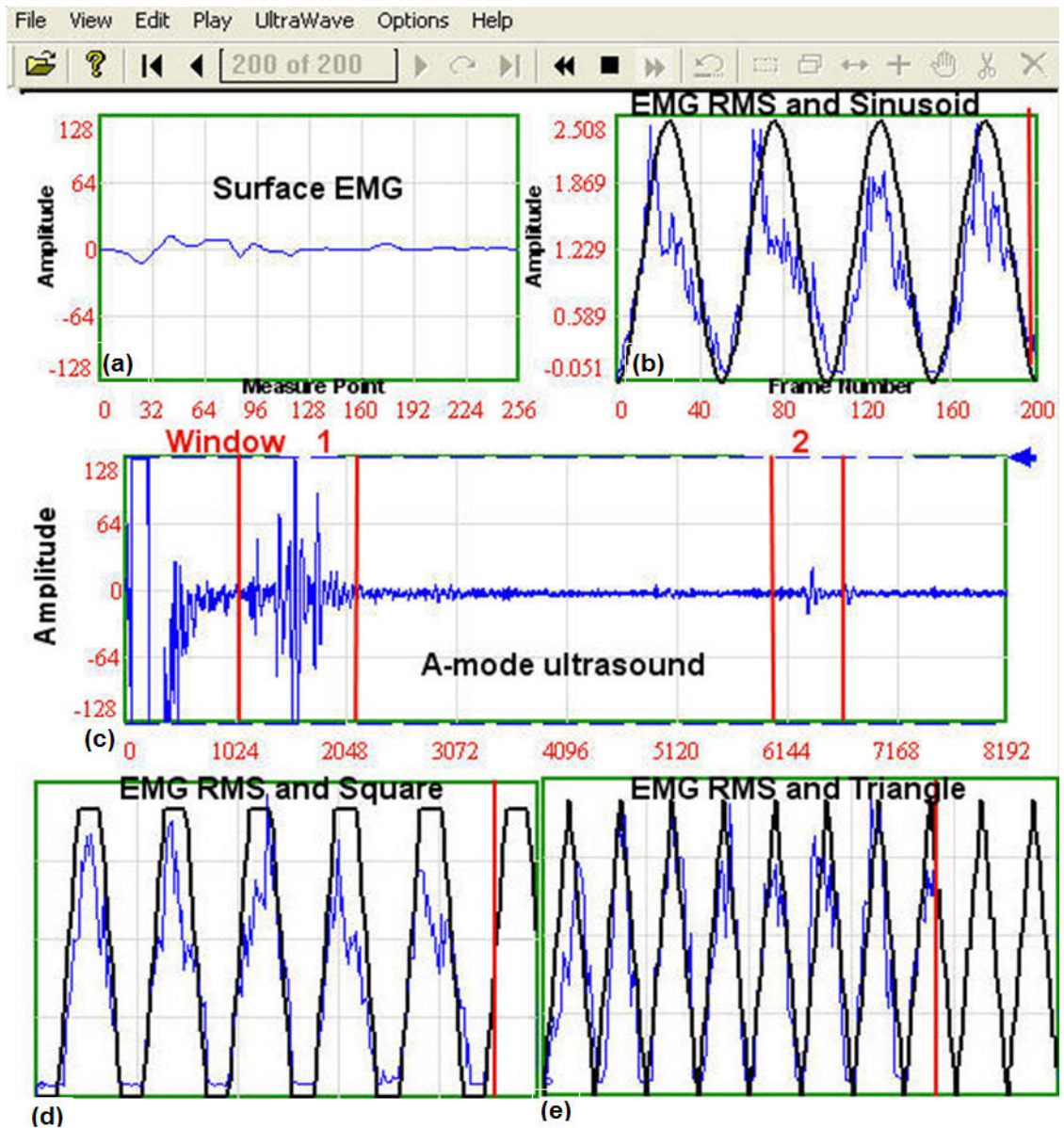


Fig. 3. 5 The software interface used to collect the surface EMG and A-mode ultrasound signals. (a) Surface EMG signal was collected; (b) The sinusoidal waveform with a rate of 20 cycles/min was used to guide the wrist extension movement; SEMG RMS was calculated to track the sinusoidal pattern; (c) A-mode ultrasound signal was also collected for reference; (d) Surface EMG RMS was tracking the square waveform at a rate of 30 cycles/min; (e) Surface EMG RMS was tracking the triangular waveform at a rate of 50 cycles/min.

3.3.1.3 RMS Tracking Error

The SMG and EMG RMS data were respectively normalised by expressing measures as a percentage of the largest SMG and EMG RMS signals detected any time during the testing procedure. The RMS tracking error between SMG/EMG RMS and the corresponding guiding waveforms were calculated separately according to the following equation:

$$\text{RMS tracking error} = \sqrt{\frac{1}{N} \sum_{n=1}^N (\text{Sig}_1(n) - \text{Sig}_2(n))^2} \quad (3-12)$$

where $\text{Sig}_1(n), \text{Sig}_2(n)$ are signals with N points of values.

The performances of SMG and EMG RMS to follow the three guiding waveform patterns were compared using paired t-test. One-Way ANOVA was also used to determine whether there were any differences in the performances of the SMG signals under the three different movement rates. All the data were calculated using Minitab (Minitab Inc., Pennsylvania, USA). Statistical significance was set at the 5% probability level.

3.3.2 Comparison of 1D SMG and Surface EMG in Visuomotor “E” Cancellation Test

3.3.2.1 Subjects

Ten healthy adults, five males and five females (age: 29.5 ± 5.6 (mean \pm SD) years; body weight: 60.6 ± 16.6 kg; height: 166.6 ± 8.0 cm), volunteered to participate in this study.

3.3.2.2 SMG-EMG Compound Sensor

As it is described earlier, an ultrasound pulser/receiver (model 5052 UA, GE Panametrics, Inc. West Chester, OH, USA) was used to drive a 10 MHz single element ultrasound transducer (model 10C6SJ, Shantou Institute of Ultrasonic Instruments Ltd., Shantou, Guangdong, China), and to amplify the received signals. The A-mode ultrasound signal was digitized by a high speed A/D converter card with a sampling rate of 100 MHz (Gage CS82G, Gage Applied Technologies, Inc, Canada). The surface EMG signal, captured from the EMG bipolar Ag-AgCl electrodes (Noraxon U.S.A. Inc., USA), was amplified by a custom-designed EMG amplifier with a gain of 2000 and filtered by a 10-400 Hz band-pass analog filter within the amplifier.

The ultrasound transducer with a diameter of 7.0 mm was firmly fixed by silicone gel onto a 5.8 cm long custom-designed printed circuit board. The EMG electrodes were attached, one to each end of the circuit board. The ultrasound-EMG compound sensor was positioned on the skin over the belly of extensor carpi radialis (Fig. 3. 6). Before the attachment of the sensors, hair in the affected area was shaved using a razor and alcohol was applied to clean the skin. Ultrasound gel was imposed between the A-mode transducer and skin and an additional reference EMG electrode was placed near the head of ulna.

An electrical goniometer (model XM110, Penny & Giles Biometrics, Ltd., Gwent, United Kingdom) was employed to collect the wrist angle signal (Fig. 3. 6). The isometric force was detected by a custom-made force sensor with a strain gauge (model KFG-6-120-C1-11, Kyowa Electronic Instruments Co. Ltd., Japan) on one of its arms (Fig. 3. 7). EMG, angle and force signals were digitized with a 12-bit data acquisition

card (NI-DAQ 6024E, National Instruments Corporation, Austin, TX, USA) with a sampling rate of 1 KHz in a PC with two 2.33 GHz Intel quad-core processors and 3.25 GB RAM.

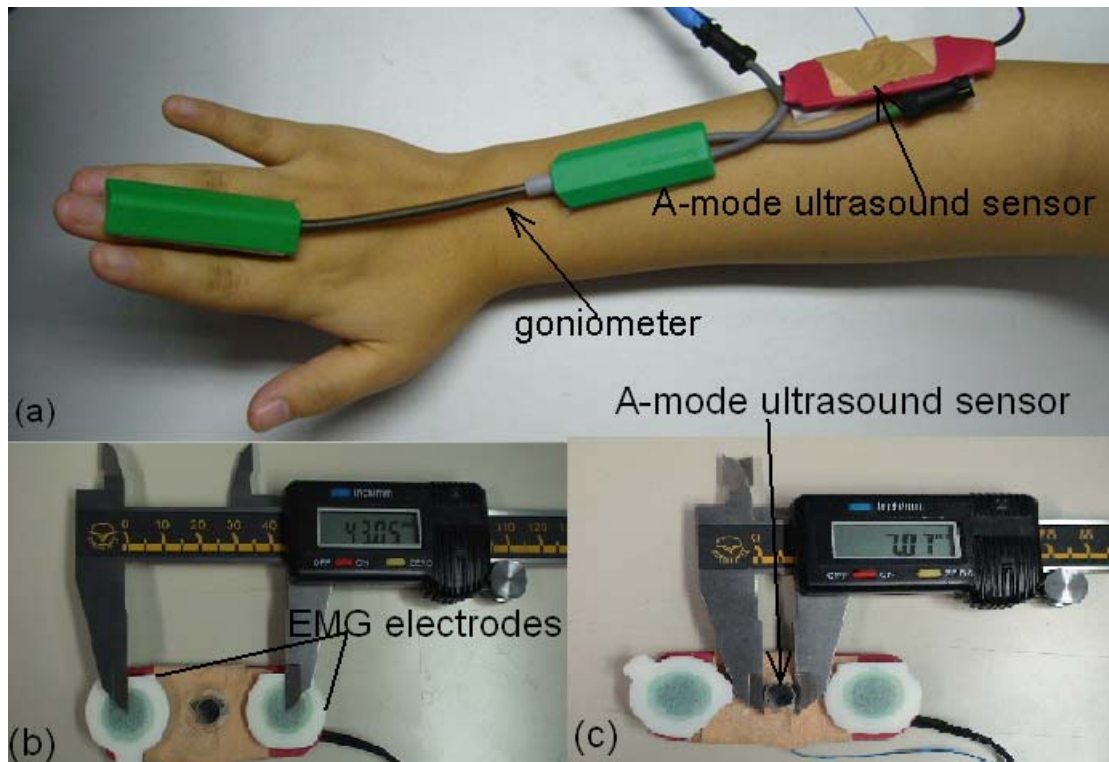


Fig. 3. 6 (a) The ultrasound-EMG compound sensor (1D ultrasound transducer, SEMG electrodes) placed on the extensor carpi radialis muscle of the subject during the wrist extension. A goniometer was placed across the wrist joint; (b) The length between the centres of the EMG sensors was 4.3 cm; (c) The diameter of A-mode ultrasound sensor was 0.7cm.

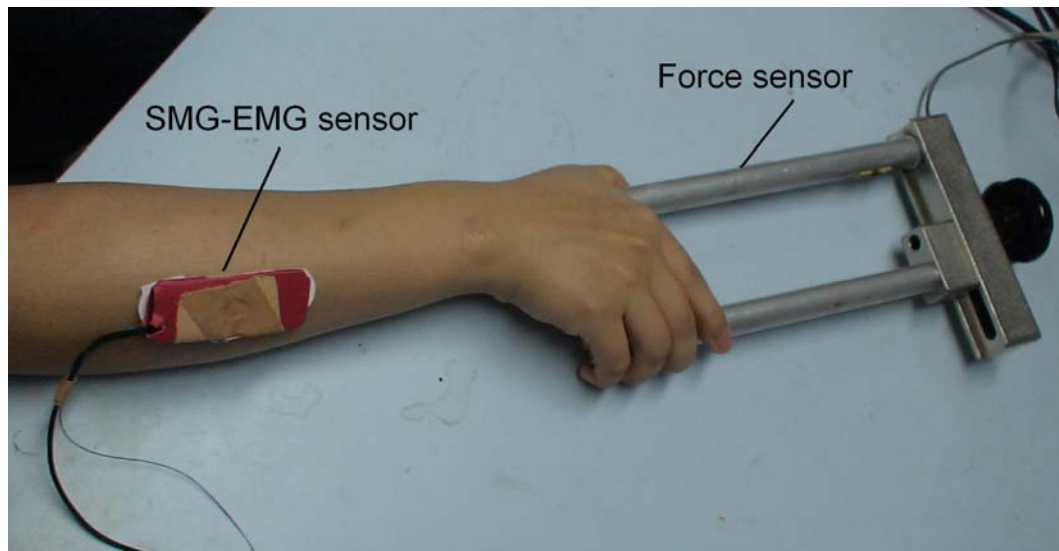


Fig. 3. 7 The ultrasound-EMG compound sensor placed on the belly of the extensor carpi radialis muscle when the subject was performing the force control task. The force of the hand was detected using a custom-made force sensor.

3.3.2.3 Protocol in the Visuomotor “E” Cancellation Test

A similar protocol to that reported by Canderle (2004) was adopted. The protocol comprised a series of one-dimensional visuomotor cancellation tests presented on a computer screen. The set of tests contained two elements, a study of motor control alone and a dual-task study, in which a cognitive load was also explicitly imposed. The cognitive load task was based on the Elevator Counting subset of the Test of Everyday Attention (TEA) (Robertson et al., 1994). Therefore, each subject performed a total of 12 trials, 6 with and 6 without the concurrent TEA test. The 6 trials included using 2 reference signals and SMG and EMG signal under both wrist extension and isometric contraction tests:

- isometric force
- wrist extension

- SMG (during wrist extension)
- SMG (during isometric contraction)
- EMG (during wrist extension)
- EMG (during isometric contraction)

The order of these tasks was randomized prior to the start of each testing session by lucky draw.

In each test, the subject was asked to either perform a wrist extension movement (Fig. 3. 6) or, by using the thumb and fingers in opposition, to apply an isometric, compressive force to a purpose-built force transducer (Fig. 3. 7). In addition to measuring both the wrist movement and applied force directly, muscle activities (either EMG or SMG) during both wrist extension and force application were also collected via a compound EMG-ultrasound sensor located over the easily-accessible extensor carpi radialis muscle. Performances on the visuomotor cancellation tests when using force (isometric contraction) or wrist angle (wrist extension) were considered to be “reference” data, against which subjects’ performance when using each of the other 2 signals (SMG and EMG) as control inputs were judged.

Each test was divided into three parts, including calibration, practice and test (Fig. 3. 8). During the calibration, the system would record the respective maximal and minimal values of the relevant signals (force/angle and EMG or SMG) when the subject was performing either the isometric contraction or wrist extension. As demonstrated in Fig. 3. 9, the minimal value corresponded to the lowest icon (“NEXT”) while 90% of maximum corresponded to the highest icon (“E”). The choice of 90% of maximal value was to reduce the effort required to reach the top icon, thereby avoiding muscle fatigue

during the 90 seconds test. After calibration, the subject could go to the practice part to examine the results of the calibration. If he/she was satisfied with the results of the calibration, the testing would begin; otherwise calibration would be repeated to reset the maximal and minimal values.

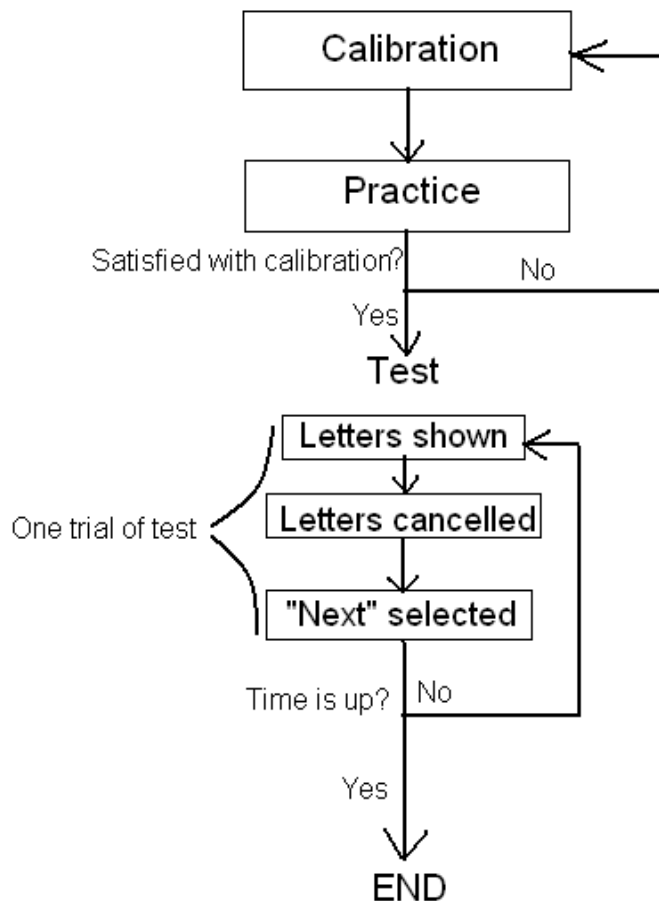


Fig. 3. 8 The diagram of the experimental protocol. Each motor control test was divided into calibration, practice and test. During the calibration, the system recorded the maximal and minimal values of each signal during movements. Then, the subject could go to practice stage to exam the result of calibration. If satisfied with the calibration result, they could begin the test; otherwise, they had to go back to calibration part to reset the maximal and minimal values. There were repeated trials in a test session of 90s.

In both the practice and test sessions, the wrist angle, force, EMG and SMG collected from the extensor carpi radialis muscle were separately used to control the cursor moving on a series of five letters displayed on the computer screen (Fig. 3. 9). The task was to control the cursor to cancel the letter “E”, whenever it appeared on the screen. For example, for the test of SMG control during wrist extension, the vertical position of the cursor was determined by a linear scaling of the SMG signal generated during the wrist extension. Upon appearance of a letter “E”, the subject was asked to move the cursor to the position of this letter and, once the position was reached, a button held in the other hand of the subject was pressed. As a result of the combination of these actions, the letter “E” was cancelled from the screen. After all of the “E”s was cancelled, the cursor was moved to “NEXT” as illustrated in Fig. 3. 9 and a new set of letters appeared on the computer screen. The participants were asked to correctly cancel the letter “E” as many times as possible within a session of 90 seconds. At any time during the test, the subject could select “NEXT”, thereby “skipping” any remaining target letters and moving on to another set of letters. During each test, the number of “E”s correctly cancelled by the subject and the number of letters wrongly cancelled or skipped were recorded automatically by the software.

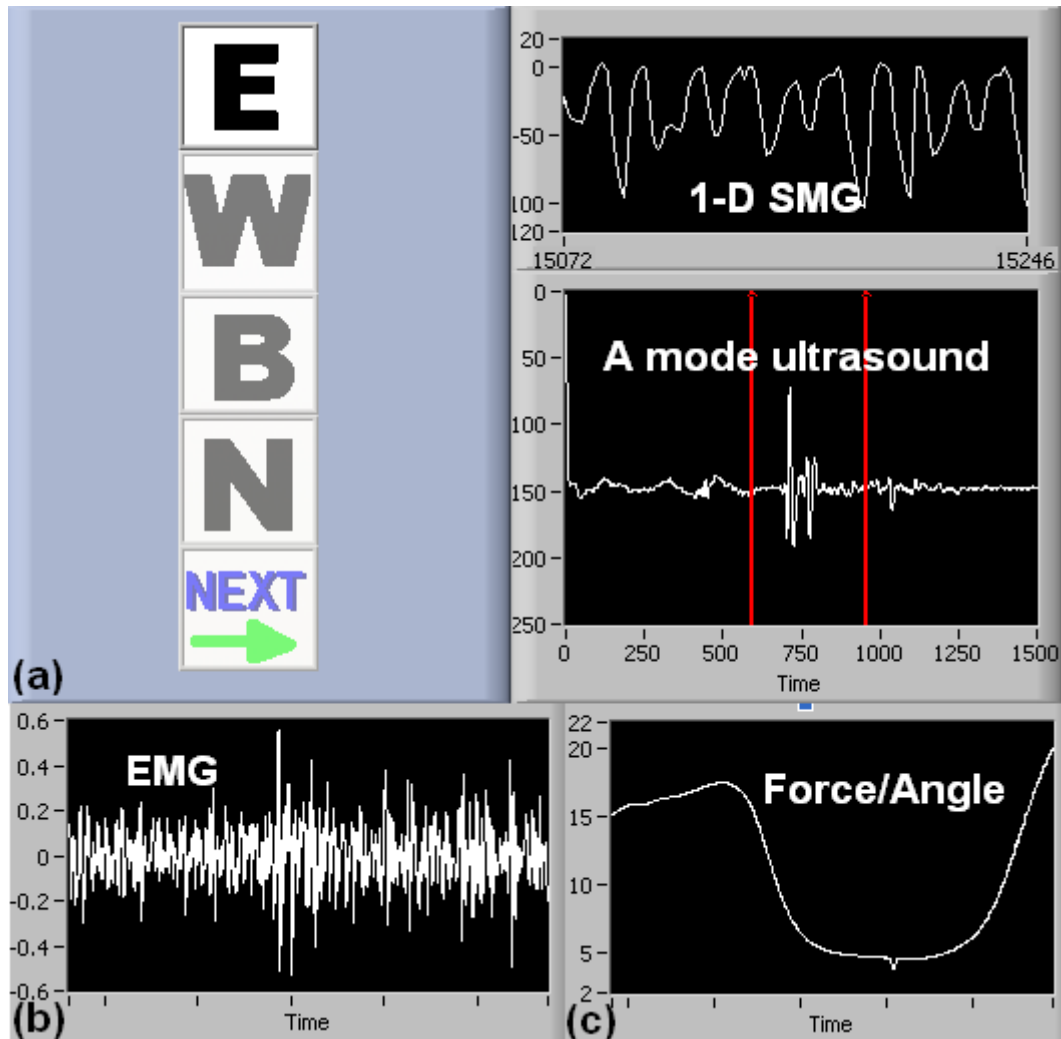


Fig. 3. 9 (a) The software interface used to collect 1D SMG signal. The muscle deformation signal (i.e. SMG) extracted from A-mode ultrasound was displayed for controlling the cursor to cancel the letters. The muscle deformation was measured according to the echo movement reflected from the muscle-bone interface. Window was selected to include the ultrasound echoes. (b) The EMG signal collected from the extensor carpi radialis muscle and EMG RMS was used to control the cursor. (c) The force collected from force sensor or angle detected by electrical goniometer was used to control the cursor.

The set of tests were also repeated while the subjects were asked to concurrently focus on a secondary, sustained attention task, to allow comparison between signals in terms of their cognitive demands. In this test, the subject was presented with a quasi-random

number of sound “bleeps”. The time interval between two neighboring bleeps varied in the range of 3-6 s and was automatically set by the software. The subjects were required to perform the TEA test and letter cancellation test at the same time and the sets of bleeps occurred asynchronously to the letter cancellation task. At the end of the sequence of bleeps, the subject was asked to respond to a question asking how many “bleeps” were given in the previous sequence, the researcher recorded the number, and the next series of bleeps was initiated. The cognitive requirement of each signal was investigated through comparing the results between the dual task and single task (cancellation task alone). The decrement between force/angle signals (the reference) and SMG/EMG in the number of “bleeps” estimated was compared between SMG and EMG signal to demonstrate the different cognitive requirements of the two signals. A greater decrement in counting bleeps was indicative of an increased demand on cognitive resources.

3.3.2.4 Selection of Sampling Rate and Number of Epoch of EMG

Since the sampling rate of 1D SMG for control was 17 Hz, limited by the current system configuration, we used 17 Hz data rate for EMG RMS signal for comparison. The RMS value of the EMG signal was calculated from data points collected over a short time window. A pilot study with 10 healthy subjects was carried out to investigate the effects of different window sizes and sampling rates on the performance in the letter cancellation task using EMG RMS. The effect on the number of letters correctly cancelled was investigated under the sampling rates of 10, 20, 30, 40, 50Hz. The result of the pilot study showed that there was no significant difference in the number of letters correctly cancelled among various sampling rates (one-way ANOVA, $p=0.966$). In addition, the performance based on a 0.2 sec epoch was compared with other epochs.

According to the oral report of the subjects, they could feel an obvious delay when controlling the cursor position using the epochs higher than 0.2 sec to calculate RMS values, such as 0.25 sec and 0.3 sec. On the other hand, it was observed that the number of letters correctly cancelled was significantly higher when using 0.2 sec epoch, compared to 0.1 sec and 0.15 sec epochs, to calculate the EMG RMS (one-way ANOVA, $p=0.016$). Therefore, in our study the 0.2 sec epoch was used to calculate RMS values, which were sampled at 17Hz.

3.3.2.5 Data Analysis

Three-way repeated measure ANOVAs with Least Significant Difference (LSD) pairwise comparisons were used to demonstrate the effects of different signals [Force / Angle vs SMG vs EMG], movement patterns [isometric control vs wrist extension] and types of task [single vs dual] on the number of “E” correctly and wrongly cancelled, i.e., either missed or incorrectly selected letters. The percentage differences of performance were also reported. Linear correlations were used to study the relationship between the performances under single and dual tasks for using SMG and EMG signals. All the data were analyzed using SPSS (Version 15.0, SPSS Inc. Chicago, IL, USA) and statistical significance was set at 5% probability level.

3.3.3 Prosthesis Control by 1D SMG and Surface EMG

3.3.3.1 Subjects

Nine healthy adults, seven males and two females (age: 31 ± 4 years; weight: 67.9 ± 16.7 kg; height: 170.1 ± 9.4 cm), volunteered to participate in the study of prosthetic control by SMG and EMG.

3.3.3.2 Experimental Setup

Hardware Setup

An ultrasound pulser/receiver (model 5052 UA, GE Panametrics, Inc. West Chester, OH, USA) was used to drive a 10 MHz single element ultrasound transducer (model V129, GE Panametrics, Inc., West Chester, OH, USA), and to amplify the received signals. The A-mode ultrasound signal was digitized by a high speed A/D converter card (Gage CS82G, Gage Applied Technologies, Inc, Canada) with a sampling rate of 100 MHz. A prosthetic hand (MH11, Shanghai Kesheng Prostheses Co., Shanghai, China) was controlled to open and close by the analog pulse outputted from an NI DAQ card (NI-DAQ 6024E, National Instruments Corporation, Austin, TX, USA). The prosthetic opening-closure degree, defined by the angle between the middle finger and the back of the hand, was measured by an electronic goniometer (model XM110, Penny & Giles Biometrics, Ltd; Gwent, United Kingdom) attached on the back of the prosthesis (Fig. 3. 10). The collected angle signal was also digitized by the NI DAQ card using the same sampling rate as the frame rate of A-mode ultrasound (17 Hz). The surface EMG signal, captured from the EMG bipolar Ag-AgCl electrodes (Noraxon U.S.A. Inc., USA), was amplified by a custom-designed EMG amplifier with a gain of 1000 and filtered by a 10-400 Hz band-pass analog filter within the amplifier, and then digitized by the same NI DAQ card with a sampling frequency of 1 KHz.

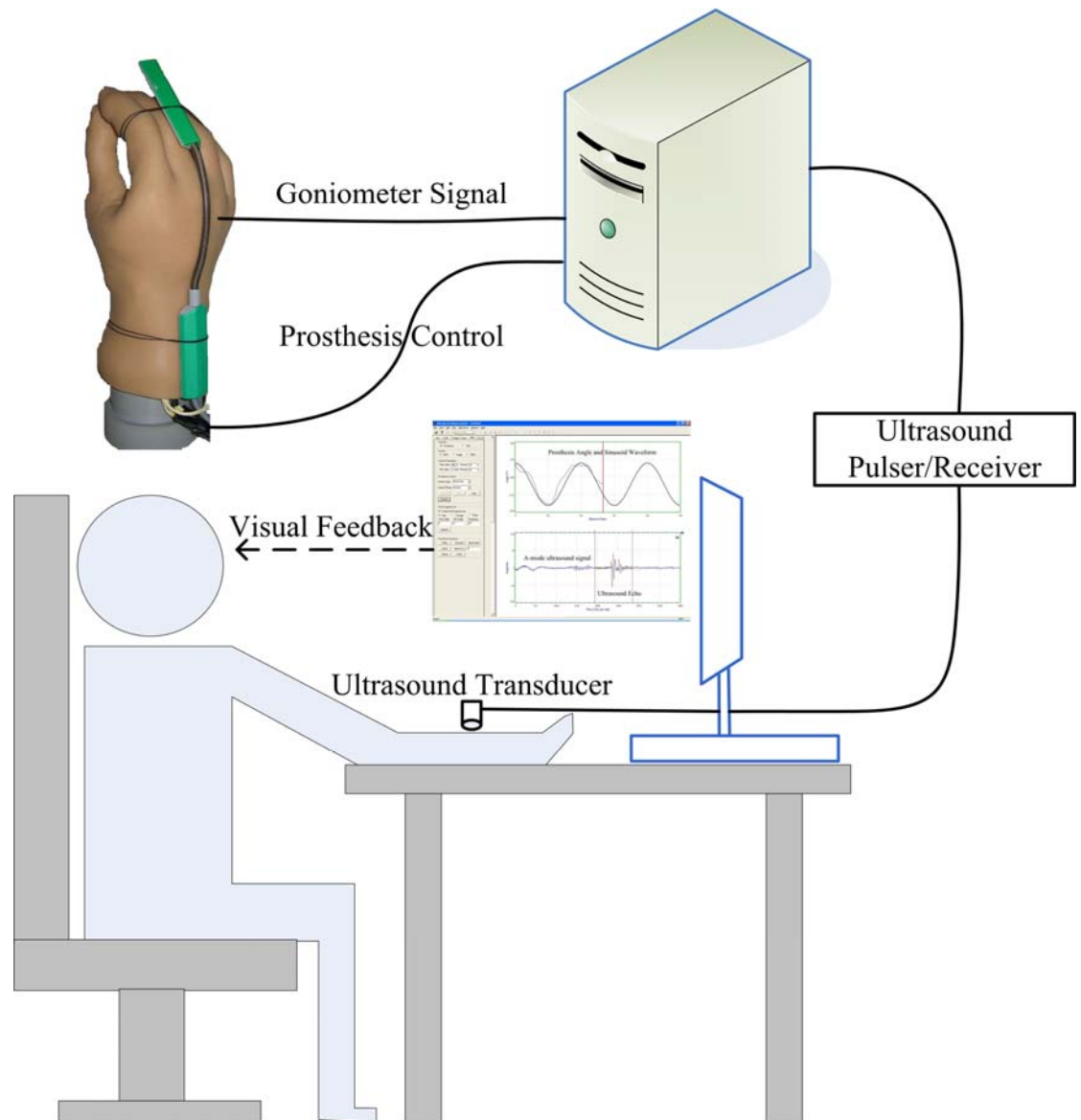


Fig. 3. 10 An illustration of the SMG prosthesis control experiment.

Software Design

The signal acquisition, synchronization, analysis, display, as well as prosthetic control tasks were achieved using custom-designed software UMME developed in Microsoft VC++6.0 platform. Fig. 3. 11 shows the interface of the software developed to capture and process the ultrasound signals. A-mode ultrasound signal was captured frame by frame according to the trigger output of the pulser/receiver. The A-mode ultrasound

echoes reflected from the muscle-bone interfaces were selected by the tracking windows in the first frame. When muscle contracted, the dimensional change induced variations in the distance between the interface of fat-muscle and that of muscle-bone, causing the A-mode ultrasound echo to shift by a certain distance-dependent time-of-flight. To estimate the echo shift in the subsequent frames, we utilized the cross-correlation algorithm to search the segment of signal most similar to the reference echo signal in each frame.

SMG signal was then applied to open and close the prosthesis. The amplitude of the SMG signal was linearly correlated with the opening position of the prosthesis. Once an instantaneous SMG value was extracted from muscle contraction in wrist extension, pulse commands were sent to the prosthetic hand through a DAQ card to drive the hand to the corresponding opening position. The metacarpophalangeal (MCP) joint angle of the middle finger of the prosthesis was measured by a goniometer to evaluate the opening position of the prosthetic hand. Both the angle signal and a pre-designed target track were plotted on the computer screen to give the subject a visual feedback, through which the subject could adjust his/her wrist movements to track the target as accurately as possible (Fig. 3. 11). The software can also collect continuous EMG signal and control the prosthesis with similar interface as shown in Fig. 3. 11. The RMS value was extracted from the EMG signal to control the prosthesis in the same manner as SMG control.

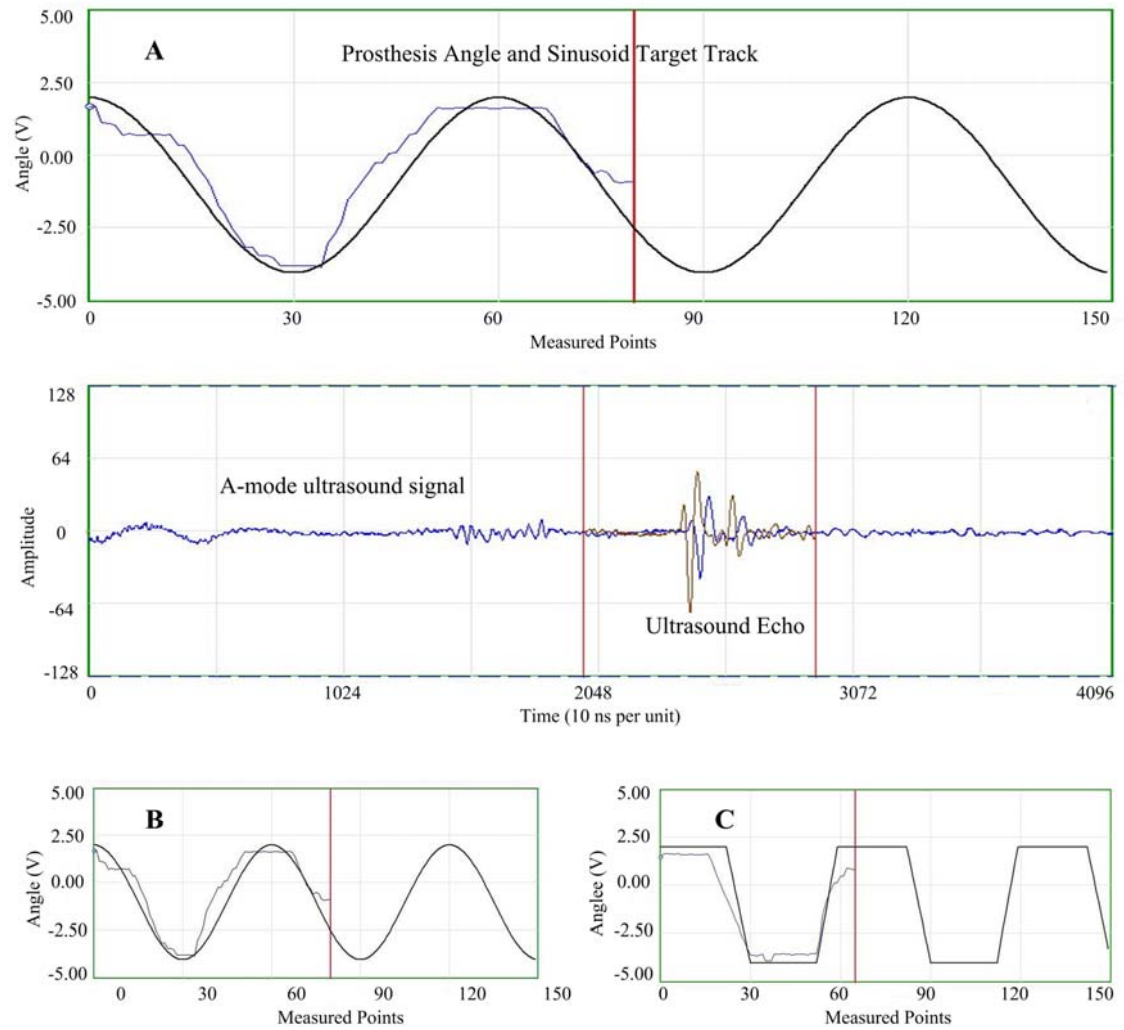


Fig. 3. 11 An illustration of the software interface used to simultaneously collect 1D SMG and goniometer signal and to control prosthesis. (a) The top window illustrates the sinusoidal waveform used to guide the wrist extension movement along with the goniometer signal which represents the prosthesis open-close level. The bottom window shows the ultrasound signal with the selected reference echo used for tracking the muscle thickness change; (b) A typical sinusoid waveform with a rate of 10 cycles/min; (c) A typical square waveform with a rate of 10 cycles/min.

3.3.3.3 Experimental Protocol

The subject sat on a comfortable chair with his/her forearm rested on the table. The computer screen was also placed on the table in front of the subject. Ultrasound-EMG

compound sensor was positioned on the belly of extensor carpi radialis. Double-sided adhesive tape was used to fix the compound sensor, and ultrasound gel was applied between the transducer and skin for better coupling.

Before experiment, the subject was asked to perform several wrist extensions in order to determine prosthetic open-close range according to the maximal and minimal values of muscle deformation. For each task, five repeated trials were performed. The first two were used for training, in which the amplitude of waveform was designed to proportionally correspond to the fully open and close position of prosthetic hand, and the data of the last three trials was collected for further analysis to evaluate the performance.

During the test, the subject was instructed to perform wrist extension and try to match the prosthetic angle signal with the pre-designed guiding waveform. They could adjust the speed of wrist movement to match the prosthetic angle signal with the waveform, i.e., sinusoid or square, which performed as a standard to assess the control performance of SMG and SEMG signals. The sinusoid waveform was employed to investigate the subject's ability to continuously control the prosthesis; while the square waveform was used to study the ability of maintaining the prosthesis at two different stationary levels. The wrist extension movement rates were set to be 4, 6, 10 cycles/min for each guiding waveform. Therefore, each subject performed a total of six tasks (3 x 2) of wrist extension. The accuracy of SMG and surface EMG control was quantified using the RMS tracking error between the guiding waveform and the prosthetic angle.

3.4 Case Study on Amputee

3.4.1 Subject

One male amputee subject (age: 47 years; body weight: 64 kg; height: 168 cm) with bilateral wrist amputation was recruited to validate whether 1D SMG signal was applicable to the limb-deficient person for prosthetic control.

3.4.2 Experimental Protocol

Similar experiment protocol for healthy subjects was applied to the amputee. He was instructed to intend extending his phantom wrist in the tracking guided patterns of wrist extension, visuomotor “E” cancellation, and prosthetic control test as follows.

3.4.2.1 Performances of 1D SMG and Surface EMG in Tracking Guided Patterns of Wrist Extension

The amputee was asked to follow the waveform patterns (sinusoid, square, and triangle) using 1D SMG or surface EMG by intending extending his phantom wrist at the rate of 5 cycles/min and 10 cycles/min. The reason for choosing the slower movement rates was that the amputee has difficulty in following the high rates as used by healthy subjects. Three repeated trials were performed for each task and there was a rest of 3 minutes between two adjacent trials to avoid muscle fatigue. The ultrasound-EMG compound sensor was attached on the extensor carpi radialis muscle of the amputee.

Both 1D SMG and surface EMG signals were tested for their accuracy in following the displayed waveform patterns using RMS tracking error.

3.4.2.2 Comparison of 1D SMG and Surface EMG in Visuomotor “E” Cancellation Test

The amputee as instructed intended extending his phantom wrist to control the cursor in 4 trials including using 1D SMG and surface EMG signal with and without TEA tests:

- 1D SMG
- 1D SMG (with TEA test)
- EMG
- EMG (with TEA test)

The order of these tasks was randomized. Because the amputee is with bilateral wrist amputation, a pedal foot switch was used instead of a button (Fig. 3. 12).

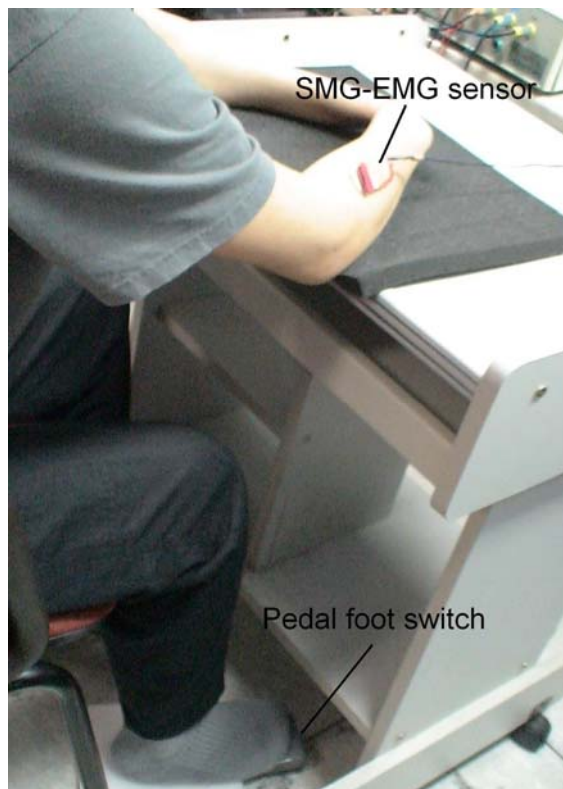


Fig. 3. 12 A pedal foot switch was utilized for the amputee with bilateral wrist amputation to make decision during visuomotor “E” cancellation test.

3.4.2.3 Prosthesis Control by 1D SMG and Surface EMG

During the test, the amputee was instructed to intend extending his phantom wrist and try to match the prosthetic angle signal with the pre-designed guiding waveform. Compared with the healthy subjects, the amputee has difficulty in following the pattern at the rate of 10 cycles/min. Therefore, only 4, 6 cycles/min were tested in this study. During the trial, the amputee could adjust the speed of wrist movement to match the prosthetic angle signal with the waveform, i.e., sinusoid or square. Therefore, there were a total of 6 tasks (2 x 2 x 2). The accuracy of SMG and surface EMG control was quantified using the RMS tracking error between the guiding waveform and the prosthetic angle.

CHAPTER 4 RESULTS

In this chapter, the main findings are presented, including the linear relationship between 1D SMG and wrist extension angle; SMG -based wrist angle prediction; the comparisons of the control performances of the subjects using 1D SMG and surface EMG in tracking guided patterns of wrist extension, visuomotor “E” cancellation and prosthetic control tasks. Finally, the result of the control performance of the amputee using 1D SMG signal is given.

4.1 Muscle Thickness Change Detected by 1D SMG

4.1.1 The Relationship between Muscle Deformation (SMG) and Wrist Angle

Fig. 4. 1 shows the muscle deformation and the wrist extension angle of a typical trial obtained from subject C at the rate of 30 cycles/min. The three cycles indicated the three repeated wrist extension cycles in a single trial. The ascending part of each cycle corresponded to the muscle contracting action and the descending portion corresponded to the muscle relaxing stage. It was found that on subject C the muscle deformation correlated very well with the wrist extension angle with the correlation coefficient $r = 0.940$ using a linear regression in Fig. 4. 2. The experimental data obtained from the other subjects showed a similar trend and the overall mean r value for the nine subjects was 0.907 ± 0.077 (mean \pm S.D.).

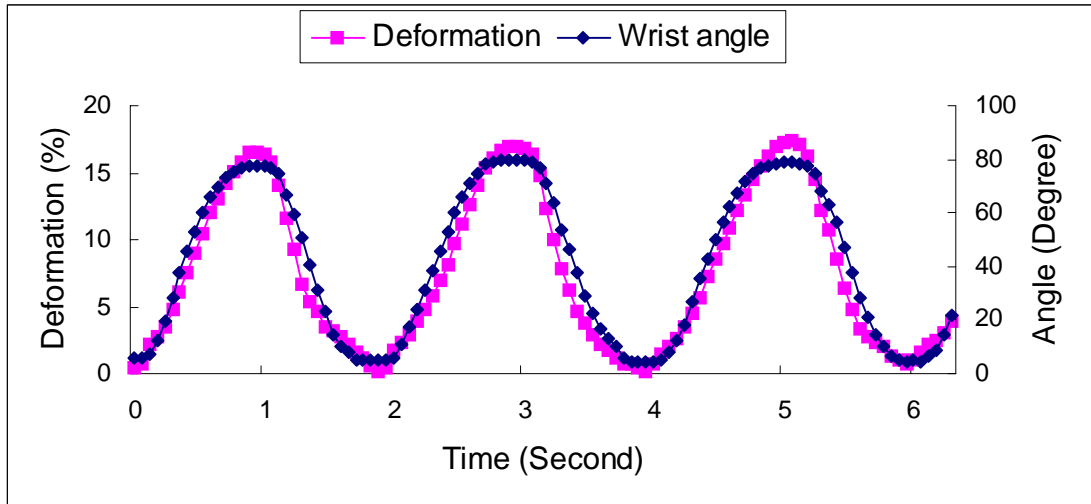


Fig. 4. 1 The muscle deformation and the wrist extension angle of a typical trial with three cycles of wrist extension of subject C at the rate of 30 cycles/min.

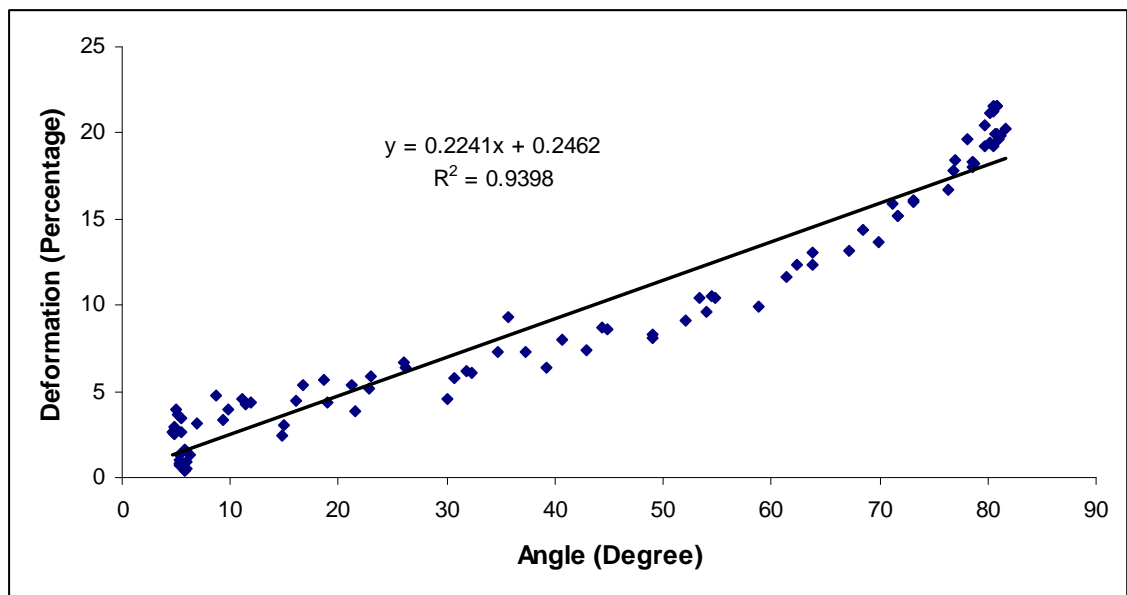


Fig. 4. 2 The relationship between the percentage of muscle deformation and wrist extension angle of the trial shown in Fig. 4. 1. The linear regression was used to represent the correlation between the two signals.

The relationship between the wrist extension angle and the corresponding muscle deformation was further studied using their ratio, i.e. the slope of the linear regression in

Fig. 4. 2. The overall mean value of the angle-deformation ratio was $0.130 \pm 0.058\%$ per degree. One-way ANOVA revealed that the ratios were significantly ($P < 0.001$) different among the subjects but not among the trials under different extension rates for each subject ($P = 0.9$). Fig. 4. 3 and Table 4. 1 show the summary of the ratios of the muscle deformation and the wrist angle for individual subjects at different extension rates. The intraclass correlation coefficient (ICC) for the three repeated trials was 0.87, indicating a good repeatability.

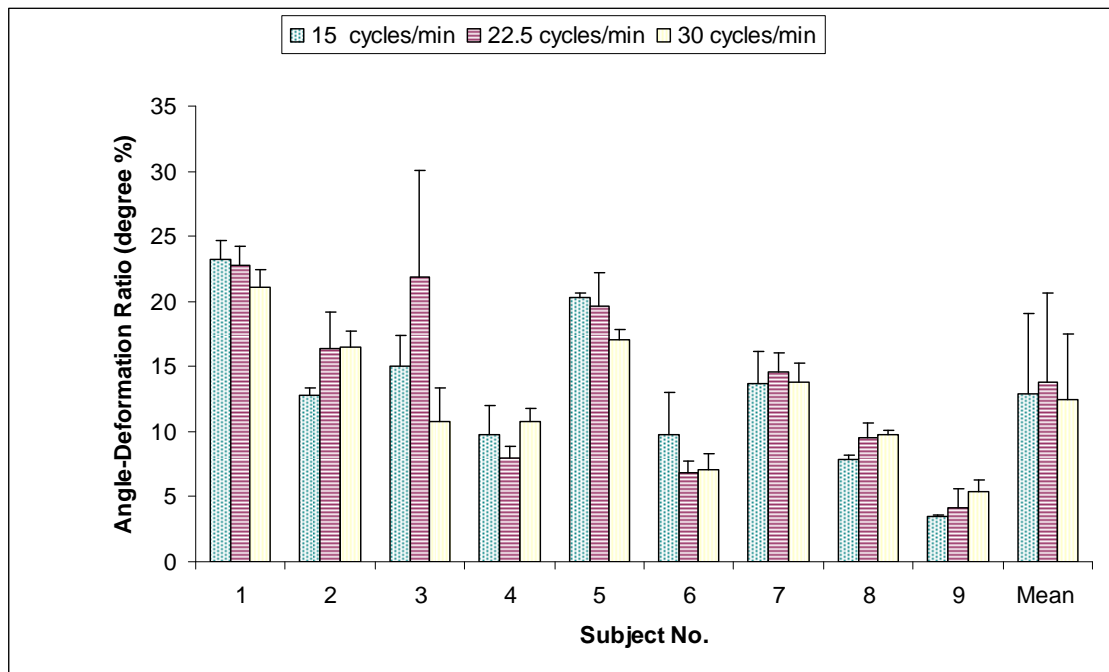


Fig. 4. 3 The ratios between the muscle deformation and the wrist angle for the nine subjects (1-9) under different extension rates. The error bar represents the standard deviation of the results of the three trials for each subject at each rate. The last bar (mean) represents the overall mean and standard deviation of the results of the nine subjects.

Table 4. 1 The mean and standard deviations (STDEV) of the ratio between muscle deformation and wrist extension angle among the nine subjects. The results were calculated from the data obtained under three different rates of wrist extension.

<i>Subject No.</i>	<i>1</i>	<i>2</i>	<i>3</i>	<i>4</i>	<i>5</i>	<i>6</i>	<i>7</i>	<i>8</i>	<i>9</i>
<i>Mean of ratio (%/degree)</i>	0.224	0.152	0.159	0.095	0.190	0.079	0.140	0.090	0.043
<i>STDEV of ratio (%/degree)</i>	0.011	0.021	0.056	0.014	0.017	0.016	0.004	0.010	0.010

4.1.2 Relationship between Surface EMG RMS and Wrist Angle

Fig. 4. 4 shows a typical relationship between the EMG RMS and the wrist angle obtained from subject C at the extension rate of 30 cycles/min. The relationship could also be represented by a linear regression with the correlation coefficient $r = 0.832$ (Fig. 4. 5). The results obtained from the other subjects showed a similar trend. The mean r value of the tests for all the subjects was 0.864 ± 0.071 . The relationship between the EMG RMS and the wrist angle showed poorer correlation in comparison with that between the SMG and the wrist angle.

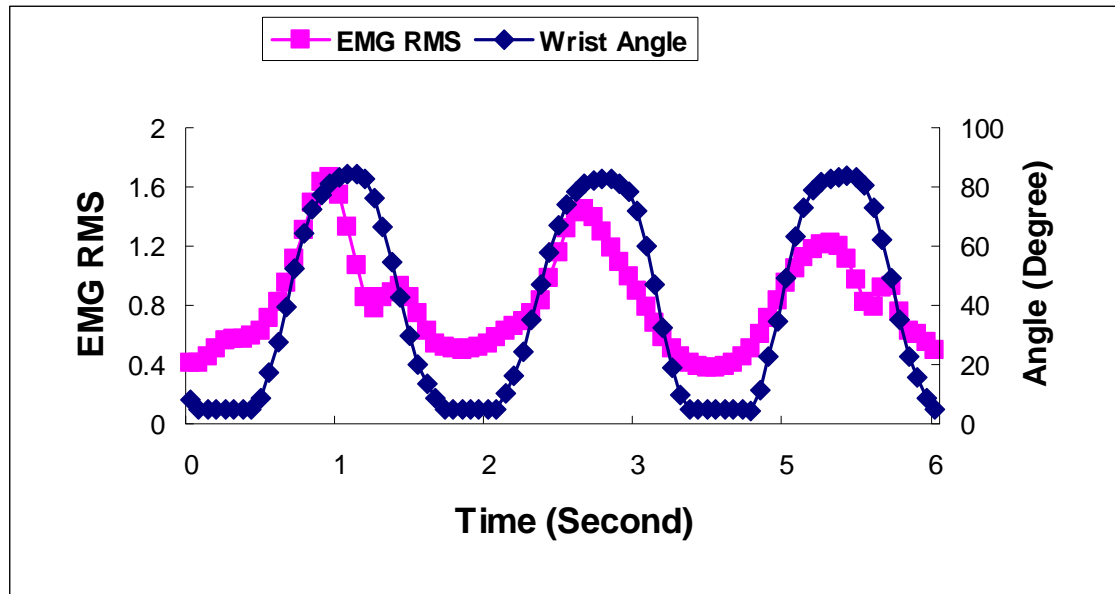


Fig. 4. 4 The EMG RMS and the wrist extension angle of a typical trial with three cycles of wrist extension of subject C at the extension rate of 30 cycles/min.

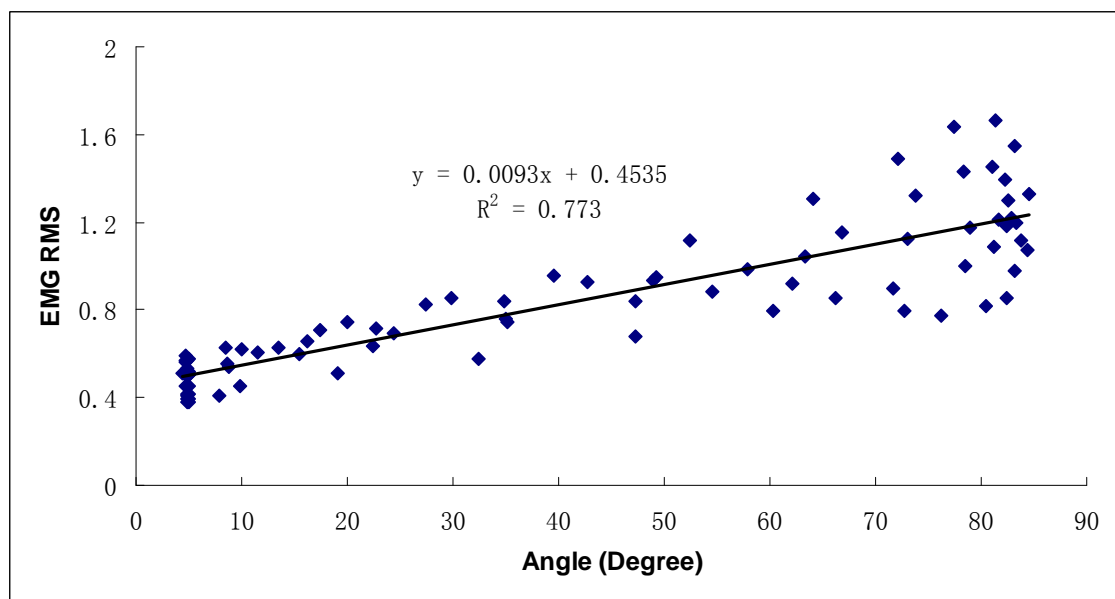


Fig. 4. 5 The relationship between the EMG RMS and the wrist extension angle of the trial shown in Fig. 4. 4. The two signals were also found to be linearly correlated.

4.2 SMG-Based Wrist Angle Estimation

4.2.1 RMSD and CC of SVM, BP and RBF ANN

The examples of measured wrist angle signal and the signal predicted by SVM, BP ANN and RBF ANN for subject C at the extension rates of 15, 30 cycles/min were displayed in Fig. 4. 6 and Fig. 4. 7, respectively.

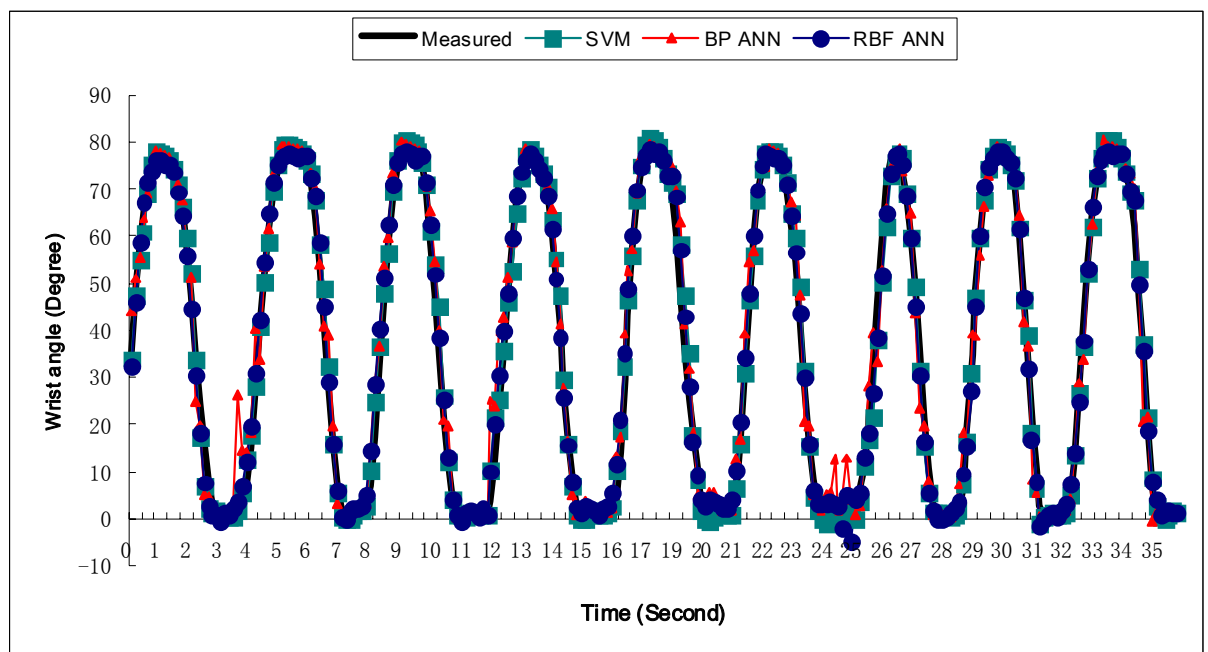


Fig. 4. 6 Comparison of the predicted and measured wrist angles at the extension rate of 15 cycles/min by LS-SVM, BP ANN and RBF ANN.

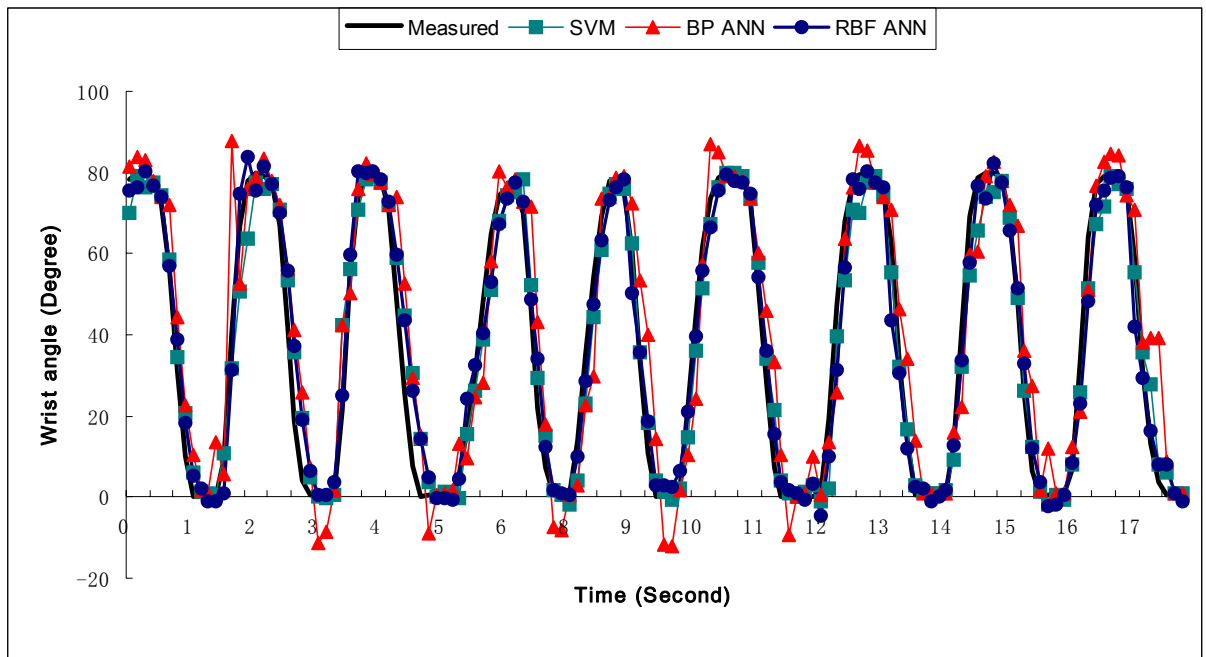


Fig. 4. 7 Comparison of the predicted and measured wrist angles under the extension rate of 30 cycles/min by LS-SVM, BP ANN and RBF ANN.

The averaged RMSD and CC among the nine subjects for different extension rates were shown in Fig. 4. 8 and Fig. 4. 9.

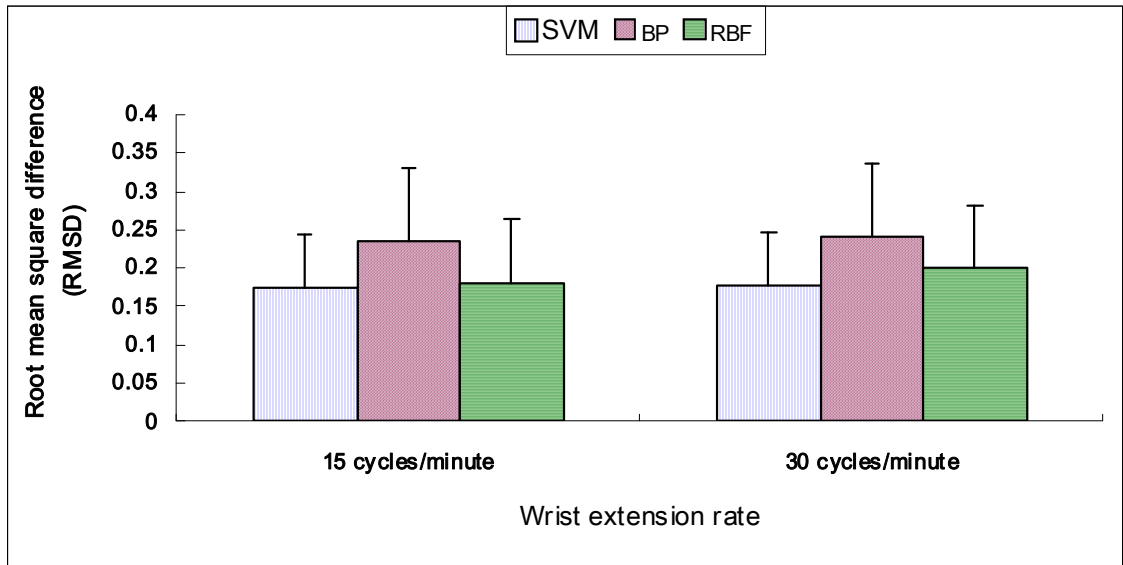


Fig. 4. 8 The mean and standard deviation of prediction RMSD of the nine subjects at extension rates of 15, 30 cycles/min, by LS-SVM, BP ANN and RBF ANN.

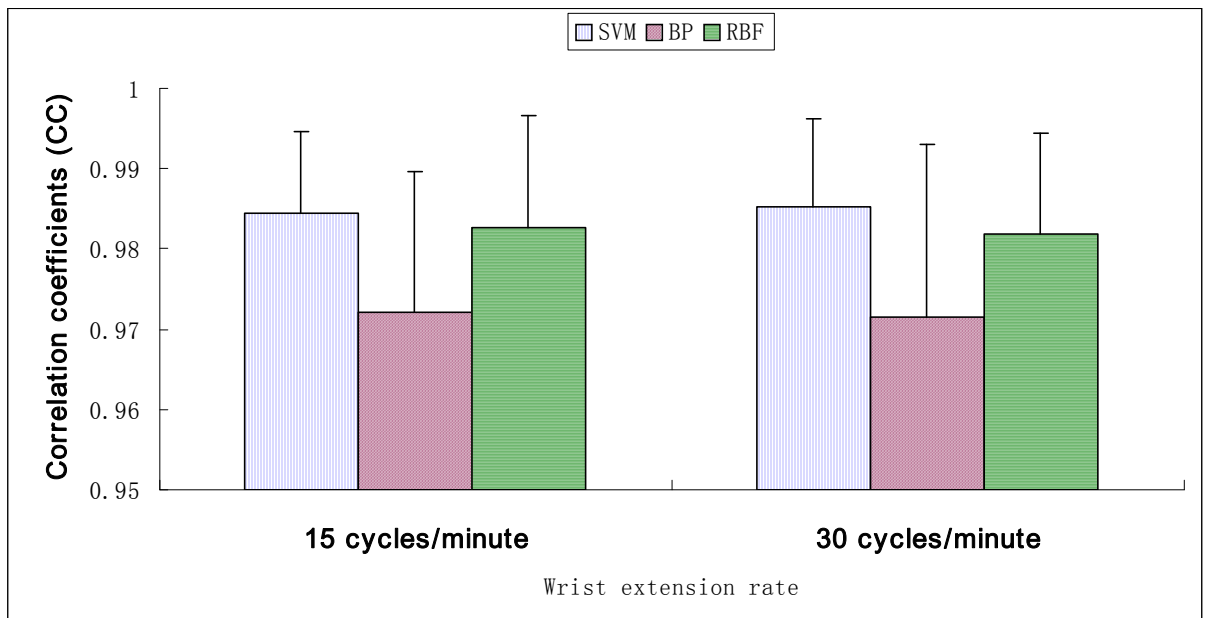


Fig. 4. 9 The mean and standard deviation of prediction CC of the nine subjects at 15, 30 cycles/min extension rate by LS-SVM, BP ANN and RBF ANN.

It was found that the mean of CC of the three models for each test condition was all larger than 0.9, with LS-SVM having the highest CC among all test conditions, followed by RBF and BP ANN. Moreover, the mean of RMSD of LS-SVM at the three different extension rates was smaller than those of BP and RBF ANN. The results revealed that LS-SVM had better generalization power compared with BP and RBF ANN for the wrist angle prediction, though they all showed good learning power during the training. It was also demonstrated that the models established for the rate of 22.5 cycles/min could be used for the prediction of wrist angle from SMG data set obtained under other rates. Statistical analysis showed that only different models affected the RMSD and CC significantly ($p = 0.018$ and $p = 0.021$). Both LS-SVM and RBF ANN achieved significantly higher prediction accuracy in term of RMSD and CC as compared with BP ANN (both $p < 0.05$), while no significant difference between BP ANN and LS-SVM methods was observed ($p = 0.05$).

4.3 Performance of 1D SMG and Surface EMG in Tracking Guided Patterns of Wrist Extension

4.3.1 Comparison in RMS Tracking Error between 1D SMG and Surface EMG among Various Guiding Waveforms

Totally 432 data sets were recorded from the sixteen subjects. Table 4. 2 summarizes the RMS tracking error of 1D SMG and surface EMG for the three guiding waveform patterns under different movement rates. The overall mean RMS tracking error of SMG under the three movement rates was $18.9 \pm 2.6\%$ (mean \pm S.D.), $18.3 \pm 4.5\%$, and $17.0 \pm 3.4\%$ for the sinusoid, square, and triangle guiding waveforms, while the corresponding value for EMG was $30.3 \pm 0.4\%$, $29.0 \pm 2.7\%$, and $24.7 \pm 0.7\%$,

respectively. Paired t-test revealed that the overall mean RMS tracking error of SMG was significantly ($P < 0.01$) smaller than that of EMG for all the three guiding waveforms (Fig. 4. 10).

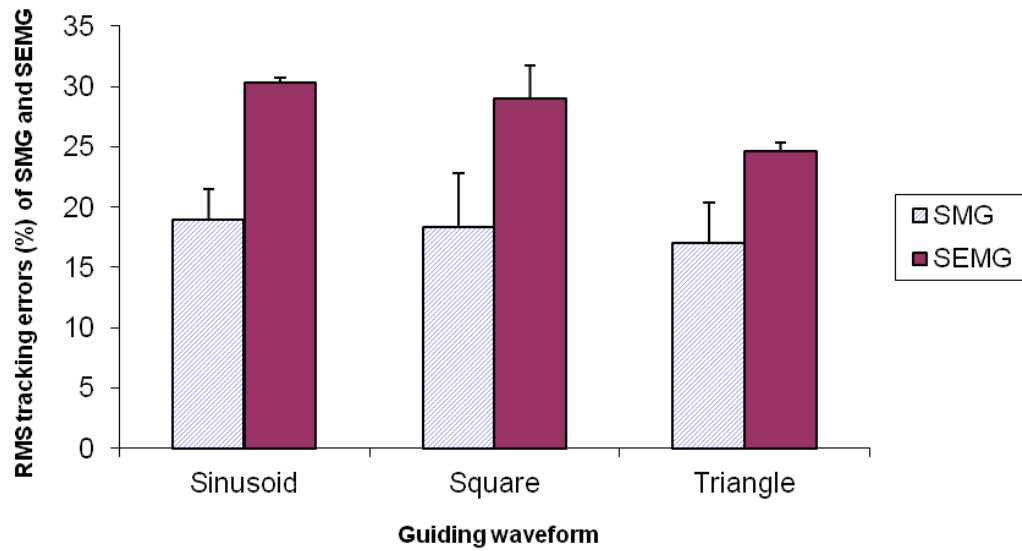


Fig. 4. 10 The RMS tracking error (%) of 1D SMG and surface EMG for the different guiding waveforms. The error bar represents the standard deviation of the results obtained at three different movement rates.

Table 4. 2 The RMS tracking error (%) between 1D SMG/surface EMG and the guiding waveforms at the three movement rates (Mean \pm S.D.) and the mean RMS tracking error averaged over the three movement rates for sinusoid, square, and triangle guiding waveforms.

<i>Rate</i> (Cycles/min)	<i>SMG</i>			<i>Surface EMG</i>		
	<i>sinusoid</i>	<i>square</i>	<i>triangle</i>	<i>sinusoid</i>	<i>square</i>	<i>triangle</i>
20	16.3 \pm 7.8	14.6 \pm 1.7	14.0 \pm 1.9	30.5 \pm 4.7	27.0 \pm 4.2	24.2 \pm 4.4
30	19.0 \pm 3.0	17.1 \pm 1.6	16.3 \pm 2.5	29.9 \pm 6.4	27.8 \pm 3.0	24.4 \pm 6.3
50	21.5 \pm 3.2	23.3 \pm 3.7	20.7 \pm 3.1	30.6 \pm 5.5	32.1 \pm 4.1	25.4 \pm 4.8
<i>Mean</i>	18.9 \pm 2.6	18.3 \pm 4.5	17.0 \pm 3.4	30.3 \pm 0.4	29.0 \pm 2.7	24.7 \pm 0.7

4.3.2 RMS Tracking Error of 1D SMG/surface EMG for Three Guiding Waveforms under Different Movement Rates

One-way ANOVA showed that there were significant differences in the RMS tracking error of 1D SMG among the three wrist extension rates (all $p < 0.01$) for all the three guiding waveforms as demonstrated in Fig. 4. 11. An apparent increasing trend of the RMS tracking error using SMG was observed with the increase of the movement rate for all the different guiding patterns. However, for EMG, statistical analysis revealed that the RMS tracking error was significantly different among the three movement rates only for the square waveform ($P=0.001$), but not for sinusoid ($P=0.921$) and triangle ($P=0.762$) waveforms. As shown in Fig. 4. 12, the RMS tracking error for EMG generally showed smaller variations under different rates of wrist extension.

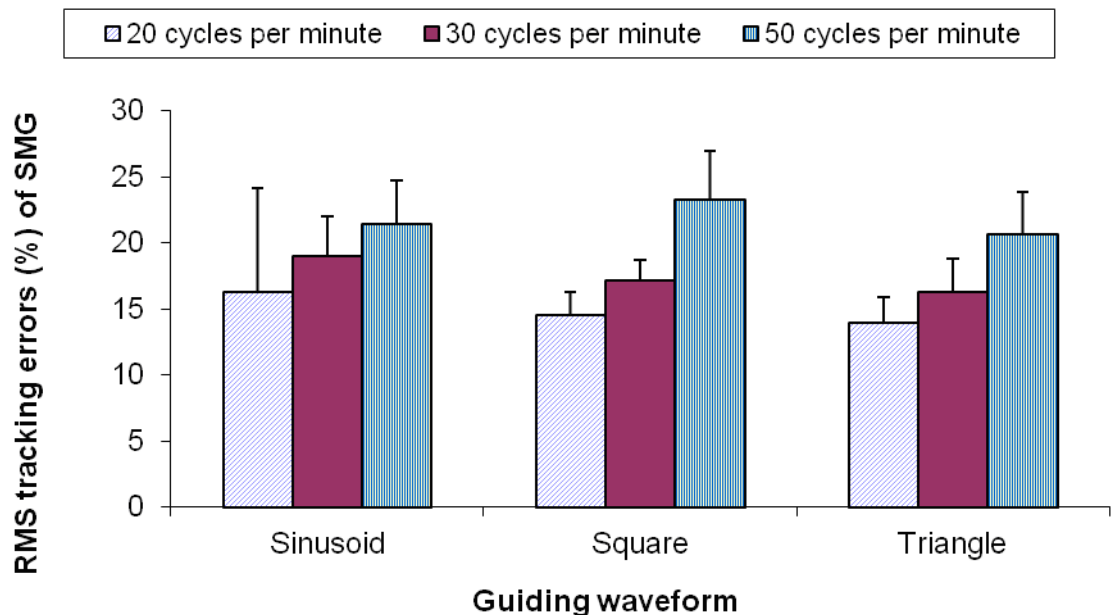


Fig. 4. 11 The tracking errors of SMG for the three guiding waveforms under different movement rates. The error bar represents the standard deviation of the results of the sixteen subjects.

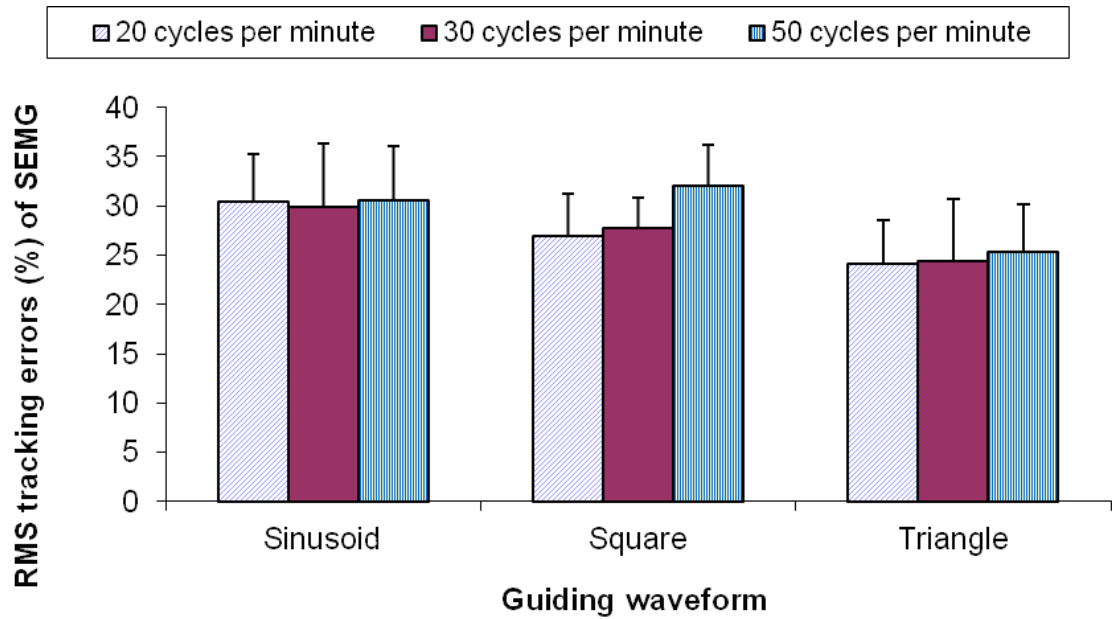


Fig. 4. 12 The RMS tracking error of surface EMG under the three different wrist extension rates for various guiding waveforms. The error bar represents the standard deviation of the results obtained from the sixteen subjects.

4.4 Comparison of 1D SMG and Surface EMG in Visuomotor “E” Cancellation Test

Table 4. 3 shows the result of “E” canceling for the single and dual tasks together with the number of bleeps counted by the subjects during the dual task test. It was found that only the signal type had significant effect on the number of “E” successfully and wrongly cancelled (all $p < 0.001$) and that the force/angle signals in the corresponding tests provided significantly better performance than SMG and EMG signals for both single and dual task tests, in terms of the number of “E” successfully cancelled (all $p < 0.001$), and there was no significant difference in the performance of successfully cancelling “E” between SMG and EMG ($P=0.081$). However, a significant increase in the number of “E” wrongly cancelled was observed when using the EMG signal in

comparison with using force/angle and SMG signals in both the single and dual task tests (both $p < 0.001$) and no such significance was found between using SMG and force/angle signals ($p = 0.791$).

Table 4. 3 The number of “E” correctly cancelled or that of letters wrongly cancelled in a period of 90 sec using different signals and under conditions of wrist movement and isometric contraction for both single and dual tasks. The number of bleeps counted by the subjects during the dual task test was also included.

Task	Item	Isometric force control						Wrist extension					
		Force		SMG		EMG		Angle		SMG		EMG	
		C	W	C	W	C	W	C	W	C	W	C	W
Single task	<i>E cancel mean</i>	48	7	35	7	29	18	44	8	34	7	30	23
	<i>SD</i>	7	4	10	5	13	6	10	5	9	4	13	14
Dual task	<i>E cancel mean</i>	47	8	34	8	30	23	45	6	32	7	31	21
	<i>SD</i>	10	5	9	7	9	7	8	3	9	3	8	10
	<i>Bleep count</i>	16	1	15	1	17	1	13	1	16	1	15	1
	<i>SD</i>	3	1	3	1	2	1	2	1	2	2	3	1

* C represents the number of “E” correctly cancelled or the number of bleeps correctly counted. W represents the number of the letters wrongly cancelled, either “E” was skipped or a wrong letter was cancelled, or the number of bleeps wrongly counted.

The result of the single task showed that the number of *successfully* cancelled “E” using SMG decreased by $27 \pm 15\%$ and $21 \pm 11\%$ in isometric contraction and wrist extension tests, in compared with using force and angle signal, while the corresponding reduction recorded by using EMG was $37 \pm 29\%$ and $31 \pm 23\%$, respectively, but the difference in decrements between the two signals was not significant ($p = 0.15$). Meanwhile, using SMG generated significantly lower number of “E” *wrongly* canceled than using EMG

for both isometric contraction ($p=0.0005$) and wrist extension ($p=0.006$) controls. Similar result was obtained in the dual task test (Table 4. 3).

Statistical analysis also revealed that there was no significant difference in the performances of cancelling “E” between the single and dual tasks among the control signals, i.e. force/angle, SMG and EMG signals (all $p>0.2$). In addition, it was found that the number of bleeps correctly counted by the subjects was very close (15.3 ± 1.4 bleeps) in all the tests. As shown in Table 4. 3, the number of wrongly counted bleep was very small ($5 \pm 1\%$) with small variations among different situations using different signals. The result tended to show that the signals tested had similar control performance in the TEA test in this study. Further analysis revealed that there was no significant difference between SMG and EMG regarding the percentage reduction in the number of “E” correctly cancelled ($p=0.07$) or the percentage increase of the number of “E” wrongly cancelled ($p=0.17$) caused by the change from the single to dual task. We further studied the correlation between the numbers of “E” correctly cancelled in the single and dual task tests for both SMG and EMG control. As shown in Fig. 4. 13, the numbers of “E” correctly cancelled by using SMG under the single and dual tasks showed a much higher correlation in comparison with those using EMG.

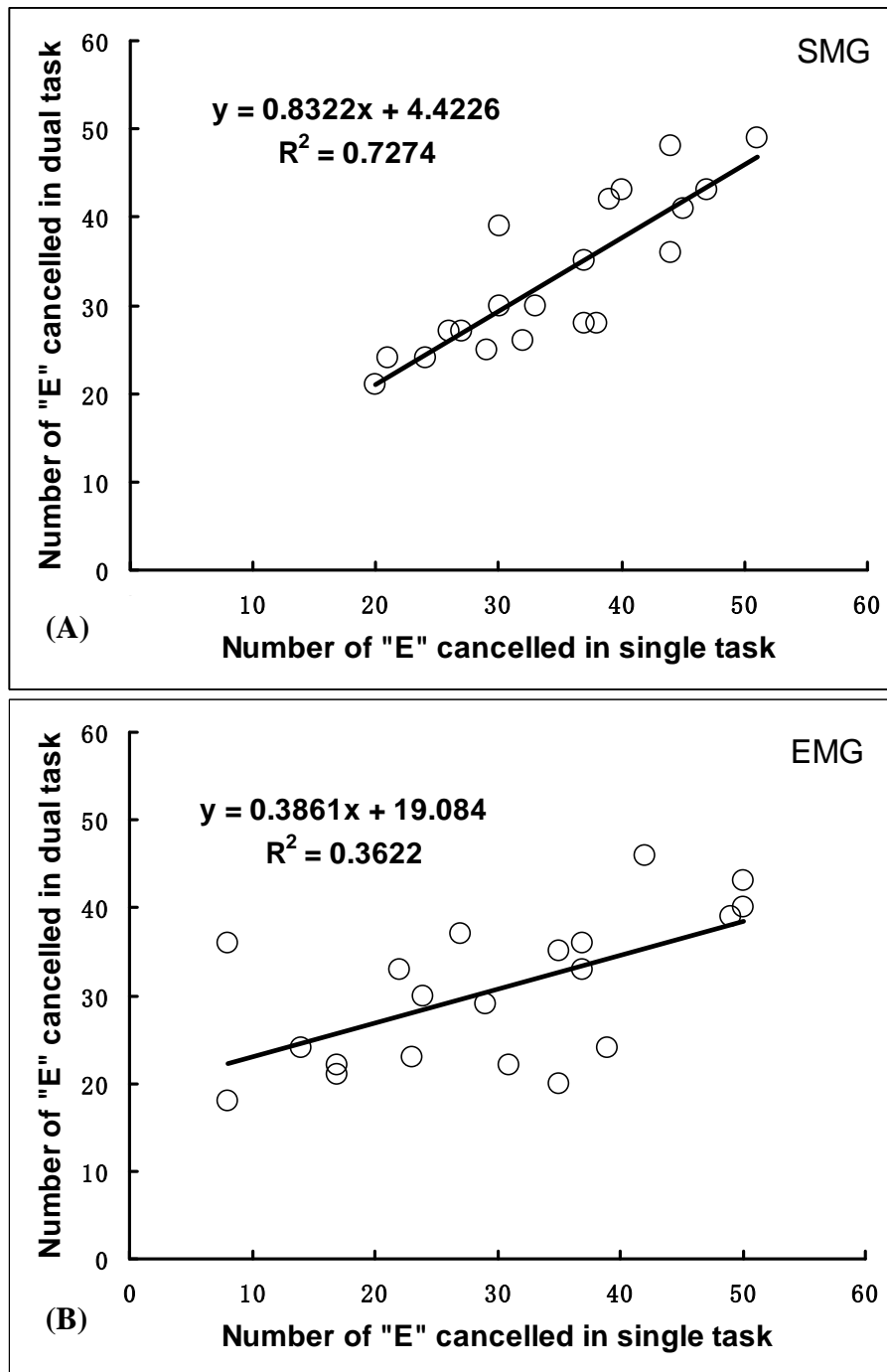


Fig. 4. 13 Correlations between the numbers of "E" correctly cancelled in 90s under the single and dual tasks when (a) SMG and (b) EMG were used as control signals, respectively.

4.5 Comparison of 1D SMG and Surface EMG in Prosthetic Control

Table 4. 4 summarizes the RMS tracking error of 1D SMG and surface EMG for the two guiding waveform patterns under three different movement rates. The overall mean RMS tracking error of SMG under the three movement rates was $12.8 \pm 3.2\%$ (mean \pm S.D) and $14.8 \pm 4.6\%$ for the sinusoid and square guiding waveforms, while the corresponding values for EMG were $24.1 \pm 4.9\%$ and $22.9 \pm 5.5\%$, respectively. The overall mean RMS tracking error of each subject for all the movement rates and waveform patterns are shown in Fig. 4. 14. Paired t-test showed that the RMS tracking error by SMG control was significantly smaller than that of surface EMG control ($p < 0.05$). For SMG control, it was observed that both the wrist extension rate and the guiding waveform pattern had significant effects ($p = 2.0 * 10^{-6}$ for extension rate and $p = 0.007$ for guiding waveform pattern) and their interaction effect was also significant ($p = 0.02$). However for EMG control, neither the factor had significant effect ($p = 0.059$ for extension-flexion rate and $p = 0.27$ for guiding waveform pattern).

Table 4. 4 The RMS percentage tracking errors of 1D SMG and surface EMG between the prosthesis angle and the guiding waveform at the three movement rates (Mean \pm S.D.) and the mean RMS tracking error averaged over the three movement rates for sinusoid and square guiding waveforms.

<i>Rate</i> (Cycles/min)	<i>SMG</i>		<i>EMG</i>	
	<i>sinusoid</i>	<i>square</i>	<i>sinusoid</i>	<i>square</i>
4	11.2 \pm 2.4	10.9 \pm 2.2	21.1 \pm 3.5	22.2 \pm 6.9
6	13.5 \pm 3.4	15.3 \pm 4.0	25.6 \pm 6.0	22.2 \pm 4.6
10	13.8 \pm 3.0	18.3 \pm 3.8	25.6 \pm 3.3	24.2 \pm 4.3
<i>Mean</i>	12.8 \pm 3.2	14.8 \pm 4.6	24.1 \pm 4.9	22.9 \pm 5.5

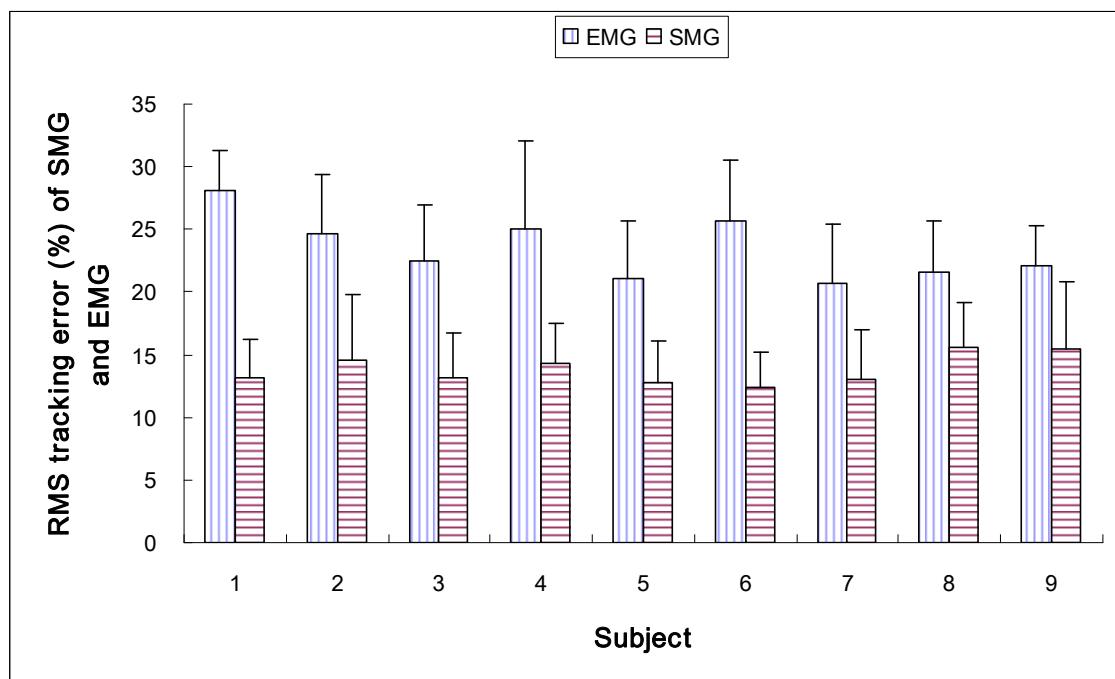


Fig. 4. 14 The overall mean RMS tracking error of SMG and surface EMG for each subject for all the movement rates and waveforms. The error bar represents the standard deviation from the mean.

Fig. 4. 15 illustrates a typical data set of the 1D SMG signal and the angle signal in one trial (the movement rate or input signal frequency is 4 cycles/min). The left Y-axis represents the SMG signal, i.e. the muscle deformation in percentage, while the right Y-axis indicates the prosthesis angle normalized to the maximal angle at full opening position. The X-axis indicates the measurement time in seconds. The input-output relationship was constructed by plotting the instantaneous angle values as the function of SMG values. Linear regression was applied and R^2 coefficient was obtained to characterize the linearity of the relationship (Fig. 4. 16). Fig. 4. 17 shows the R^2 coefficients of all the nine subjects under different movement rates, with the error bar representing the standard deviation (S.D.) of the three trials for each subject, and the relationship between R^2 and movement rate was further plotted in Fig. 4. 18. One-way ANOVA was used to test the effect of movement rate on the linearity. It was found that the rate had significant effect ($p = 4.7 \times 10^{-8}$). There was an obvious trend of decrease of R^2 value with the increase of movement rate.

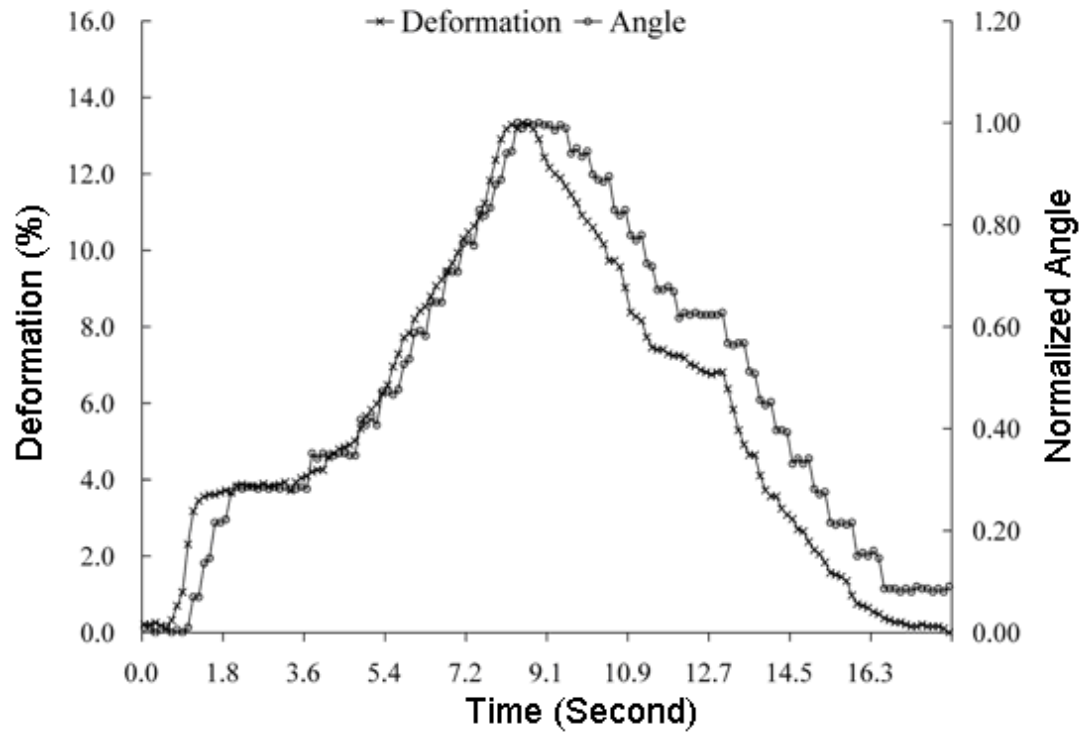


Fig. 4. 15 Plots of muscle deformation (SMG) and angle curves as function of time in one trial. The left Y-axis indicates the SMG signal, while the right Y-axis represents the prosthesis angle normalized to the maximal angle at full opening position.

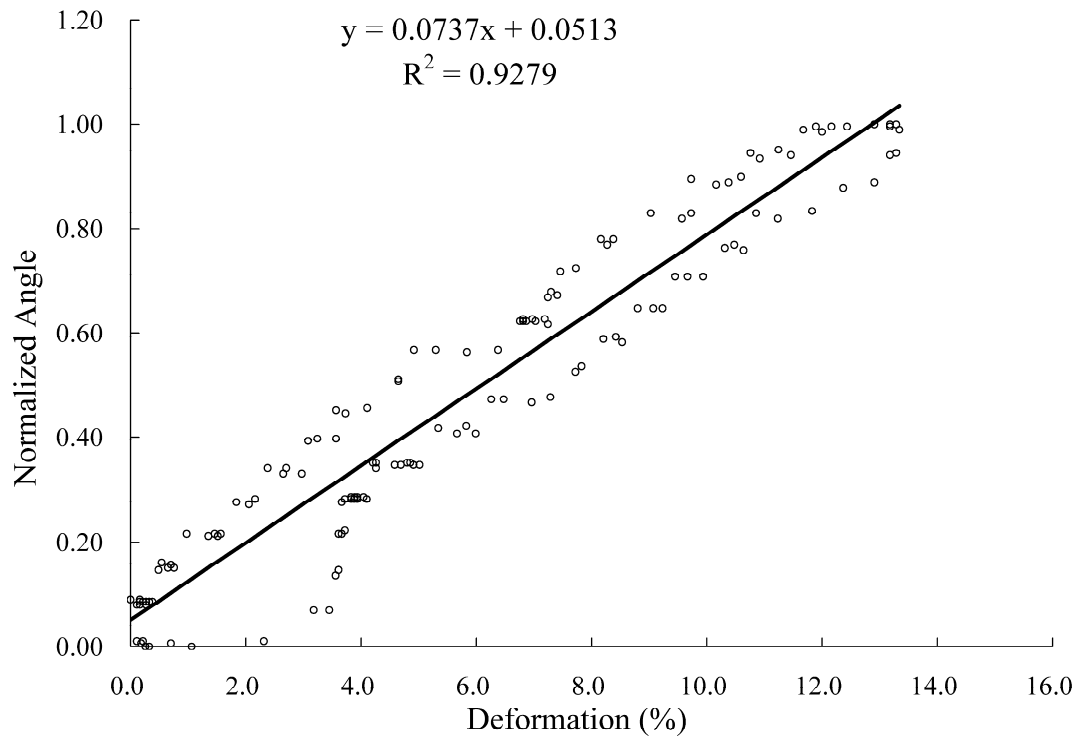


Fig. 4. 16 The input-output relationship of the prosthetic control system where the input was the SMG signal, and the output was the prosthesis opening position represented by goniometer angle. Linear regression was applied to indicate their relationship.

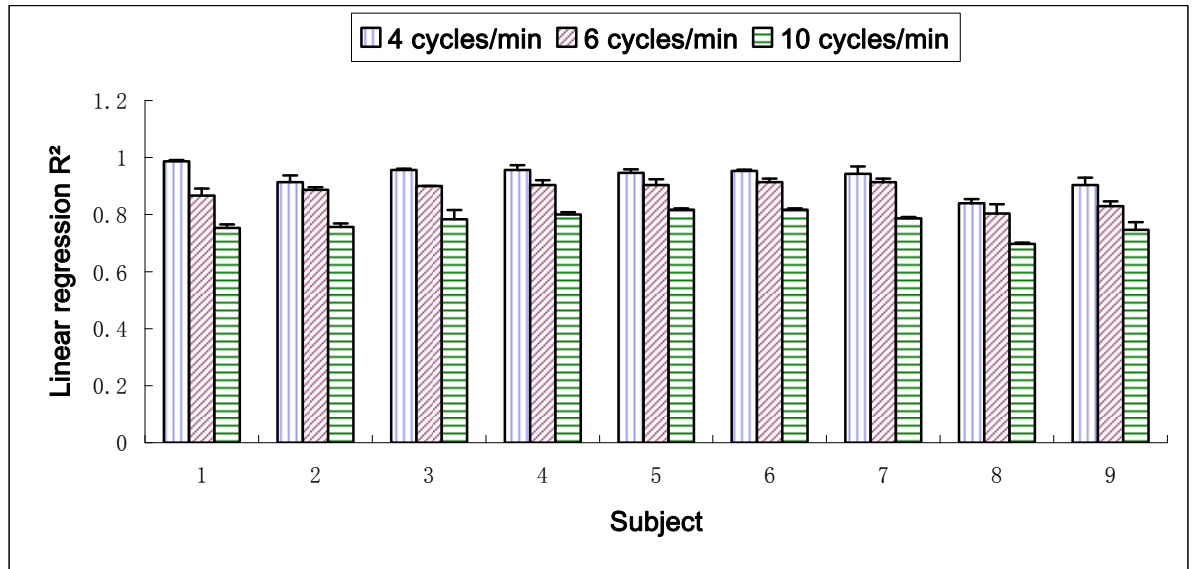


Fig. 4. 17 The R^2 values of linear regression for each subject under three movement rates. The error bar represents the standard deviation from the mean of the three trials. For all the subjects, higher movement rate resulted in lower R^2 value.

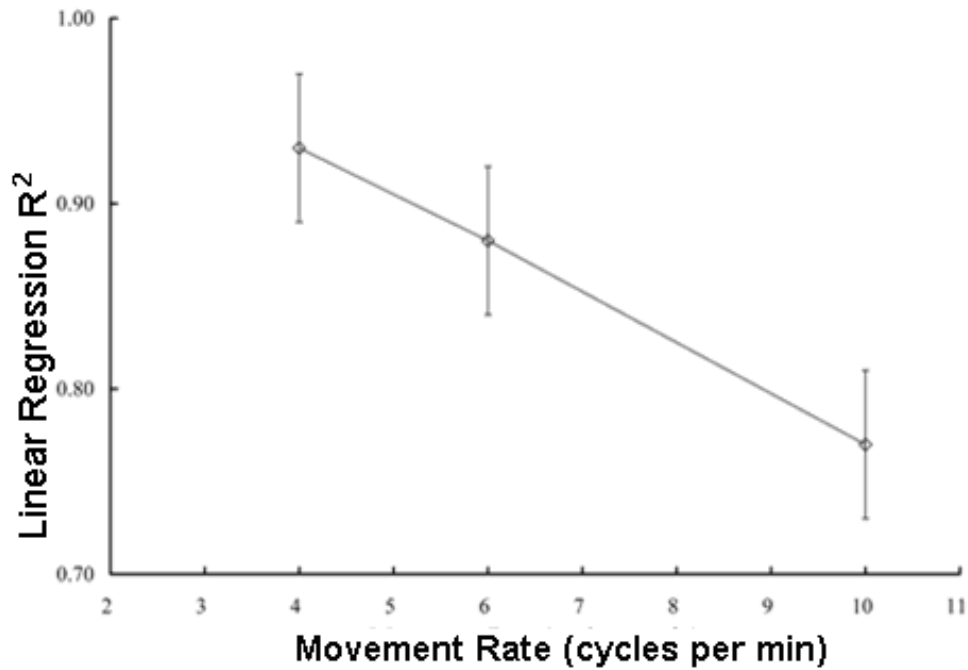


Fig. 4. 18 The relationship between R^2 value and movement rate. The error bar represents the standard deviation from the mean of the nine subjects.

Totally 162 data sets were obtained from the nine subjects. For each data set, the RMS tracking error between the target waveform and prosthesis angle was calculated according to Eq. (3-11) to evaluate the control performance. Typical tracking result is shown in Fig. 4. 19 (movement rate of 4 cycles/min), in which the angle value was normalized to the maximal angle at full opening position. Fig. 4. 19 (A) and (B) illustrates the prosthesis angle trajectories in tracking the sinusoid target and square target respectively. The overall mean RMS tracking error of each subject for all the movement rates is shown in Fig. 4. 20. The overall mean RMS tracking error of SMG under three movement rates was $12.8 \pm 3.2\%$ and $14.8 \pm 4.6\%$ for sinusoid and square tracking, respectively. Two-way repeated ANOVA was used to test the effects of both the movement rate and the track patterns on the RMS tracking error. It was observed that both factors had significant effects ($p = 2.0 \times 10^{-6}$ for movement rate and $p = 0.007$

for target track pattern) and their interaction effect was also significant ($p = 0.02$). Fig. 4. 21 illustrates the increasing trend of RMS tracking error for both sinusoid and square targets with the increase of the movement rate.

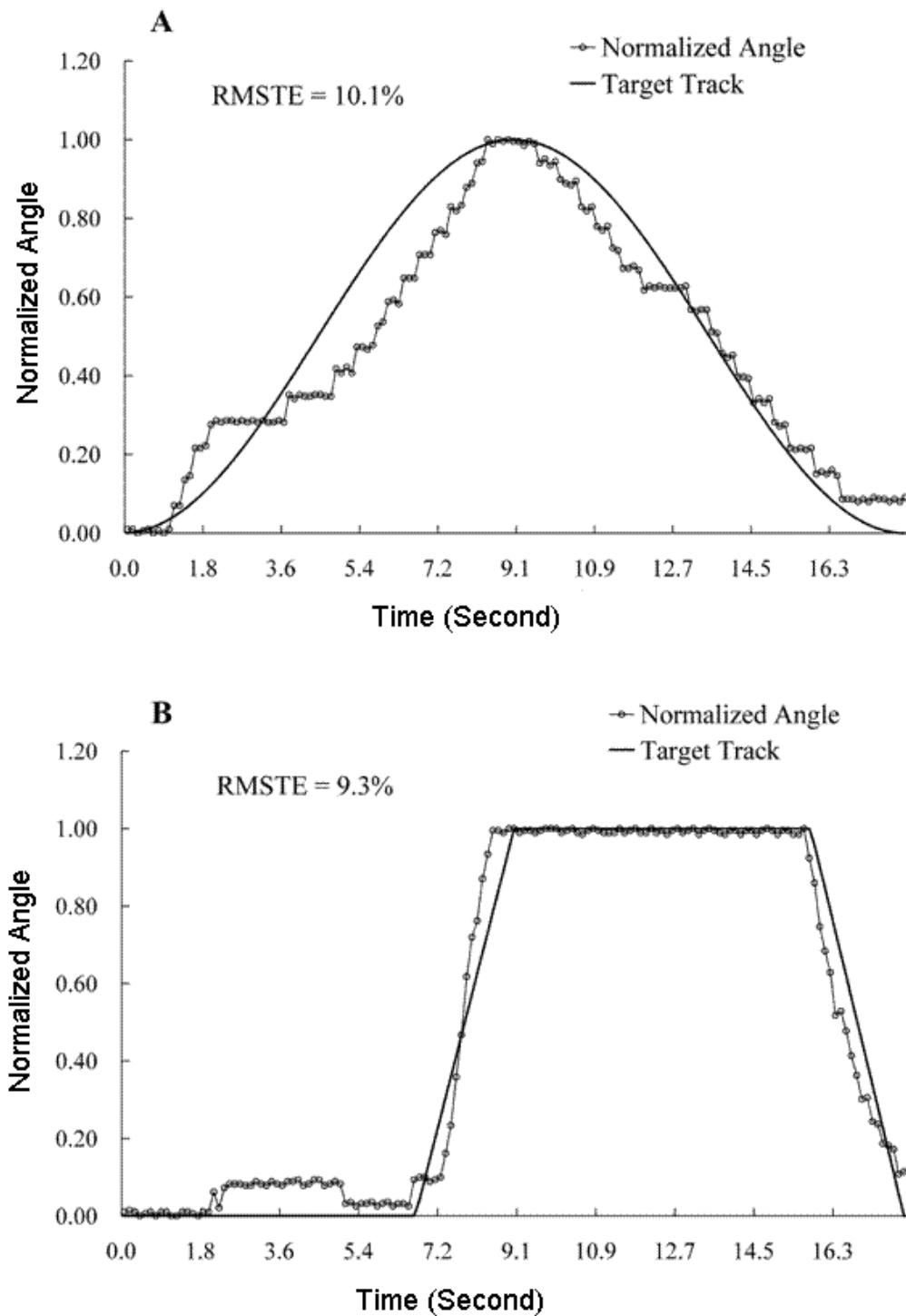


Fig. 4. 19 The tracking result of a typical trial under the movement rate of 4 cycles/min. Good consistency is shown between the target and the prosthesis response. (A) Tracking result of sinusoid target; (B) Tracking result of square target, RMSTE indicates the RMS tracking error.

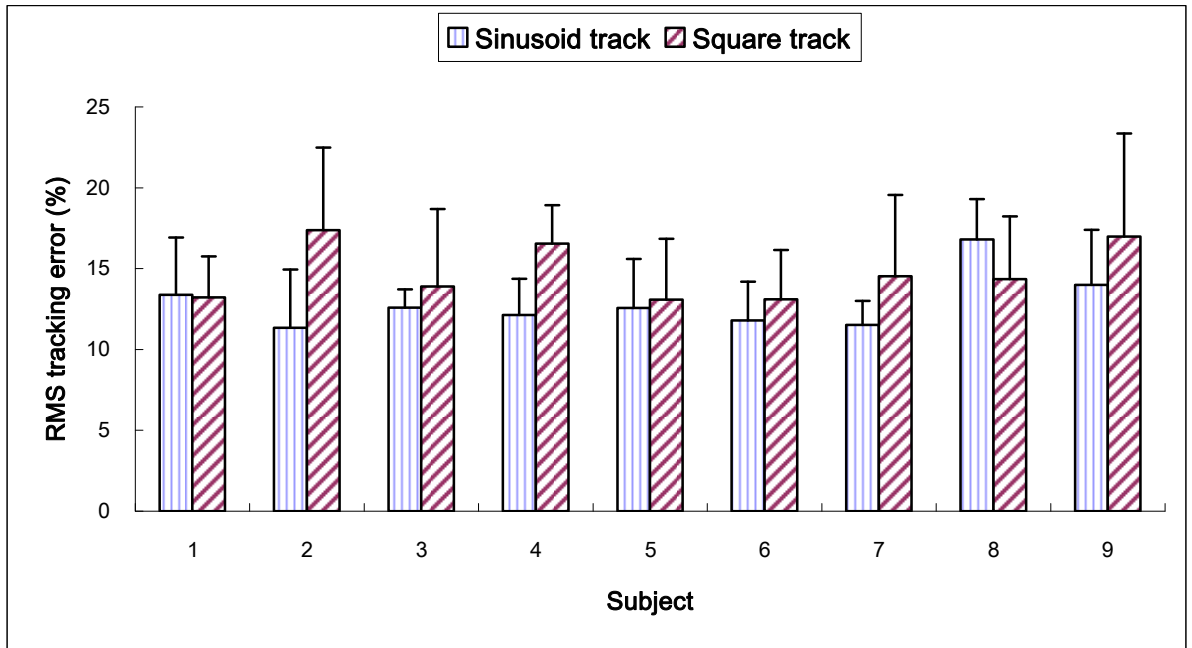


Fig. 4. 20 The overall mean RMS tracking error of each subject for all the movement rates. The error bar represents the standard deviation from the mean.

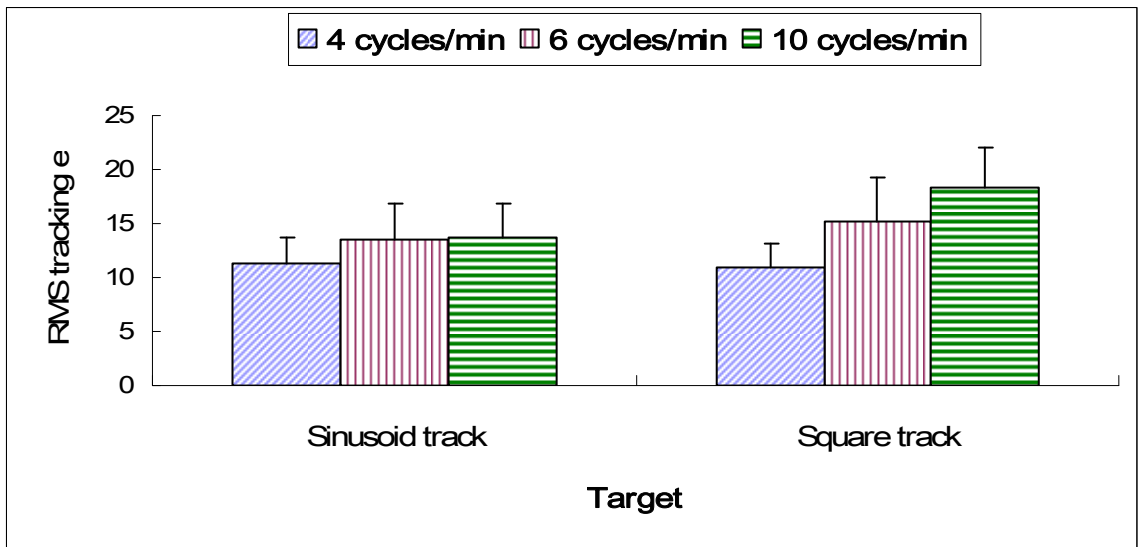


Fig. 4. 21 The RMS tracking error of for the two target tracks under three different movement rates. The error bar represents the standard deviation from the mean of the nine subjects. An increasing trend of RMS tracking error for both sinusoid and square targets was observed with the increase of the movement rate.

4.6 The Performance of Amputee using 1D SMG and Surface EMG Signals for Control Purpose

4.6.1 Performances of 1D SMG and Surface EMG in Tracking Guided Patterns of Wrist Extension

Table 4. 5 summarizes the RMS tracking error of using 1D SMG and surface EMG for tracking the three guiding waveform patterns under different movement rates by the amputee. The overall mean RMS tracking error of 1D SMG under the two movement rates was $17.2\pm 4.0\%$ (mean \pm S.D.), $16.5\pm 2.1\%$, and $15.0\pm 0.9\%$ for the sinusoid, square, and triangle guiding waveforms, while the corresponding value for EMG was $22.4\pm 2.3\%$, $22.1\pm 1.1\%$, and $15.5\pm 3.3\%$, respectively. Fig. 4. 22 shows that the averaged RMS tracking errors of SMG were smaller than those of EMG for all the three waveforms. Furthermore, as shown in Fig. 4. 23, the RMS tracking error for SMG was generally smaller under the slower rate.

Table 4. 5 The RMS tracking error (%) between 1D SMG/surface EMG and the guiding waveforms at the two movement rates (Mean \pm S.D.) and the mean RMS tracking error averaged over the two movement rates for the three guiding waveforms.

<i>Rate</i> (Cycles/min)	<i>SMG</i>			<i>Surface EMG</i>		
	<i>sinusoid</i>	<i>square</i>	<i>triangle</i>	<i>sinusoid</i>	<i>square</i>	<i>triangle</i>
5	14.4 \pm 2.6	15.0 \pm 3.4	14.3 \pm 1.8	24.0 \pm 4.2	22.9 \pm 4.2	13.2 \pm 1.0
10	20.1 \pm 1.8	18.0 \pm 2.0	15.7 \pm 3.0	20.8 \pm 4.1	21.3 \pm 2.9	17.9 \pm 4.3
<i>Mean</i>	17.2 \pm 4.0	16.5 \pm 2.1	15.0 \pm 0.9	22.4 \pm 2.3	22.1 \pm 1.1	15.5 \pm 3.3

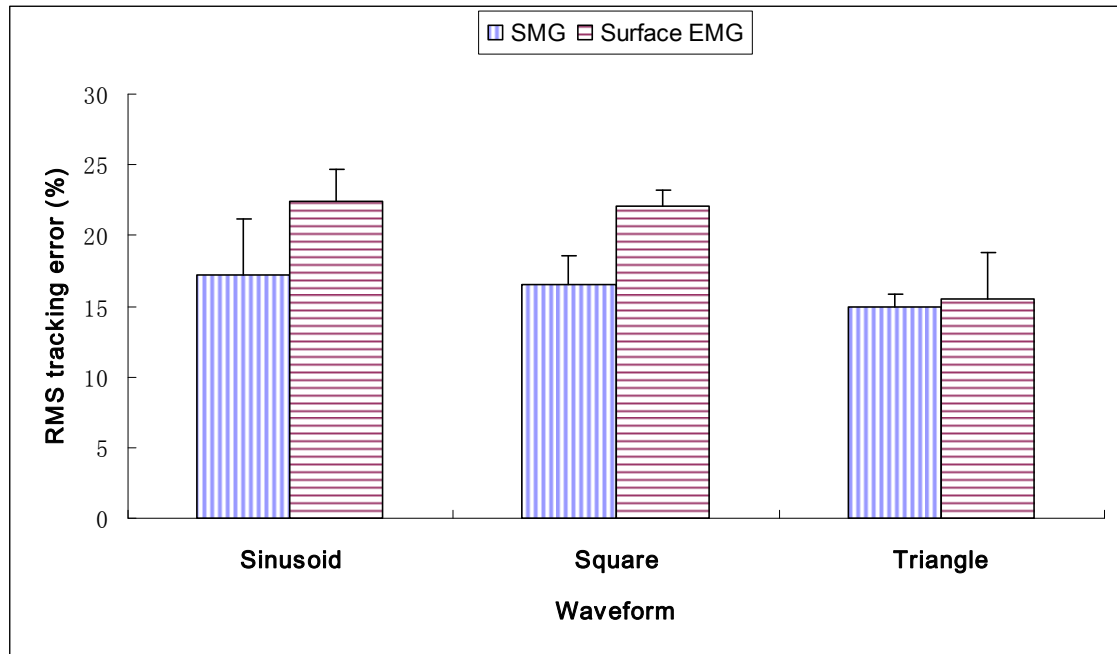


Fig. 4. 22 The RMS tracking error (%) between 1D SMG/surface EMG and the guiding waveforms. The error bar represents the standard deviation of the results of two different movement rates.

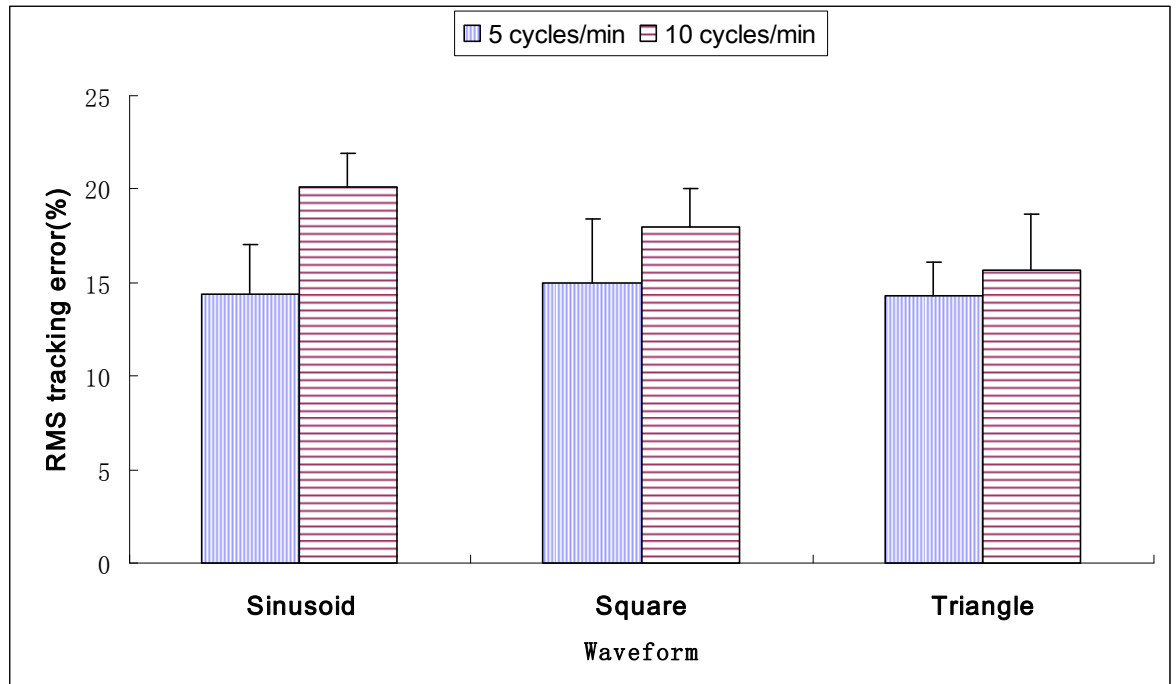


Fig. 4. 23 The tracking errors of SMG for different guiding waveforms under the two movement rates. The error bar represents the standard deviation of the three repeated trials.

4.6.2 Comparison of 1D SMG and Surface EMG in Visuomotor “E” Cancellation Test

Table 4. 6 shows the result of “E” cancelling for the single and dual tasks of amputee together with the number of bleeps counted during the dual task test. It was observed that the number of “E” *wrongly* cancelled greatly increased when using the EMG signal instead of SMG signal in both the single and dual task tests. Moreover, there was a 50% drop in the number of “E” *correctly* cancelled in using EMG in dual task when compared with single task and no such result was found in using SMG.

Table 4. 6 The number of “E” correctly cancelled and that of letters wrongly cancelled using 1D SMG and surface EMG signals for both single and dual tasks. The number of bleeps counted during the dual task test was also included.

<i>Task</i>	<i>Item</i>	<i>SMG</i>		<i>EMG</i>	
		<i>Correct</i>	<i>Wrong</i>	<i>Correct</i>	<i>Wrong</i>
<i>Single task</i>	<i>E cancel</i>	11	4	12	13
<i>Dual task</i>	<i>E cancel</i>	16	5	6	11
	<i>Bleep count</i>	15	5	11	1

4.6.3 Prosthesis Control by 1D SMG and Surface EMG

The RMS tracking error of 1D SMG and surface EMG for the two guiding waveform patterns under two different movement rates is shown in Table 4. 7. The overall mean RMS tracking errors of SMG under the two movement rates were $21.3\pm 1.6\%$ (mean \pm S.D) and $23.0\pm 1.3\%$ for the sinusoid and square guiding waveforms, while the corresponding values for EMG were $26.8\pm 2.0\%$ and $27.4\pm 1.8\%$, respectively. It was observed that the mean RMS tracking error of SMG control was smaller than that of surface EMG control for both the waveforms (Fig. 4. 24). For SMG control, it was also observed that the RMS tracking error under 4 cycles/min extension rate was smaller than that under the rate of 6 cycles/min for the sinusoid waveform. However, reverse result was obtained for the square waveform (Fig. 4. 25).

Table 4. 7 The RMS tracking errors in percentage of 1D SMG and surface EMG between the prosthesis angle and the guiding waveforms at the two movement rates (Mean \pm S.D.) and the mean RMS tracking error averaged over the two movement rates for sinusoid and square guiding waveforms.

Rate (Cycles/min)	SMG		EMG	
	<i>sinusoid</i>	<i>square</i>	<i>sinusoid</i>	<i>square</i>
4	20.1 \pm 2.4	24.0 \pm 1.9	25.4 \pm 5.5	28.7 \pm 3.3
6	22.4 \pm 1.8	22.1 \pm 0.9	28.2 \pm 6.8	26.1 \pm 2.0
Mean	21.3 \pm 1.6	23.0 \pm 1.3	26.8 \pm 2.0	27.4 \pm 1.8

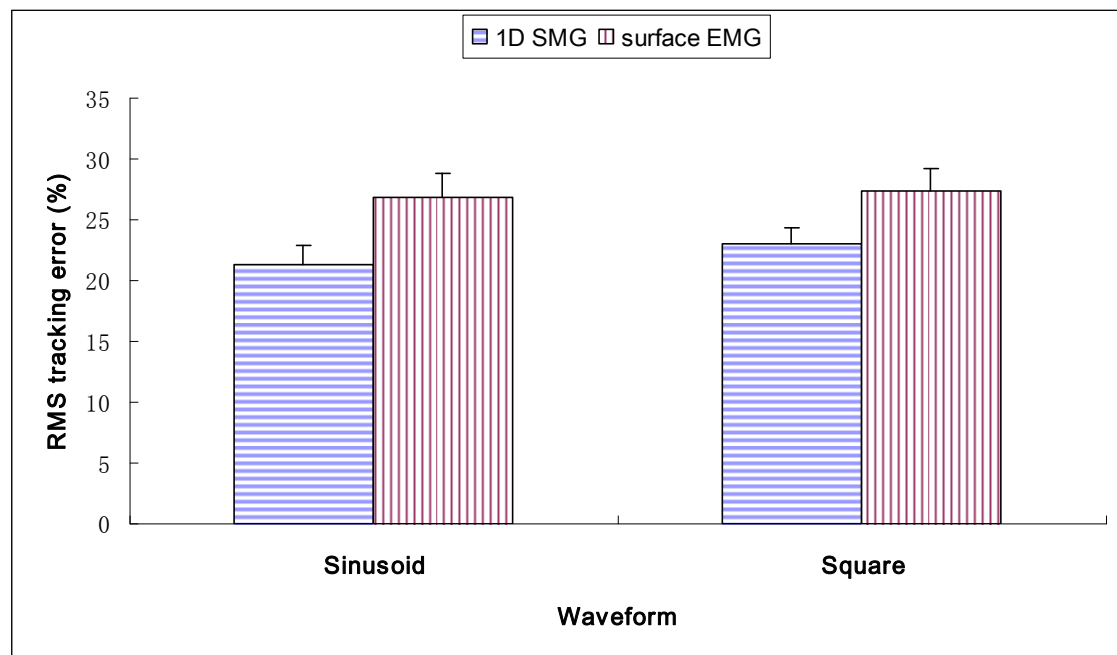


Fig. 4. 24 The overall mean RMS tracking error of using 1D SMG and surface EMG for control by the amputee for the two guiding waveforms. The error bar represents the standard deviation from two different movement rates.

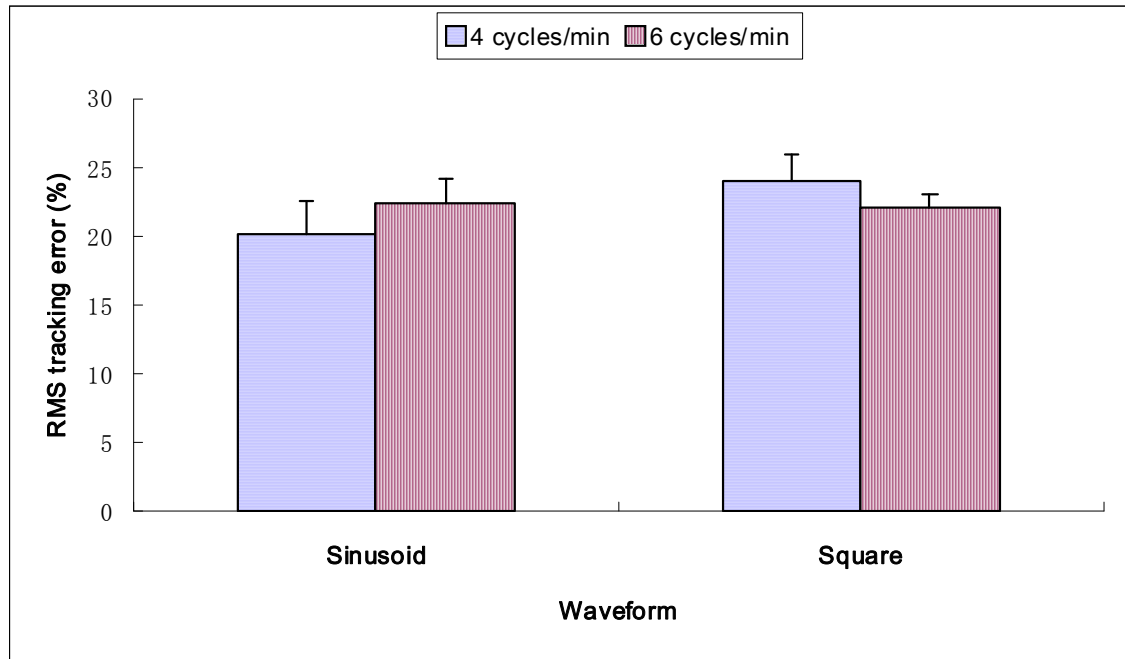


Fig. 4. 25 The overall mean RMS tracking errors of using 1D SMG to control prosthesis by the amputee under the two extension rates. The error bar represents the standard deviation from three repeated trials.

CHAPTER 5 DISCUSSION

In this chapter, the performance of the subjects using 1D SMG to evaluate the muscle contraction and to control prosthesis is discussed in separate sections. The possible reasons are given to explain the advantages of 1D SMG signal in skeletal muscle assessment and in prosthetic control.

5.1 Skeletal Muscle Evaluated by 1D SMG

5.1.1 The Relationship between 1D SMG and Wrist Angle

A-mode ultrasound signal with a single element ultrasound transducer, named as 1D SMG, was used to detect the thickness change of forearm muscle during wrist extension. It was found that there was a good linear correlation ($r = 0.907 \pm 0.077$) between the 1D SMG signal and the corresponding wrist extension angle for the healthy subjects tested ($n=9$), demonstrating that the morphological changes of forearm muscles were significantly correlated to the motion of the related joint. The deformation-angle ratio was also calculated to further study the relationship between the muscle thickness change and wrist extension angle. This ratio was found to be significantly different among the nine subjects. The results were calculated from the data obtained in three different rates of wrist extension. However, for each subject, no significant difference was observed among the ratios for different wrist extension rates. Therefore, it was possible to use a single ratio to describe the relationship between the muscle deformation and the wrist angle signal for one subject. More experiments on subjects with different ages and genders are required to better understand the factors that affect the deformation-angle ratio. The surface EMG as a reference signal was collected

simultaneously and the result demonstrated that there was also a linear correlation between the EMG RMS and the wrist angle ($r = 0.864 \pm 0.071$). Since surface EMG has been widely used to assess muscle function and prosthesis control, we suggested that 1D SMG could also be used in this area to provide more information by detecting muscle thickness changes.

Recently, the change of muscle thickness has been used as a parameter to characterize muscle fatigue process (Shi et al., 2007), evaluate the effect of resistance training (Abe et al., 2000), and reveal muscle morphological decline of the supraspinatus muscle due to a shoulder injury (Hasegawa et al., 2003). Ultrasound measurement can be more spatially localized in comparison with surface EMG. The diameter of the ultrasound sensor used in this study was only 5 mm. The muscle thickness changes were calculated through detecting the shift of the reflected ultrasound echoes from the fat-muscle and muscle-bone interfaces. Therefore, the 1D SMG signal provided the potential advantage of being able to detect the thickness changes of muscles at different depths or locations with single-element ultrasound transducers non-invasively, which would effectively avoid adjacent muscle cross talk. Compared with the MMG signal, the 1D SMG signal was more stable as it would not be influenced by external noises, such as movement artefact or power line noise. In addition, the magnitudes of both surface EMG and MMG can be significantly affected by changes of coupling conditions between the skin surface and the electrodes / sensors. And the body motion can easily induce the change of the coupling condition resulting in the distortion of surface EMG or MMG signals. In the case of 1D SMG, the coupling between the ultrasound transducer and the skin may also be affected by the body motion. However, such effects may only affect the magnitude of ultrasound echoes but not the time between echoes, which represents

muscle thickness. For this reason, 1D SMG may be more robust to motion artifacts in comparison with surface EMG. Therefore, it was expected that the 1D SMG signal could be used as complementary information tool for surface EMG and MMG during various contractions for the assessment of muscle function, muscle fatigue and pathology, and for the control of prosthesis. However, the advantages of 1D SMG should be further verified together with other factors that may affect the collection and extraction of this signal.

5.1.2 1D SMG Based Wrist Angle Estimation

In the present work, it was demonstrated that the models established for the rate of 22.5 cycles/min could be used for the prediction task of 1D SMG data sets obtained under other rates and within different trials. Erfanian et al. (1994) reported the use of EMG signals obtained from surface electrodes to determine the knee joint angle in paraplegic subjects when the quadriceps muscle was electrically stimulated using percutaneous intramuscular electrodes. They found that the peak amplitude of the evoke EMG signal and its power spectrum increased as the joint angle increased. Suryanarayanan et al. (1995) developed a neural network model to estimate joint angle at the elbow using the EMG signal of biceps as an input. However, there was only one subject in their trials and the prediction RMS error was as large as 20%. Compared with these EMG-based modelling, the present 1D SMG-based joint angle prediction models demonstrated better performances. Moreover, the EMG-angle relationship in the literature remained controversial and unsolved. For example, some previous studies (Leedham and Dowling, 1995; Vredenburg and Rau, 1973) claimed that the EMG activity was the same at different joint angles under maximal contraction of biceps brachii muscle. This was not consistent with the EMG-elbow joint angle prediction model reported by

Suryanarayanan et al. (1995). Joint angle models reportedly heavily relied on the EMG inputs to ‘drive’ them. It has been demonstrated that the EMG relates more to the input of muscle contraction, i.e. the intension of an action, while the muscle architecture is a primary determination of muscle function (Shi et al., 2007). As the architectural changes of skeletal muscle were claimed to correlate more with the output of muscle contraction, and could be detected using ultrasound (Shi et al., 2007; Zheng et al., 2006; Hodges et al., 2003), thus SMG had the potential to be a better candidate to describe the relationship between joint angle patterns and the activities of corresponding muscles during the human movement.

The previous studies on non-parameter modelling for muscle systems were mostly based on ANN. This study investigated the feasibility of using LS-SVM method for wrist angle prediction. The result indicated that the LS-SVM model performed better in comparison with the ANN models in terms of prediction accuracy and correlation coefficient. This was in line with the findings of previous studies that the LS-SVM model outperformed the ANN in predicting the joint angle from the EMG or SMG signals (Suryanarayannan et al., 1995; Shi et al., 2006).

In the present study, several factors, such as the location of ultrasound sensor, signal resolution, tracking algorithm and the frame rate of the ultrasound, may contribute to the prediction error. To improve the estimation accuracy, ultrasound frame rate and imaging resolution should be increased and other algorithms for tracking the two interfaces (muscle-skin, muscle-bone) should be explored. In addition, multiple channels of 1D SMG signal could be utilized to improve the control accuracy.

5.2 Comparisons of 1D SMG and Surface EMG for Prosthetic Control

5.2.1 1D SMG in Tracking Guided Patterns of Wrist Extension

In this study, the performances of surface EMG and 1D SMG, i.e. real-time muscle thickness change detected using A-mode ultrasound, in tracking three different movement patterns of the wrist extension were assessed, guided by waveforms shown on the PC screen. It was found that the RMS tracking error of SMG under different wrist extension rates (ranged from $14.0\pm 1.9\%$ to $23.3\pm 3.7\%$) was statistically significantly ($P<0.01$) smaller than the corresponding value of surface EMG (ranging from $24.2\pm 4.4\%$ to $32.1\pm 4.1\%$) for all the movement patterns studied, indicating that SMG performed better than surface EMG in following the given movement patterns in terms of tracking accuracy.

It was interesting to explore why 1D SMG could perform significantly better than surface EMG in tracking different given movement patterns of the joint under different movement rates. It has been reported that there is an exponential relationship between EMG magnitudes and the strengths generated by different skeletal muscles (DeLuca 1997; Hodges et al., 2003; Zheng et al., 2006; Shi et al., 2008). Previous studies reported that SMG signals of a skeletal muscle have approximately linear relationships with the strengths generated by this muscle, represented either by torques for isometric contractions (Shi et al., 2008) or by joint angles for isotonic contractions (Zheng et al., 2006). It appears that SMG and the corresponding joint angle follow a relatively simple relationship in comparison with the relation between EMG and joint angle. The results of this study and previous ones appear to imply that the architectural changes during muscle contraction relate more directly to the actuation achieved (mechanical output),

while the EMG is a measure of activation intended (electrical input). In relation to the findings of the present study, we may interpret that our motor control and visual feedback system could perform better when the control signal has a linear relationship with the target signal to control, which was the wrist angle in this case. This may probably reduce the training efforts when the SMG signal was used for the prosthetic control. Further studies are required to study how many training efforts can be saved when using 1D SMG for control instead of surface EMG. And more normal and residual limbs should be tested to ensure a solid conclusion.

As expected, it was found that as the movement rates increased, the RMS tracking error of SMG increased (Fig. 4. 11). When the movement rates increased, the subjects were required to perform the same movement in a shorter time period. Furthermore, according to subjects' verbal reports, the visual feedback used to provide instantaneous performance indication during the test slightly distracted their attention. Thus, as the movement rates increased, the possibility for SMG to "move away" from the guiding waveform may also increase, resulting in higher tracking errors. However, this increasing trend in tracking error with the increase of movement rate was not observed in EMG RMS. It was also noted that the performance of SMG tracking at the highest rate was still better than the best performance of the EMG tracking among all the tests. This difference between the two signals may result from a number of potential reasons. First, the frame rate of A-mode ultrasound (approximately 17 Hz), which also determines how fast the data points of SMG signal are given, was relatively low in the study. With the increase of the wrist flexion-extension rate, the SMG data collected in each cycle would be reduced. Therefore, the subject had fewer data points to refer to for following the given waveform. Since we also controlled the data rate of EMG RMS to

17 Hz during the test, this effect should have affected the performance of EMG tracking as well when the movement speed was increased, however, it was not observed in this study. A higher frame rate could be used to further investigate the effect of data collection speed in future studies. The second possible reason was that SMG is a signal not only related to the bioelectrical properties of muscles, i.e. how muscles are activated, but also dependent on the mechanical properties of muscle-tendon complex, i.e. viscoelastic properties. With the increase of the muscle contraction speed, the hysteresis of SMG signal may also increase. This made it more challenging for the subjects to follow the given movement patterns using SMG signals. However, EMG signal would not be affected by this effect, as it is more related to bioelectrical properties of muscles. Again, further studies are needed to better understand the effect of the viscoelasticity of muscles and other tissues on the generation and applications of SMG signal.

5.2.2 1D SMG in Visuomotor “E” Cancellation Test

We compared the control performances of force/angle, 1D SMG, and surface EMG signals during both isometric force contraction and wrist extension. These signals were used to proportionally control a cursor’s vertical location on PC screen so as to cancel letter “E” from a sequence of vertically arranged letters. The number of “E”s correctly cancelled and the number of letters wrongly cancelled were recorded to allow the comparison of control performances of subjects using various signals. It was found that the percentage of “E” correctly cancelled was the highest when using either force or wrist angle as the control signal. Using the performance of force/angle signal as reference, the performances of using both SMG and EMG signals dropped significantly ($p < 0.001$). The performance reduction when using surface EMG was observed to be

10% larger than that observed when using SMG for both the isometric contraction ($37\pm 29\%$ vs $27\pm 15\%$) and wrist extension tests ($31\pm 23\%$ vs $21\pm 11\%$). Although the number of “E” correctly cancelled using SMG and EMG did not show significant differences, the numbers of “E” wrongly cancelled using EMG was significantly larger than that using SMG under both the isometric contraction and wrist extension tests ($p < 0.001$). These findings supported our hypothesis that 1D SMG signal could provide the user with an improved degree of control compared to surface EMG.

Two signal processing parameters were believed to have potential effect on the control performance using surface EMG signal. One was the sampling rate of EMG RMS used to perform the control task. The other was the number of data points used for the calculation of EMG RMS. The sampling rate determined the rate at which the signal controlled the cancelling task. In this study, comparison of the performance among various sampling rates (10~50Hz) showed no significant difference. As the sampling rate of 1D SMG was 17 Hz in our current system, the same sampling rate was also adopted for EMG RMS to allow for a better comparison between the two signals. It may be worthwhile to further study whether the sampling rate of SMG would affect its performance, by using a faster ultrasound measurement system and an improved real-time tracking algorithm. Meanwhile, the number of data points was found to significantly affect the performance of EMG ($p = 0.016$). Some subjects verbally reported a delay when using the data points larger than 200 and the number of letters correctly cancelled was significantly higher when using 0.2 sec epoch, compared to 0.1 and 0.15 sec epochs, to calculate the EMG RMS (one-way ANOVA, $p = 0.016$). Therefore, 200 data points (equivalent to 0.2 sec) for each epoch, which was observed to be associated with the highest accuracy, was chosen to calculate EMG RMS in this study.

In the dual task test, the control performances of using all the signals were not significantly decreased in comparison with the corresponding results of the single task test under both the isometric contraction and wrist extension ($p > 0.05$). It appeared that the disturbance to the subject's attention on "E" cancelling task caused by the TEA test was not significant. According to the verbal reports from some of the subjects, they became more alert upon hearing the sound of bleeps, encouraging them to react more quickly than without sound. In this study, the sample size ($n=10$) was relatively small, and hence a study with a larger subject number would be required to better understand this effect. It was also worth noting that the results were based on a specific auditory attentional task and hence could not be generalized to other cognitive tasks, such as a visual attentional task. Visual attentional task in which subjects could do concurrently with the visual cancelling task should be devised to further explore the generalisability of the results reported here.

We originally hypothesized that using 1D SMG signal to perform a visuo-motor tracking task may require less attentional effort than using surface EMG signal, i.e. we expected that the performance drop when using EMG for control would be significantly serious than that using 1D SMG. This hypothesis was not verified in this study. However, we found the correlation between the numbers of "E" correctly cancelled in the single and dual tests using 1D SMG ($R^2 = 0.73$) was much higher than that using surface EMG ($R^2 = 0.36$), implying that using SMG could generate a more consistent control performance in comparison with using EMG under different cognitive requirements. Such a consistency is important for real prosthesis control. Again, this finding needs to be further confirmed with a large sample size and tests with different types of secondary tasks.

5.2.3 Evaluation of 1D SMG for Prosthetic Control

The study also investigated the feasibility of controlling powered prosthesis by 1-D SMG signal and compared the performances of SMG and EMG in tracking the guided patterns of wrist extension. The statistical analysis showed that the RMS tracking error of SMG control was significantly smaller than that of EMG control, indicating that SMG could have better performance than EMG in controlling the prosthesis. This result confirmed our hypothesis that SMG had the potential to be an alternative signal to surface EMG for control purpose. The finding from this part of the study was consistent with those from the tracking guided patterns. The performance of SMG was significantly better than EMG in tracking different given movement patterns under different movement rates. One potential reason was that these two signals had different relationship with the joint movement. In the guided pattern tracking test, we have demonstrated that SMG signals of the extensor carpi radialis had linear relationships with the joint angles while the relationship between muscle architectural parameters measured from the ultrasound images and EMG was nonlinear (Hodges et al., 2003). In the part of study, it was further confirmed that 1D SMG and the corresponding joint angle follow a relatively simple relationship in comparison with the relation between surface EMG and joint angle. During the experiment, the subjects controlled the prosthesis with the function of open-close by the wrist joint movement. This simpler relationship of SMG may help to reduce the conscious efforts of the subject and in turn increase the control accuracy. Moreover, surface EMG signal is the summation of asynchronous electrical pulses from many muscle fibres; therefore it is difficult to decode the joint movement from one-channel EMG signal.

This study utilized an open-loop control system with input of 1D SMG signal and output of prosthesis angle. Since a linear control algorithm was used, theoretically the input-output relationship was expected to be linear. However, according to Fig. 4. 18, we observed an obvious decrease of linearity which was significantly affected by the frequency of input signal ($p < 0.005$). The main reason for this frequency-dependent property is due to the intrinsic mechanical deficiency of the prosthesis which has a nonlinear response upon quick movement. Subjects may still be able to control the system even if the input-output property is nonlinear, although the subject may have to make more effort in control and the performance is unlikely to be optimal.

The visual pursuit tracking task was applied in the study to test the 1D SMG control performance which was similar to the study in tracking guided patterns of wrist extension. The RMS tracking error of SMG control under different movement rates in Table 4. 4 ranged from $10.9 \pm 2.2\%$ to $18.3 \pm 3.8\%$, while in the guided pattern tracking study the range was from $14.0 \pm 1.9\%$ to $23.3 \pm 3.7\%$ (Table 4. 2). Two factors may contribute to the difference between the two data sets. The first possible reason was the lower wrist extension rates used in this prosthesis study (4-10 cycles/minute), taking into account the motion speed of the prosthesis. The maximal motion speed of the prosthesis was less than 15 cycles/min, limiting the maximal wrist movement rate. As shown in Table 4. 4, lower movement rates would decrease the RMS tracking error which has also been proved in the previous work. The second possible reason was that the limited motion resolution of the prosthesis might have negative effect on the performance. The prosthesis could control only 20 positions in its full motion range. Thus, when the subject performed wrist extension, SMG signal could follow muscle deformation in a smooth manner, while the prosthesis was only able to move one step at

a time (Fig. 4. 19). This resolution limitation might cause a decrease of the control accuracy compared with the guided pattern study. Moreover, this stepwise trajectory in visual feedback might increase the subject's conscious effort during the tracking process. The guided pattern tracking study has shown that the 1D SMG signal has a better performance than the surface EMG signal in tracking the guided patterns of wrist extension when linearly recruited. In the current study, we focused on the real time control of the prosthetic hand by the 1D SMG signal to further demonstrate the potential of SMG as a control signal. However, further studies should be carried out to evaluate the performance using multiple channels of EMG and SMG with more efficient methods in the future.

Two-way ANOVA showed that the wrist extension movement rate had the most significant effect ($p < 0.005$) on the RMS tracking error. An increasing trend of tracking error was observed with the increase of the movement rate for both sinusoid and square waveforms. When the movement rate increased, the subject was required to perform the tracking task in a shorter time period which in turn required more conscious effort from the subject. Hence, with the increase of movement rate, the possibility for the subject to make errors may also increase, resulting in larger tracking errors. The target track pattern also had a significant effect ($p < 0.005$) on the RMS tracking error. As shown in Fig. 4. 21, although the tracking error increased for both sinusoid and square tracks with the increase of movement rate, it tended to increase faster for the square track in comparison with the sinusoid track. The major possible reason might come from the nature of square track, which included stable-state (high level and low level) and transient-state (changes between two levels) in its waveform (Fig. 3. 11). The transient-state part contributed most of the errors because it was quite difficult for subject to

follow this quick change. The proportion of transition-state parts was larger in square waveforms with higher rates, thus causing a larger tracking error.

Compared with surface EMG control, the major advantage of 1D SMG control is that it is more suitable to provide an intuitive control, because it is directly extracted from the morphological changes of muscle, which is originally closely correlated to the joint motion. Intuitiveness relieves the mental burden on a user during long-term operation and natural daily work. In the guided pattern tracking study, we found that the SMG signal of skeletal muscle had an approximate linear relationship with the corresponding joint angle. In this study, a simple linear algorithm was used to map the magnitude of SMG signal to the prosthesis opening position. Therefore the relationship between the control signal, namely the wrist angle, and the target signal of prosthesis position was approximately linear. This intuitive control method helped subjects to perform better in using SMG in comparison with EMG. To achieve similar performances in EMG control much more complex algorithm should be applied and more training efforts were required (Cipriani et al. 2008). Another advantage of the 1D SMG control is its potential of detecting contraction of individual muscles at neighbouring locations and different depths, providing the feasibility of fine control in multi-function artificial hands. Due to the challenges in surface EMG signals generated by different neighbouring muscles, i.e., cross talk, the commercially available prostheses controlled by surface EMG could only provide limited number of DOF. We employed only one channel SMG from forearm extensor muscle to control the prosthesis in the present work. To provide multiple DOF prosthetic control, multi-channel SMG signals from different groups of muscles are required to predict the motions of individual joint. Further experiments are being planned to explore the potential of controlling multiple DOF prosthesis using

multi-channel SMG signals. Furthermore, as mentioned above, the performance of the prosthesis can affect the control accuracy to some degree. Therefore, more dexterous prostheses with higher reaction speed and motion resolution should be utilized in further study. In this study, 90% of the maximal wrist extension was selected as the maximal open position that the prosthesis can reach which could cover most of the wrist range and also purposely prevent muscle fatigue. In addition, it would be very interesting to explore the prosthetic performance using the subject's strength, for example, using 80% of the maximal voluntary contraction (MVC) as the maximal open position of the prosthesis. Further studies are needed to systematically test the effects of the prosthetic performance. Moreover, the ability to control the prosthesis using different degrees of extension should also be tested by using stepwise waveforms in a future study.

In summary, we developed the 1-D SMG prosthetic control system to realize the control of prosthesis with one DOF, and then evaluated the performance of prosthetic control in tracking different opening-closure patterns by SMG in this study. The results indicated that the continuous change of prosthetic hand could be well controlled by SMG. It suggests that SMG provides an alternative method to surface EMG for prosthetic control. It is very natural for us to conduct experiments on amputee subjects as a next step.

5.2.4 Amputee's Performance using 1D SMG to Control

5.2.4.1 Performances of 1D SMG and Surface EMG in Tracking Guided Patterns of Wrist Extension

Similar with the result of the healthy subject, the test on the amputee showed that the RMS tracking error of 1D SMG under different wrist extension rates were smaller than the corresponding values of surface EMG for all the movement patterns studied, indicating that SMG performed better than surface EMG in following the given movement patterns in term of tracking accuracy. Moreover, the RMS tracking error increased with the increase of the movement rate under all the movement patterns. These results were consistent with those obtained from the healthy subjects. However, we also noticed that the amputee subject showed great difficulties in following the movement rate used by healthy subject, i.e. 20, 30, 50 cycles/min and he could only follow the rate of 5, 10 cycles/min, instead. The main reason maybe that during the hypothetical movement of intending extension of the phantom wrist, there was little feedback for the amputee to regulate his strength. Unlike the healthy subject, the amputee could not adjust his strength according to the wrist angle change. In this situation, far more effort was required in order to better follow the predesigned waveform for the amputee and once the movement rate increased, the effort required was beyond the amputee's ability.

5.2.4.2 Comparison of 1D SMG and Surface EMG in Visuomotor "E" Cancellation Test

As expected, it was found that the number of "E" correctly cancelled of amputee subject greatly decreased when compared with that of healthy subjects using both 1D SMG and

surface EMG (Table 4. 3 and Table 4. 6) mainly because of the greater effort required for the amputee. The number of “E” wrongly cancelled was greatly increased in using the EMG signal in comparison with using SMG signals in both the single and dual task tests. This finding supported our hypothesis that the 1D SMG signal may provide the user with an improved degree of control compared to that offered through use of surface EMG. A drop of 50% in the number of “E” correctly cancelled in using EMG in dual task may indicate a greater cognitive requirement. No such a great drop in the number of “E” correctly cancelled in using 1D SMG may indicate that 1D SMG is a better alternative of EMG for prosthetic control, especially when performing two tasks at the same time.

5.2.4.3 Control Prosthesis by 1D SMG and Surface EMG

RMS tracking error of 1D SMG control was smaller than that of EMG control, indicating that SMG had better performance than EMG in controlling the prosthesis. For the square waveform, as the movement rate increased, the RMS tracking error tended to be smaller. The reason maybe that there is no significant difference between these two. However, it is difficult to make a solid conclusion as only one amputee was recruited in this study and the two movement rates tested, i.e. 4 and 6 cycles/min are close. A statistically significant result should be obtained by recruiting more amputees.

In summary, the case study on the amputee showed the consistent result with healthy subject that 1D SMG is a promising alternative signal for prosthetic control with smaller RMS tracking error and better performance in all the three tests in comparison with EMG. However, more amputees should be recruited in future studies in order to form a solid conclusion. More consideration should be given if we want to make the SMG

control method suitable for amputees. In a previous study (Zheng, et al, 2006), SMG signals were successfully collected from 3 amputees to demonstrate that the SMG signal had the potential for prosthetic control. In this thesis, we used SMG signal from both normal subjects and an amputee to control a prosthesis. Although encouraging results were achieved, there are three major differences between our experiment setup and the clinical setup. First, our experiment used computer-based control system instead of microcontroller-based one. Second, clinical setup uses patient-specific socket to fit the prosthetic hand with residual limb and to mount the EMG electrode. Third, the training processes are different. In clinical application, a patient should be trained for a long time to learn to control the prosthesis to accomplish various specific functions such as grasping and holding objects. With training, failure to perform adequately in the initial stages can be overcome. In our experiment, the subjects were trained only for the specific task in a short time. The RMS tracking error is the quantitative evaluation of the task performance in the experiment. However, it is hard to assess the subject's ability to control the prosthesis just according to this parameter. We can only conclude that the smaller RMS tracking error, the higher possibility that the subject can successfully control the prosthesis. To put this SMG control technique in clinical use in the future, further developments work are needed such as integrating the computer-based control system into a microcontroller-based control system, as well as finding out the best way of mounting the ultrasound transducer into the prosthetic socket. Furthermore, the thermal effect of ultrasound should be carefully considered in the development. The ultrasound technology of our method belongs to the category of diagnostic ultrasound. Guidelines for the safe use of diagnostic ultrasound equipment would need to be followed (such as the safety guidelines of the British Medical Ultrasound Society, see

<http://www.bmus.org>). The future ultrasound control equipment should be designed to meet the requirement of the Thermal Index (TI) in the guidelines for long time use.

In this chapter, discussions were made on the results of investigating the morphological changes of skeletal muscle during various movements, assessed by 1D SMG signal and the possibility of using 1D SMG in prosthetic control compared with surface EMG. Possible reasons leading to those results were explored in details. Important findings obtained in this study, limitations for each test and, suggested future works are introduced in the next chapter.

5.2.5 Summary

According to the above discussion, this thesis clearly demonstrated that 1D SMG has the potential to be an alternative signal for skeletal muscle assessment and prosthetic control. It was further confirmed in this thesis that SMG has a more linear relationship with muscle outputs in comparison with EMG signals. Using proper modeling techniques, such as SVM, the joint angle can be precisely predicted using the SMG signal of corresponding muscles. The performance of SMG in guided motion pattern tracking, visuomotor “E” cancellation test, and prosthetic control test all showed that the SMG control has a better performance in comparison with the EMG control. The feasibility of the SMG control has also been demonstrated by the test of the amputee subject. Despite of these encouraging findings, the current experimental setup still have various limitations and future works are needed before SMG can be clinically applicable. Important findings obtained in this study, limitations for each test and, suggested future works are introduced in the next chapter.

CHAPTER 6 CONCLUSIONS AND FUTURE STUDIES**6.1 Conclusions**

In this thesis, the relationship between 1D SMG and wrist extension angle was investigated and the wrist extension angle was predicted by the morphological changes of skeletal muscle using ultrasound, i.e., 1D SMG signal. And the potential of using 1D SMG as a control signal further explored by comparison with surface EMG. The findings of this study are summarized as follows.

1. 1D SMG- EMG compound sensor

In this study, 1D SMG and surface EMG signals were collected simultaneously by a custom-made compound sensor, which make it possible to fix the A-mode ultrasound transducer in the middle and at the same time to minimize the size of the sensor. We then further evaluate this sensor by comparing subjects' performance in a series of tracking task. It is showed that 1-D SMG provides a more portable, compact, inexpensive, and practical solution to detect muscle thickness changes than 2-D SMG. Moreover, A-mode ultrasound transducers may be easily attached to the skin during dynamic activities of muscles and are of a sufficiently small size to potentially be embedded in prosthetic sockets.

2. Linear relationship between the 1D SMG and the wrist angle signals

Compared with surface EMG signal, 1D SMG signal provided the potential advantages of being able to detect the thickness changes of muscles at different depths or locations with a single ultrasound transducer non-invasively, which effectively avoids adjacent muscle cross talk. In addition, the results of our experiments demonstrated a significant linear relationship between the 1D SMG and the wrist angle signals. Based on this simple linear relationship, we expect that the 1D SMG could be used along with the surface EMG signal to provide more comprehensive information of skeletal muscle contractions.

3. 1D SMG based wrist angle prediction by LS- SVM and ANN models

It was investigated that the wrist angle could be accurately estimated from the muscle deformation signal, i.e.1D SMG, using the LS-SVM and ANN models. The results also revealed that the estimation performance of LS-SVM model was significantly better than that of ANN models. Accurate joint angle prediction is crucial for human-computer interface devices in many different areas. There have been growing interests in determining the joint angles in different areas, such as functional electrical stimulation (FES), prosthesis control, virtual reality, telerobotics and medical hand function assessment (Crago et al., 1998; Hart et al., 1998). Therefore, the models developed in the current study could potentially offer a feedback signal of the wrist joint extension angle for wrist position control in these areas.

4. 1D SMG could result in a smaller RMS tracking error compared with surface EMG

It was demonstrated in this study that 1D SMG signal obtained using A-mode ultrasound could provide better performance of wrist extension in comparison with surface EMG in tracking different given patterns under different wrist extension rates. The use of single element transducer in A-mode image allowed great flexibility in designing SMG sensor, thus, it is practically feasible to attach such a probe on the skin surface for the purposes of control or muscle function evaluation, similar to the use of surface EMG.

5. The control performance using 1D SMG was better than that using surface EMG

Our study found that the control performance using the single channel of 1D SMG signal, obtained using A-mode ultrasound was better than using surface EMG signal under both the isometric contraction and the wrist extension conditions. Furthermore, it was demonstrated that introducing the additional task of counting bleeps tends to have insignificant effects to the control performance for all the signals. The results also showed that 1D SMG provided more consistent performance under the single and dual task tests in comparison with surface EMG.

6. 1D SMG showed potential for prosthetic control

The 1D SMG prosthetic control system was conducted to realize the control of a single DOF prosthesis, and the performance of prosthetic control in tracking different wrist extension patterns by 1D SMG was evaluated in this study. It was indicated that the prosthetic hand could be better controlled by 1D SMG with lower RMS tracking error in

comparison with EMG. It suggests that 1D SMG provides an alternative method to surface EMG for prosthetic control.

7. The similar performance of amputee using 1D SMG to control with that of healthy subjects

The case study on amputee showed the consistent result with healthy subject that 1D SMG is a promising alternative signal for prosthetic control with smaller RMS tracking error and better performance when compared with surface EMG. However, more amputees should be recruited in order to acquire a solid conclusion.

6.2 Further Studies

Based on the findings of the present study, it is necessary to propose several further experiments to comprehensively assess skeletal muscle function and to control prosthesis by 1D SMG.

1. The relationship between 1D SMG and wrist angle signal should be further tested with various movement patterns and muscle groups

Although the current experiment showed that 1D SMG was a promising method for muscle assessment, it had some limitations. In this study, the 1D SMG signal was found to be significantly correlated with wrist extension angle when there was no external resistance during the wrist extension movement, which, however, needs further investigation for the condition when external resistance exists in future studies. In addition, skeletal muscles usually work as a group to perform certain movement. In this experiment, only the extensor carpi radialis muscle was studied during the wrist extension movement. Future investigations may hope to detect co-activated muscles by using a multiple SMG sensing system. Finally, we found that it was difficult to place both SMG and surface EMG sensors on their optimal sites when the superficial area of the muscle is small. This problem should also be addressed in further studies for the 1D SMG signal.

2. Multi-channels of 1D SMG and other bio-signals should be utilized to improve the prediction accuracy

Only the single channel of SMG signal obtained from the extensor carpi radialis muscle

was used to predict the limited wrist extension movement using the LS-SVM and ANN models. To improve the wrist angle prediction performance, SMG signal extracted from the flexor carpi ulnaris and other forearm muscles may be added to the model input in the future work. With multi-channel SMG data, it is believed that the prediction performance can be improved, as the information of different muscles contributing to the same action can be combined. Moreover, other biomedical or biomechanical signals such as mechanomyography (MMG) may be employed to provide complementary information of muscle movement behaviors. Thus, combination of SMG and MMG could potentially offer richer input features for identifying the relationship between muscle activity and arm kinematics during the execution of motor tasks. In addition, further studies are required to investigate whether the findings in this study could be applied to the movements of other joints.

3. Comparison of 1D SMG and surface EMG in tracking extension test should be verified with different muscles and conditions

It was demonstrated in this study that SMG signal obtained using A-mode ultrasound could provide better performance of wrist extension in comparison with surface EMG in tracking different given patterns under different wrist extension rates. However, further studies are required to verify the performances of 1D SMG signal on different muscles under different conditions. The mechanism of how the increasing movement rate of wrist extension affects the SMG tracking performances should also be further investigated. Further studies are required to demonstrate these advantages quantitatively. It would also be very interesting to further investigate whether the good performance of 1D SMG on the extensor carpi radialis muscle for wrist control observed in this study can be applied to other skeletal muscles.

4. 1D SMG in the Visuomotor “E” Cancellation Test should be tested with more muscle and movement pattern

Our study found that the control performance using the single channel of 1D SMG signal, obtained using A-mode ultrasound was better than using surface EMG signal under both the isometric contraction and the wrist movement conditions. The results of the present study tend to support that the control of either an isometric or dynamic task could be performed better when the control signal has a linear relationship with the muscle strength signals. Further studies are required to evaluate whether this observation would also lead to a reduction in the training required to use 1D SMG for control instead of surface EMG. The current study only evaluated the control performance of the signals measured over the extensor carpi radialis muscle of able-bodied subjects and one amputee subject. Therefore, the performance using 1D SMG from other skeletal muscles is still unknown. Further, only one isometric setup and one type of movement at one joint were examined. Thus, further work examining performance with other muscles and different test scenarios should be carried out to reach a final conclusion.

5. Multi-channels of 1D SMG to control prosthesis

We used only one channel of 1D SMG from forearm extensor muscle to control prosthesis in the present work. To provide multiple DOF prosthetic control, multi-channel SMG signals from different groups of muscles are required to predict the motions of individual joints. One major advantage of multi-channel SMG control is that there is no cross talk among SMG signals from different channels, because ultrasonography can individually detect the morphological changes of muscles in

neighboring locations. Further experiments should be planned to explore the potential of controlling multiple DOF prosthesis using multi-channel SMG signals. Furthermore, as mentioned above, the performance of the prosthesis can affect the control accuracy to some degree. Therefore, more dexterous prostheses with higher reaction speed and motion resolution should be utilized in further study. In addition, more amputees with wrist amputation should be recruited to test the performance of control prosthesis using 1D SMG signals.

6. More amputee subjects should be recruited

In this study, several healthy subjects and one amputee were recruited to test the control performance 1D SMG compared with that of surface EMG. More amputee subjects with residual forearm muscles should be recruited to give a solid conclusion on the 1D SMG control.

REFERENCES

- Abboudi RL, Glass CA, Newby NA, Flint JA, and Craelius W. A biomimetic controller for a multifinger prosthesis. *IEEE Transactions on Rehabilitation Engineering* 1999; 7:121-9.
- Abe T, DeHoyos DV, Pollock ML, and Garzarella L. Time course for strength and muscle thickness changes following upper and lower body resistance training in men and women. *European Journal of Applied Physiology* 2000; 81:174-80.
- Ajiboye AB and Weir RF. A heuristic fuzzy logic approach to EMG pattern recognition for multifunctional prosthesis control. *IEEE Transactions on Neural Systems and Rehabilitation Engineering* 2005; 13: 280-91.
- Akataki K, Mita K, Watakabe M and Itoh K. Mechanomyogram and force relationship during voluntary isometric ramp contractions of the biceps brachii muscle. *European Journal of Applied Physiology* 2001; 84:19-25.
- Akataki K, Mita K, Itoh K, Suzuki N and Watakabe M. Acoustic and electrical activities during voluntary isometric contraction of biceps brachii muscles in patients with spastic cerebral palsy. *Muscle and Nerve* 1996; 19:1252-7.
- Akasaka K, Onishi H, Momose K, Ihashi K, Yagi R, Handa Y and Hoshimiya N. EMG power spectrum and integrated EMG of ankle planterflexors during stepwise and ramp contractions. *Tohoku Journal of Experimental Medicine* 1997; 182:207-16.
- Akima H, Kuno S, Takahashi H, Fukunaga T and Katsuta S. The use of magnetic resonance images to investigate the influence of recruitment on the relationship between torque and cross-sectional area in human muscle. *European Journal of Applied Physiology* 2000; 83:475-80.

- Al-Assaf Y. Surface myoelectric signal analysis: Dynamic approaches for change detection and classification. *IEEE Transactions on Biomedical Engineering* 2006; 53: 2248-56.
- Alemu M, Kumar DK and Bradley A. Time-frequency analysis of SEMG - with special consideration to the interelectrode spacing. *IEEE Transactions on Neural Systems and Rehabilitation Engineering* 2003; 11: 341-5.
- Alkner BA, Tesch PA and Berg HE. Quadriceps EMG/force relationship in knee extension and leg press. *Medicine & Science in Sports & Exercise* 2000; 32:459-63.
- Almstrom C and Kadefors R. Methods for transducing skin movements in the control of assistive devices. In: *Proceedings of Third International Conference on Medical Physics*. vol. 33, p 2. Sweden, 1972.
- Andrade AS, Gavião MBD, Derossi M and Gameiro GH. Electromyographic activity and thickness of masticatory muscles in children with unilateral posterior crossbite. *Clinical Anatomy* 2009; 22: 200-6.
- Arendt-Nielsen L, Gantchev N, and Sinkjaer T. The influence of muscle length on muscle fibre conduction velocity and development of muscle fatigue. *Electroencephalography and Clinical Neurophysiology* 1992; 85:166-72.
- Au ATC, and Kirsch RF. EMG-based prediction of shoulder and elbow kinematics in able-bodied and spinal cord injured individuals. *European Journal of Applied Physiology* 2000; 8: 471–80.
- Bader DS, Maguire TE and Balady GJ. Comparison of ramp versus step protocols for exercise testing in patients $>$ or $=$ 60 years of age. *The American journal of cardiology* 1999; 83: 11-4.

References

- Bakke M, Tuxen A, Vilmann P, Jensen Br, Vilmann A and Toft M. Ultrasound image of human masseter muscle related to bite force, electromyography, facial morphology, and occlusal factors. *Scandinavian Journal of Dental Research* 1992; 100: 164-71.
- Balogh I, Hansson GA, Ohlsson K, Stromberg U and Skerfving S. Interindividual variation of physical load in a work task. *Scandinavian Journal of Work, Environment & Health* 1999; 25:57-66.
- Barry DT, Leonard JA Jr, Gitter AJ and Ball RD. Acoustic Myography as a Control Signal for an Externally Powered Prosthesis. *Archives of Physical Medicine and Rehabilitation* 1986; 67: 267-9.
- Benoit DL and Dowling JJ. In vivo assessment of elbow flexor work and activation during stretch-shortening cycle tasks. *Journal of Electromyography and Kinesiology* 2006; 16: 352-64.
- Beck TW, Housh TJ, Johnson GO, Weir JP, Cramer JT, Coburn JW and Malek MH. Mechanomyographic amplitude and mean power frequency versus torque relationships during isokinetic and isometric muscle actions of the biceps brachii. *Journal of Electromyography and Kinesiology* 2004; 14:555-64.
- Beck TW, Housh TJ, Johnson GO, Weir JP, Cramer JT, Coburn JW and Malek MH. Gender comparisons of mechanomyographic amplitude and mean power frequency versus isometric torque relationships. *Journal of Applied Biomechanics* 2005; 21:96-109.
- Bernathova M, Felfernig M, Rachbauer F, Barthi SD, Martinoli C, Zelger B and Bodner G. Sonographic Imaging of Abdominal and Extraabdominal Desmoids. *Ultraschall in Der Medizin* 2008; 29: 515-9.

- Besio W and Prasad A. Analysis of skin-electrode impedance using concentric ping electrode. In: 28th Annual International Conference of the IEEE-Engineering-in-Medicine-and-Biology-Society. pp 3269-72. New York, NY, 2006.
- Bianchi S and Martinoli C. Ultrasound of the Musculoskeletal System. Springer Berlin Heidelberg, 2007.
- Biddiss E and Chau T. Upper-limb prosthetics: critical factors in device abandonment. *American Journal of Physical Medicine and Rehabilitation* 2007; 86: 977-87.
- Bilodeau M, Arsenault AB, Gravel D and Bourbonnais D. EMG power spectra of elbow extensors during ramp and step isometric contractions. *European Journal of Applied Physiology and Occupational Physiology* 1991; 63: 24-8.
- Bilodeau M, Cincera M, Arsenault AB and Gravel D. Normality and stationarity of EMG signals of elbow flexor muscles during ramp and step isometric contractions. *Journal of Electromyography and Kinesiology* 1997; 7: 87-96.
- Bilodeau M, Goulet C, Nadeau S, Arsenault AB and Gravel D. Comparison of the EMG power spectrum of the human soleus and gastrocnemius muscles. *European Journal of Applied Physiology and Occupational Physiology* 1994; 68: 395-401.
- Bojsen-Moller J, Hansen P, Aagaard P, Kjaer M and Magnusson SP. Measuring mechanical properties of the vastus lateralis tendon-aponeurosis complex in vivo by ultrasound imaging. *Scandinavian Journal of Medicine & Science in Sports* 2003; 13:259-65.
- Boostani R and Moradi MH. Evaluation of the forearm EMG signal features for the control of a prosthetic hand. *Physiological Measurement* 2003; 24:309-19.
- Botteron S, Verdebout CM, Jeannet PY and Kiliaridis S. Orofacial dysfunction in Duchenne muscular dystrophy. *Archives of Oral Biology* 2009; 54: 26-31.

- Bolton CF, Parkers A, Thompson TR, Clark MR, and Sterne CJ. Recording sound from human skeletal muscle: technical and physiological aspects. *Muscle and Nerve* 1989; 12: 126-34.
- Brorsson S, Nilsson A, Hilliges M, Sollerman C and Aurell Y. Ultrasound evaluation in combination with finger extension force measurements of the forearm musculus extensor digitorum communis in healthy subjects. *BMC Medical Imaging* 2008; 8:6.
- Brunner C, Allison BZ, Krusienski DJ, Kaiser V, Muller-Putz GR, Pfurtscheller G, and Neuper C. Improved signal processing approaches in an offline simulation of a hybrid brain-computer interface. *Journal of Neuroscience* 2010; 188: 165-173.
- Bu N, Tsukamoto J, Ueno N, Shima K, and Tsuji T. Measuring Muscle Movements for Human Interfaces using a Flexible Piezoelectric Thin Film Sensor. In: 30th Annual International Conference of the IEEE Engineering in Medicine and Biology Society, vols. 1-8, pp 112-6, 2008.
- Burges CJC. A tutorial on support vector machines for pattern recognition. *Data Mining and Knowledge Discovery* 1998; 2: 121–67.
- Canderle J, Kenney LPJ, Bowen A, Howard D, and Chatterton H. A dual-task approach to the evaluation of the myokinematic signal as an alternative to EMG. In: Proceedings of the 26th Annual International Conference of the IEEE Engineering in Medicine and Biology Society, vol. 6, pp 4548-51, 2004.
- Castillo-Valdivieso PA, Merelo JJ, Prieto A, Rojas I, Romero G. Statistical analysis of the parameters of a neuro-genetic algorithm. *IEEE Transactions on Neural Networks* 2002; 13: 1374–94.

References

- Chan FF, Yang YS, Lam FK, Zhang YT, Parker PA. Fuzzy EMG classification for prosthesis control. *IEEE Transactions on Rehabilitation Engineering* 2000; 8: 305-11.
- Chang PF, Arendt-Nielsen L, Graven-Nielsen T and Chen AC. Psychophysical and EEG responses to repeated experimental muscle pain in humans: pain intensity encodes EEG activity. *Brain Research Bulletin* 2003; 59: 533-43.
- Chan FHY, Yang YS, Lam FK, Zhang YT, and Parker PA. Fuzzy EMG classification for prosthesis control. *IEEE Transactions on Rehabilitation Engineering* 2000; 8: 305-11.
- Chapin JK. Using multi-neuron population recordings for neural prosthetics. *Nature Neuroscience* 2004; 7: 452-5.
- Chapin JK, Moxon KA, Markowitz RS and Nicolelis Miguel AL. Real-time control of a robot arm using simultaneously recorded neurons in the motor cortex. *Nature Neuroscience* 1999; 2: 664-70.
- Chester R, Costa ML, Shepstone L, Cooper A and Donell ST. Eccentric calf muscle training compared with therapeutic ultrasound for chronic Achilles tendon pain-A pilot study. *Manual Therapy* 2008; 13: 484-91.
- Cipriani C, Zaccone F, Micera S, and Carrozza MC. On the shared control of an EMG-controlled prosthetic hand: Analysis of user-prosthesis interaction. *IEEE Transactions on Robotics* 2008; 24: 170-84.
- Coburn JW, Housh TJ, Cramer JT, Weir JP, Miller JM, Beck TW, Malek MH and Johnson GO. Mechanomyographic and electromyographic responses of the vastus medialis muscle during isometric and concentric muscle actions, *Journal of Strength and Conditioning Research* 2005; 19: 412-20.

References

- Coifman RR and Wickerhauser MV. Experiments with adapted wavelet de-noising for medical signals and images. In: Time Frequency and Wavelets in Biomedical Signal Processing, IEEE Press Series in Biomedical Engineering, pp 323-46, 1995.
- Cope TC and Pinter MJ. The size principle: still working after all these years, News in Physiological Sciences, 1995; 10: 280-86.
- Crago PE, Memberg WD, Usey MK, Keith MW, Kirsch RF, Chapman GJ, Katorgi MA and Perreault EJ. An Elbow Extension Neuroprosthesis for Individuals with Tetraplegia. IEEE Transactions on Rehabilitation Engineering 1998; 6: 1-6.
- Cristianini N and Shawe-Taylor J. An introduction to support vector machines and other kernel-based learning methods. Cambridge, UK: Cambridge Univ. Press. 2000.
- Curcie DJ, Flint JA and Craelius W. Biomimetic finger control by filtering of distributed forelimb pressures. IEEE Transactions on Neural Systems and Rehabilitation Engineering 2001; 9:69-75.
- David S, Ricki L, and Jackie B. Hole's Human Anatomy & Physiology, Martin J Lange, 10th edition., 2004.
- De Bruin PF, Ueki J, Watson A and Pride NB. Size and strength of the respiratory and quadriceps muscles in patients with chronic asthma. European Respiratory Journal 1997; 10: 59-64.
- De Luca CJ. Physiology and mathematics of myoelectric signals. IEEE Transactions on Rehabilitation Engineering 1979; 26: 313-25.
- De Luca CJ, LeFever RS, McCue MP and Xenakis AP. Behaviour of human motor units in different muscles during linearly varying contractions. The Journal of Physiology 1982; 329:113-28.
- De Luca CJ. The use of surface electromyography in biomechanics. Journal of Applied Biomechanics 1997; 13: 135-63.

- De Luca CJ. Surface electromyography: detection and recording. Boston: DelSys Inc.; 2002. pp 1-6.
- Diaz JFJ, Rey GA, Matas RB, De La Rosa FJB, Padilla EL and Vicente JGV. New technologies applied to ultrasound diagnosis of sports injuries. *Advances in Therapy* 2008; 25:1315-30.
- Dipietro L, Sabatini AM, and Dario P. Artificial neural network model of the mapping between electromyographic activation and trajectory patterns in free-arm movements. *Medical & Biological Engineering & Computing* 2003; 41: 124–32.
- Ebenbichler G, Kollmitzer J, Quittan M, Uhl F, Kirtley C and Fialka V. EMG fatigue patterns accompanying isometric fatiguing knee-extensions are different in mono- and bi-articular muscle. *Electroencephalography and Clinical Neurophysiology/Electromyography and Motor Control* 1998; 109:256-62.
- Ebersole KT, Housh TJ, Johnson GO, Evetovich TK, Smith DB and Perry SR. MMG and EMG responses of the superficial quadriceps femoris muscles. *Journal of Electromyography and Kinesiology* 1999; 9: 219-27.
- Englehart K, Hudgins B, Parker PA and Stevenson M. Classification of the myoelectric signal using time-frequency based representations *Medical Engineering & Physics* 1999; 21: 431-8.
- Englehart K, Hudgins B and Parker PA. A wavelet-based continuous classification scheme for multifunction myoelectric control. *IEEE Transactions on Biomedical Engineering* 2001; 48: 302-11.
- Englehart K and Hudgins B. A robust, real-time control scheme for multifunction myoelectric control. *IEEE Transactions on Biomedical Engineering* 2003; 50: 848-54.

- Erfanian A, Chizeck HJ and Hashemi RM. The relationship between joint angle and evoked EMG in electrically stimulated muscle. In: Proceedings of the 16th Annual International Conference of the IEEE Engineering in Medicine and Biology, Vol.1, pp 345–6, 1994.
- Farella M, Bakke M, Michelotti A, Rapuano A and Martina R. Masseter thickness, endurance and exercise-induced pain in subjects with different vertical craniofacial morphology. *European Journal of Oral Sciences* 2003; 111:183-88.
- Ferreira PH, Ferreira ML and Hodges PW. Changes in recruitment of the abdominal muscles in people with low back pain - Ultrasound measurement of muscle activity. *Spine* 2004; 29:2560-6.
- Fukuda K, Umezu Y, Shiba N, Tajima F, and Nagata K. Electromyographic fatigue analysis of back muscles during remote muscle contraction. *Journal of Back and Musculoskeletal Rehabilitation* 2006; 19: 61-6.
- Fukunaga T, Ichinose Y, Ito M, Kawakami Y, and Fukashiro S. Determination of fascicle length and pennation in a contracting human muscle in vivo. *Journal of Applied Physiology* 1997; 82: 354-58,
- Fukunaga T, Kubo K, Kawakami Y, Fukashiro S, Kanehisa H and Maganaris CN. In vivo behaviour of human muscle tendon during walking. In: Proceedings of the Royal Society of London Series B-Biological Sciences, vol. 268, pp 229-33, 2001.
- Georgiakaki I, Tortopidis D, Garefis P and Kiliaridis S. Ultrasonographic thickness and electromyographic activity of masseter muscle of human females. *Journal of Oral Rehabilitation* 2007; 34:121-8.
- Gambrell C. Overuse Syndrome and the Unilateral Upper Amputee: Consequences and Prevention. *Journal of Prosthetics and Orthotics* 2008; 20: 126-32.

- Georgiakaki I, Tortopidis D, Garefis P and Kiliaridis S. Ultrasonographic thickness and electromyographic activity of masseter muscle of human females. *Journal of Oral Rehabilitation* 2007; 34: 121-8.
- Gordon G and Holbourn AH. The sounds from single motor units in a contracting muscle. *The Journal of Physiology* 1948; 107: 456-64.
- Griffiths RI. Ultrasound transit time gives direct measurement of muscle fibre length in vivo. *Journal of Neuroscience Methods* 1987; 21: 159-65.
- Guo JY, Zheng YP, Huang QH and Chen X. Dynamic monitoring of forearm muscles using 1D sonomyography (SMG) system. *Journal of Rehabilitation Research and Development*. 2008; 45:187-96.
- Guo JY, Zheng YP, Huang QH, Chen X, He JF and Chan H. Performances of one-dimensional sonomyography and surface electromyography in tracking guided patterns of wrist extension. *Ultrasound in Medicine and Biology* 2009; 35: 894-902.
- Güler NF and Kocer S. Use of support vector machines and neural network in diagnosis of neuromuscular disorders. *Journal of Medical Systems* 2005; 29: 271–84.
- Haig AJ, Gelblum JB, Rechten JJ and Gitter AJ. Technology assessment: The use of surface EMG in the diagnosis and treatment of nerve and muscle disorders. *Muscle Nerve* 1996; 19:392-5.
- Hakkinen A, Airaksinen O, Valkeinen H and Alen M. Effects of strength training on muscle strength, cross-sectional area, maximal electromyographic activity, and serum hormones in premenopausal women with fibromyalgia. *The Journal of Rheumatology* 2002; 29:1287-95.

References

- Hakkinen K and Hakkinen A. Muscle cross-sectional area, force production and relaxation characteristics in women at different ages *European Journal of Applied Physiology and Occupational Physiology* 1991; 62:410-4.
- Hakkinen K, Kallinen M, Izquierdo M, Jokelainen K, Lassila H, Malkia E, Kraemer WJ, Newton RU and Alen M. Changes in agonist-antagonist EMG, muscle CSA, and force during strength training in middle-aged and older people. *Journal of Applied Physiology* 1998; 84:1341-9.
- Hahn M E. Feasibility of estimating isokinetic knee torque using a neural network model. *Journal of Biomechanics* 2007; 40: 1107–14.
- Hart RL, Kilgore KL, and Peckham PH. A Comparison between control methods for implanted FES hand-grasp systems. *IEEE Transactions on Rehabilitation Engineering* 1998; 6: 208–18.
- Hasegawa S, Tachi T, Sasaki H, Torii S, and Kato K. Morphological and strength characteristics of the rotator cuff and deltoid muscles in collegiate baseball players. *Japanese Journal of Physical Fitness and Sports Medicine* 2003; 52: 407-19.
- Haykin S. *Neural Networks, a Comprehensive Foundation*. 2nd ed. Upper Saddle River, NJ: Prentice-Hall, 1999.
- Herda TJ, Ryan ED, Beck TW, Costa PB, DeFreitas JM, Stout JR and Cramer JT. Reliability of mechanomyographic amplitude and mean power frequency during isometric step and ramp muscle actions. *Journal of Neuroscience Methods* 2008; 171:104-9.
- Heasman JM, Scott TRD, Kirkup L, Flynn RY, Vare VA, and Gschwind CR. Control of a hand grasp neuoprosthesis using an electroencephalogram-triggered switch: demonstration of improvements in performance using wavepacket analysis. *Medical & Biological Engineering & Computing* 2002; 40:588-93.

- Heath GH. Control of proportional grasping using a myokinematic signal. *Technology and Disability* 2003; 15: 73-83.
- Herbert RD, Moseley AM, Butler JE and Gandevia SC. Change in length of relaxed muscle fascicles and tendons with knee and ankle movement in humans. *Journal of Physiology (London)* 2002; 539: 637-45.
- Henneman E, Somjen G, and Carpenter DO. Functional Significance of Cell Size in Spinal Motoneurons *Journal of Neurophysiology* 1965; 28 560-80.
- Henneman E, and Mendell LM. Functional organization of motoneuron pool and its inputs. In: Brooks VB, editor. *Handbook of physiology, the nervous system, motor control*. Bethesda (MD): American Physiological Society, 1981.
- Hides JA, Stokes MJ, Saide M, Jull GA and Cooper DH. Evidence of lumbar multifidus muscle wasting ipsilateral to symptoms in patients with acute/subacute low back pain. *Spine* 1994; 19:165-72.
- Hincapie JG and Kirsch RF. Feasibility of EMG-based neural network controller for an upper extremity neuroprosthesis. *IEEE Transactions on Neural and Rehabilitation Systems Engineering* 2009; 17: 80-90.
- Hochberg LR, Serruya MD, Friehs GM, Mukand JA, Saleh M, Caplan AH, Branner A, and Chen David. Neuronal ensemble control of prosthetic devices by a human with tetraplegia. *Nature* 2006; 442: 164-71.
- Hodges PW, Pangel LHM, Herbert RD and Gandevia SC. Measurement of muscle contraction with ultrasound imaging. *Muscle and Nerve* 2003; 27:682-92.
- Hogrel JY. Clinical applications of surface electromyography in neuromuscular disorders. *Clinical Neurophysiology* 2005; 35:59-71.
- Hornik K, Stinchcombe M and White H. Multilayer feedforward networks are universal approximators. *Neural Networks* 1989; 2: 359-66.

- Hou YF, Zurada JM, Karwowski W, Marras WS and Davis K. Estimation of the dynamic spinal forces using a recurrent fuzzy neural network. *IEEE transactions on systems, man, and cybernetics. Part B, Cybernetics* 2007; 37:100-9.
- Housh TJ, Perry SR, Bull AJ, Johnson GO, Ebersole KT, Housh DJ and deVries HA. Mechanomyographic and electromyographic responses during submaximal cycle ergometry. *European Journal of Applied Physiology* 2000; 83: 381-7.
- Huang YH, Englehart KB, Hudgins B and Chan ADC. A Gaussian mixture model based classification scheme for myoelectric control of powered upper limb prostheses. *IEEE Transactions on Biomedical Engineering* 2005; 52: 1801-11.
- Huang QH, Zheng YP, Chen X, Shi J, and He JF. Development of a Frame-Synchronized System for Continuous Acquisition and Analysis of Sonomyography, Surface EMG and Corresponding Joint Angle. *The Open Biomedical Engineering Journal* 2007; 1: 77-84.
- Huang QH, Zheng YP, Lu MH, and Chi ZR. Development of a portable 3D ultrasound imaging system for musculoskeletal tissues. *Ultrasonics* 2005; 43: 153-63.
- Huang QH, Zheng YP, Chen X, He JF, and Shi J. Synchronization between somyography, electromyography and joint angle. *Open Biomedical Engineering Journal* 2007; 1:77-84.
- Huang YL, and Chen DR. Support vector machines in sonography application to decision making in the diagnosis of breast cancer. *Clinical Imaging* 2005; 29: 179–84.
- Hudgins B, Parker P, Scott RN. A New Strategy for Multifunction Myoelectric Control. *IEEE Transactions on Biomedical Engineering* 1993; 40: 82-94.
- Ichinose Y, Kawakami Y, and Ito M. Estimation of active force-length characteristics of human vastus lateralis muscle. *Acta Anatomica (Basel)* 1997; 159: 78-83.

- Ikai M and Fukunaga T. A study on training effect on strength per unit cross-sectional area of muscle by means of ultrasonic measurement. *European Journal of Applied Physiology and Occupational Physiology* 1970; 28:173-80.
- Ishikawa M, Dousset E, Avela J, Kyrolainen H, Kallio J, Linnamo V, Kuitunen S, Nicol C and Komi PV. Changes in the soleus muscle architecture after exhausting stretch-shortening cycle exercise in humans. *European Journal of Applied Physiology* 2006; 97: 298-306.
- Masamitsu Ito, Yasuo Kawakami, Yoshiho Ichinose, Senshi Fukashiro, and Tetsuo Fukunaga. Nonisometric behavior of fascicles during isometric contractions of a human muscle. *Journal of Applied Physiology* 1998; 85: 1230-5.
- Maughan RJ, Watson JS, and Weir J. Relationship between muscle strength and muscle cross-sectional area in male sprinters and endurance runners. *European Journal of Applied Physiology* 1983; 50: 309-18.
- Jacobs R and Schenau GJV. Control of an external force in leg extensions in humans. *The Journal of Physiology* 1992; 457: 611-26.
- Jaskolska A, Brzenczek W, Kisiel-Sajewicz K, Kawczynski A, Marusiak J, and Jaskolski A. The effect of skinfold on frequency of human muscle mechanomyogram. *Journal of Electromyography & Kinesiology* 2004; 14: 217-25.
- Jaskolska A, Kisiel K, Brzenczek W and Jaskolski A. EMG and MMG of synergists and antagonists during relaxation at three joint angles. *European Journal of Applied Physiology* 2003; 90:58-68.
- Jaskolska A, Kisiel-Sajewicz K, Brzenczek-Owczarzak W, Yue GH and Jaskolski A. EMG and MMG of agonist and antagonist muscles as a function of age and joint angle. *Journal of Electromyography and Kinesiology* 2006; 16: 89-102.

- Johnson MA, Polgar J, Weightman D and Appleton D. Data on the distribution of fibre types in thirty-six human muscles. An Autopsy Study. *Journal of the Neurological Sciences* 1973; 18: 111-29.
- Jubrias SA, Odderson IR, Esselman PC and Conley KE. Decline in isokinetic force with age: muscle cross-sectional area and specific force. *Pflügers Archiv: European Journal of Physiology* 1997; 434: 246-53.
- Kasabov K. *Foundations of neural network fuzzy systems and knowledge engineering*. MIT. Press, 1996.
- Kanehisa H, Ikegawa S, Tsunoda N and Fukunaga T. Strength and cross-sectional areas of reciprocal muscle groups in the upper arm and thigh during adolescence. *International Journal of Sports Medicine*, 1995; 16: 54-60.
- Karlik B, Tokhi MO and Alci M. Fuzzy clustering neural network architecture for multifunction upper-limb prosthesis. *IEEE Transactions on Biomedical Engineering* 2003; 50: 1255-61.
- Kelly MF, Parker PA and Scott RN. The application of neural networks to myoelectric signal analysis: a preliminary study. *IEEE Transactions on Biomedical Engineering* 1990; 37: 221-30.
- Kenney LPJ, Lisitsa I, Bowker P, Heath GH and Howard D. Dimensional change in muscle as a control signal for powered upper limb prostheses: a pilot study. *Medical Engineering & Physics* 1999; 21: 589-97.
- Kinugasa R, Kawakami Y, and Fukunaga T. Quantitative assessment of skeletal muscle activation using muscle functional MRI. *Magn Reson Imaging*. 2006; 24: 639-44.
- Kanehisa H, Ikegawa S, Tsunoda N, and Fukunaga T. Strength and Cross-Sectional Areas of Reciprocal Muscle Groups in the Upper Arm and Thigh during Adolescence. *International Journal of Sports Medicine* 1995; 16: 54-60.

- Kauhanen L, Nykopp T, Lehtonen J, Jylanki P, Heikkonen J, Rantanen, P, Alaranta H and Sams M. EEG and MEG brain-computer interface for tetraplegic patients. *IEEE Transactions on Neural Systems and Rehabilitation Engineering* 2006; 14: 190-3.
- Kawakami Y, Abe T and Fukunaga T. Muscle-Fiber Pennation Angles Are Greater in Hypertrophied Than in Normal Muscles. *Journal of Applied Physiology* 1993; 74: 2740-4.
- Karlik B, Tokhi MO, and Alci M. A fuzzy clustering neural network architecture for multifunction upper-limb prosthesis. *IEEE Transactions on Biomedical Engineering* 2003; 50: 1255-61.
- Karlsson S and Gerdle B. Mean frequency and signal amplitude of the surface EMG of the quadriceps muscles increase with increasing torque- a study using the continuous wavelet transform. *Journal of Electromyography and Kinesiology* 2001; 11:131-40.
- Kanehisa H, Ikegawa S, and Fukunaga T. Comparison of muscle cross-sectional area and strength between untrained women and men. *European Journal of Applied Physiology*. 1994; 68: 148-54.
- Kanehisa H, Ikegawa S, Tsunoda N and Fukunaga T. Strength and cross-sectional areas of reciprocal muscle groups in the upper arm and thigh during adolescence. *International Journal of Sports Medicine* 1995; 16: 54-60.
- Karlsson S and Gerdle B. Mean frequency and signal amplitude of the surface EMG of the quadriceps muscles increase with increasing torque - a study using the continuous wavelet transform. *Journal of Electromyography and Kinesiology* 2001; 11:131-40.

- Kasai T and Yahagi S. Motor evoked potentials of the first dorsal interosseous muscle in step and ramp index finger abduction. *Muscle and Nerve* 1999; 22:1419-25.
- Kauhanen, L, Nykopp T, Lehtonen J, Jylanki P, Heikkonen J, Rantanen P, Alaranta H, and Sams M. EEG and MEG brain-computer interface for tetraplegic patients. *IEEE Transactions on Neural Systems and Rehabilitation Engineering* 2006; 14: 190-3.
- Kawakami Y, Abe T and Fukunaga T. Muscle-Fiber Pennation Angles Are Greater in Hypertrophied Than in Normal Muscles. *Journal of Applied Physiology* 1993; 74: 2740-4.
- Kawakami Y, Abe T, Kuno SY and Fukunaga T. Training-induced changes in muscle architecture and specific tension. *European Journal of Applied Physiology and Occupational Physiology* 1995; 72: 37-43.
- Kenney LP, Lisitsa I, Bowker P, Heath GH, and Howard D. Dimensional change in muscle as a control signal for powered upper limb prostheses: a pilot study. *Medical Engineering and Physics* 1999; 21:589-97.
- Kermani MZ, Wheeler BC, Badie K, and Hashemi TM. EMG feature evaluation for movement control of upper extremity prostheses. *IEEE Transactions on Rehabilitation Engineering* 1995; 3: 324-33.
- Kiliaridis S and Kalebo P. Masseter muscle thickness measured by ultrasonography and its relation to facial morphology. *Journal of Dental Research* 1991; 70: 1262-5.
- Koike Y, and Kawato M. Estimation of dynamic joint torques and trajectory formation from surface electromyography signals using a neural network model. *Biological Cybernetics* 1995; 73: 1015–24.

- Kouzaki M and Fukunaga T. Frequency features of mechanomyographic signals of human soleus muscle during quiet standing. *Journal of Neuroscience Methods* 2008; 173: 241-8.
- Kuiken TA Dumanian GA, Lipschutz RD, Miller LA and Stubblefield KA. The use of targeted muscle reinnervation for improved myoelectric prosthesis control in a bilateral shoulder disarticulation amputee. *Prosthetics and Orthotics International* 2004; 28: 245-53.
- Labarre VA. Assessment of muscle function in pathology with surface electrode EMG. *Revue Neurologique* 2006; 162: 459-65.
- Lamminen AE. Magnetic resonance imaging of primary skeletal muscle disease: patterns of distribution and severity of involvement. *The British Journal of Radiology* 1990; 63: 946-50.
- Lariviere C, Arsenault AB, Gravel D, Gagnon D and Loisel P. Effect of step and ramp static contractions on the median frequency of electromyograms of back muscles in humans. *European Journal of Applied Physiology* 2001; 85:552-9.
- Lebedev MA and Nicolelis MAL. Brain-machine interfaces: past, present and future. *Trends in Neurosciences* 2006; 29: 536-46.
- Lee JP, Tseng WYI, Shau YW, Wang CL, HK Wang and Wang SF. Measurement of segmental cervical multifidus contraction by ultrasonography in asymptomatic adults. *Manual Therapy* 2007; 12: 286-94.
- Lee JP, Wang CL, Shau YW and Wang SF. Measurement of cervical multifidus contraction pattern with ultrasound imaging. *Journal of Electromyography and Kinesiology* 2009; 19: 391-7.

References

- Leedham JS and Dowling JJ. Force-length, torque-angle and EMG-joint angle relationships of the human in vivo biceps brachii. *European Journal of Applied Physiology* 1995; 70: 421–6.
- Lieber RL. Hypothesis: biarticular muscles transfer moments between joints. *Developmental Medicine and Child Neurology* 1990; 32:456-8.
- Lieber RL, and Friden J. Functional and clinical significance of skeletal muscle architecture. *Muscle and Nerve* 2000; 23:1647-66.
- Liu MM, Herzog W, and Savelberg HH. Dynamic muscle force predictions from EMG: an artificial neural network approach. *Journal of Electromyography and Kinesiology* 1999; 9: 391–400.
- Loeb GE. Taking control of prosthetic arms. *Journal of American Medical Association* 2009; 301: 670-1.
- Lou B, Hong B, Gao XR and Gao SK. Bipolar electrode selection for a motor imagery based brain-computer interface. *Journal of Neural Engineering* 2008; 5: 342-9.
- Luh JJ, Chang GC, Cheng CK, Lai JS and Kuo TS. Isokinetic elbow joint torques estimation from surface EMG and joint kinematic data: Using an artificial neural network model. *Journal of Electromyography and Kinesiology* 1999; 9: 173–83.
- Macintosh BR, Gardiner PF, and McComas AJ. *Skeletal muscle: form and function*, Human Kinetics Publishers, 2nd edition. 2006.
- MacIsaac D, Englehart K, Parker P, and Rogers D. Fatigue estimation with a multivariable myoelectric mapping function. *IEEE Transactions on Biomedical Engineering* 2006; 53:694-700.
- Madeleine P, Jorgensen LV, Sogaard K, Nielsen LA and Sjogaard G. Development of muscle fatigue as assessed by electromyography and mechanomyography during continuous and intermittent low-force contractions: effects of the feedback mode.

- European Journal of Applied Physiology 2002; 87: 28-37.
- Mademli L, and Arampatzis A. Behaviour of the human gastrocnemius muscle architecture during submaximal isometric fatigue. *European Journal of Applied Physiology* 2005; 94: 611-7.
- Maganaris CN. Force-length characteristics of in vivo human skeletal muscle. *Acta physiologica Scandinavica* 2001; 172:279-285.
- Madeleine P, Bajaj P, Sogaard K and Arendt-Nielsen L. Mechanomyography and electromyography force relationships during concentric, isometric and eccentric contractions. *Journal of Electromyography and Kinesiology* 2001; 11:113-21.
- Maganaris CN and Baltzopoulos V. Predictability of in vivo changes in pennation angle of human tibialis anterior muscle from rest to maximum isometric dorsiflexion. *European Journal of Applied Physiology and Occupational Physiology* 1999; 79: 294-7.
- Mahlfeld K, Franke J, and Awiszus F. Postcontraction changes of muscle architecture in human quadriceps muscle. *Muscle and Nerve* 2004; 29:597-600.
- Mamaghani NK, Shimomura Y, Iwanaga K and Katsuura T. Mechanomyogram and electromyogram responses of upper limb during sustained isometric fatigue with varying shoulder and elbow postures. *Journal of Physiological Anthropology and Applied Human Science* 2002; 21: 29-43.
- Mannion AF, Pulkovski N, Gubler D, Gorelick M, O'Riordan D, Loupas T, Schenk P, Gerber H and Sprott H. Muscle thickness changes during abdominal hollowing: an assessment of between-day measurement error in controls and patients with chronic low back pain. *European Spine Journal* 2008; 17: 494-501.

References

- Masuda K, Masuda T, Sadoyama T, Inaki M, and Katsuta S. Changes in surface EMG parameters during static and dynamic fatiguing contractions. *Journal of Electromyography and Kinesiology* 1999; 9: 39-46.
- Maton B, Petitjean M and Cnockaert JC. Phonomyogram and electromyogram relationships with isometric force reinvestigated in man. *European Journal of Applied Physiology and Occupational Physiology* 1990; 60:194-201.
- Matsubayashi T, Kubo J, Matsuo A, Kobayashi K and Ishii N. Ultrasonographic measurement of tendon displacement caused by active force generation in the psoas major muscle. *The Journal of Physiological Sciences* 2008; 58: 323-32.
- McMeeken JM and Beith ID. The relationship between EMG and change in thickness of transversus abdominis. *Clinical Biomechanics* 2004; 19: 337-42.
- Mellinger J, Schalk G, Braun C, Preissl H, Rosenstiel W, Birbaumer N, and Kübler A. An MEG-based brain-computer interface (BCI). *Neuroimage* 2007; 36: 581-93.
- Mercuri E, Pichiecchio A, Allsop J, Messina S, Pane M, and Muntoni F. Muscle MRI in inherited neuromuscular disorders: past, present, and future. *Journal of Magnetic Resonance Imaging* 2007; 25:433-40.
- Mercuri E, Pichiecchio A, Counsell S, Allsop J, Cini C, Jungbluth H, Uggetti C, and Bydder G. A short protocol for muscle MRI in children with muscular dystrophies. *European Journal of Paediatric Neurology* 2002; 6:305-7.
- Miller LA, Stubblefield KA, Lipschutz RD, Lock BA and Kuiken TA. Improved myoelectric prosthesis control using targeted reinnervation surgery: A case series. *IEEE Transactions on Neural Systems and Rehabilitation Engineering* 2008; 16: 46-50.

- Mobasser F and Hashtrudi-Zaad K. Hand force estimation using electromyography signals. In: IEEE International. Conference in Robotics and Automation, 2005 pp 2631-6.
- Momen K, Krishnan S, and Chau T. Real-time classification of forearm electromyographic signals corresponding to user-selected intentional movements for multifunction prosthesis control. *IEEE Transactions on Neural Systems and Rehabilitation Engineering* 2007; 15: 535-42.
- Mohandes MA, Halawani TO, Rehman S, and Hussain AA. Support vector machines for wind speed prediction. *Renewable Energy* 2004; 29: 939-47.
- Muller L, Bergstrom T, Hellstrom M, Svensson E, and Jacobsson B. Standardized ultrasound method for assessing detrusor muscle thickness in children. *The Journal of Urology* 2000; 164:134-38.
- Mussa-Ivaldi FA and Miller LE. Brain-machine interfaces: computational demands and clinical needs meet basic neuroscience. *Trends in Neurosciences* 2003; 26: 329-34.
- Muzumdar, A. *Powered upper limb prostheses: control, implementation and clinical application*, Berlin; New York: Springer, 2004.
- Nicolelis MAL, Actions from thoughts. *Nature* 2001; 409:403-7.
- Nogueira W, Gentil P, Mello SNM, Oliveira RJ, Bezerra AJC and Bottaro M. Effects of power training on muscle thickness of older men. *International Journal of Sports Medicine* 2009; 30:200-4.
- Nadeau S, Bilodeau M, Delisle A, Chmielewski W, Arsenault AB and Gravel D. The influence of the type of contraction on the masseter muscle EMG power spectrum. *Journal of Electromyography and Kinesiology* 1993; 3:205-13.

- Narici MV, Binzoni T, Hiltbrand E, Fasel J, Terrier F and Cerretelli P. In vivo human gastrocnemius architecture with changing joint angle at rest and during graded isometric contraction. *The Journal of Physiology-London* 1996; 496:287-97.
- Ohata K, Tsuboyama T, Ichihashi N and Minami S. Measurement of muscle thickness as quantitative muscle evaluation for adults with severe cerebral palsy. *Physical Therapy* 2006; 86:1231-9.
- Ojanen T, Rauhala T, and Hakkinen K. Strength and power profiles of the lower and upper extremities in master throwers at different ages. *The Journal of Strength & Conditioning Research* 2007; 21:216-22.
- Okita M, Nakano J, Kataoka H, Sakamoto J, Origuchi T and Yoshimura T. effects of therapeutic ultrasound on joint mobility and collagen fibril arrangement in the endomysium of immobilized rat soleus muscle. *Ultrasound in Medicine & Biology* 2009; 35: 237-44.
- Onishi H., Yagi R, Oyama M, Ihashi K, and Handa Y. EMG-angle relationship during maximum voluntary movement. *Japanese Journal of Physical Fitness and Sports Medicine* 1999; 48: 485-92.
- Orizio C. Muscle sound: bases for the introduction of a mechanomyographic signal in muscle studies. *Critical Reviews in Biomedical Engineering* 1993; 21:201-43.
- Orizio C, Esposito F, Sansone V, Parrinello G, Meola G and Veicsteinas A. Muscle surface mechanical and electrical activities in myotonic dystrophy. *Electromyography and Clinical Neurophysiology* 1997; 37:231-9.
- Orizio C, Gobbo M, Diemont B, Esposito F, and Veicsteinas A. The surface mechanomyogram as a tool to describe the influence of fatigue on biceps brachii motor unit activation strategy. Historical basis and novel evidence. *European Journal of Applied Physiology* 2003; 90: 326-36.

- Oster G. Muscle sound. *Scientific American* 1984; 250:108–14.
- Paavolainen L, Nummela A, Rusko H, and Hakkinen K. Neuromuscular characteristics and fatigue during 10 km running. *International Journal of Sports Medicine*. 1999; 20: 516-21.
- Perry SR, Housh TJ, Weir JP, Johnson GO, Bull AJ and Ebersole KT. Mean power frequency and amplitude of the mechanomyographic and electromyographic signals during incremental cycle ergometry. *Journal of Electromyography and Kinesiology* 2001; 11: 299-305.
- Pistohl T, Ball T, Schulze-Bonhage A, Aertsen A, and Mehring C. Prediction of arm movement trajectories from ECoG-recordings in humans. *Journal of Neuroscience Methods* 2008; 167: 105-14.
- Ploutz-Snyder, LL, Convertino VA, and Dudley GA. Resistance exercise-induced fluid shifts: change in active muscle size and plasma volume. *American Journal of Physiologic Imaging* 1995 269: R536-43.
- Powell MJD. The theory of radial basis functions approximation, in advance of numerical analysis. Oxd Charendon Press, 1992; p105-210.
- Reeves ND, Maganaris CN, and Narici MV. Ultrasonographic assessment of human skeletal muscle size. *European Journal of Applied Physiology* 2004; 91:116-8.
- Robertson IH., Ward T, Ridgeway V, and Nimmo-Smith I. The structure of normal human attention: The Test of Everyday Attention. *Journal of International Neuropsychological Society* 1996; 2: 525-34.
- Ryan ED, Cramer JT, Egan AD, Hartman MJ, and Herda TJ. Time and frequency domain responses of the mechanomyogram and electromyogram during isometric ramp contractions: A comparison of the short-time Fourier and continuous wavelet transforms. *Journal of Electromyography and Kinesiology* 2008a; 18:54-67.

References

- Ryan ED, Beck TW, Herda TJ, Hartman MJ, Stout JR, Housh TJ, and Cramer JT. Mechanomyographic amplitude and mean power frequency responses during isometric ramp vs. step muscle actions. *Journal of neuroscience methods* 2008b; 168:293-305.
- Sallinen J, Ojanen T, Karavirta L, Ahtiainen JP, and Hakkinen K. Muscle mass and strength, body composition and dietary intake in master strength athletes vs untrained men of different ages. *Journal of Sports Medicine and Physical Fitness* 2008; 48:190-6.
- Sanchez JH, Solomonow M, Baratta RV and Dambrosia R. Control Strategies of the Elbow Antagonist Muscle Pair during 2 Types of Increasing Isometric Contractions. *Journal of Electromyography and Kinesiology* 1993; 3:33-40.
- Sepulveda F, Wells DM, and Vaughan CL. A neural network representation of electromyography and joint dynamics in human gait. *Journal of Biomechanics* 1993; 26: 101–9.
- Seymour JM, Ward K, Sidhu PS, Puthuchearu Z, Steier J, Jolley CJ, Rafferty G, Polkey MI and Moxham J. Ultrasound measurement of rectus femoris crosssectional area and the relationship with quadriceps strength in COPD. *Thorax* 2009; 64:418–23.
- Schalk G, Miller KJ, Anderson NR, Wilson JA, Smyth MD, Ojemann JG, Moran DW, Wolpaw JR, and Leuthardt EC. Two-dimensional movement control using electrocorticographic signals in humans. *Journal of Neural Engineering* 2008; 5: 75-84.
- Schwartz AB, Taylor DM, and Helms Tillery SI. Extraction algorithms for cortical control of arm prosthetics. *Current Opinion in Neurobiology* 2001; 11: 701-7.
- Scott RN and Parker PA. Myoelectric Prostheses - State of the Art. *Journal of Medical Engineering & Technology* 1988; 12: 143-51.

- Seymour JM, Ward K, Sidhu PS, Puthuchery Z, Steier J, Jolley CJ, Rafferty G, Polkey MI, and Moxham J.. Ultrasound measurement of rectus femoris crosssectional area and the relationship with quadriceps strength in COPD. *Thorax* 2009; 64: 418–23.
- Sikdar S, Shah JP, Gilliams E, Gebreab T and Gerber LH. Assessment of Myofascial Trigger Points (MTrPs): A New Application of Ultrasound Imaging and Vibration Sonoelastography. In: 30th Annual International Conference of the IEEE-Engineering in Medicine and Biology Society, 2008 pp 5585-8
- Silva J and Chau T. Coupled microphone-accelerometer sensor pair for dynamic noise reduction in MMG signal recording. *Electronics Letters* 2003; 39: 1496-8.
- Silva J, Chau T, Naumann S, Helm W and Goldenberg AA. Optimization of the signal-to-noise ratio of silicon-embedded microphones for mechanomyography. In: 15th IEEE Canadian Conference on Electrical and Computer Engineering, Montreal, Canada, 2003, pp 1493-6.
- Silva J, Heim W and Chau T. A self-contained, mechanomyography-driven externally powered prosthesis. *Archives of Physical Medicine and Rehabilitation* 2005; 86: 2066-70.
- Shenoy P, Miller KJ, Crawford B, and Rao RN. Online electromyographic control of a robotic prosthesis. *IEEE Transactions on Biomedical Engineering* 2008 55: 1128-35.
- Shi J, Zheng YP, Chen X, and Huang QH. Assessment of muscle fatigue using sonomyography: Muscle thickness change detected from ultrasound images. *Medical Engineering & Physics* 2007; 29: 472-9.
- Shi J, Zheng YP, Huang QH and Chen X. Continuous monitoring of sonomyography, electromyography and torque generated by normal upper arm muscles during

- isometric contraction: Sonomyography assessment for arm muscles. *IEEE Transactions on Biomedical Engineering* 2008a; 55: 1191-8.
- Shi J, Zheng YP, Huang QH and Zhu YS. Modeling the Relation between Muscle Thickness and Wrist Angle Based on Bone-Muscle Lever Model. In: 30th Annual International Conference of the IEEE-Engineering-in-Medicine-and-Biology-Society, (Vancouver, CANADA: IEEE) pp 887-90, 2008b.
- Shi J, Zheng YP, Yan ZZ, and Huang QH. Prediction of wrist angle from sonomyography Signals with artificial neural networks technique. In: 28th Annual International Conference of the IEEE Engineering in Medicine and Biology Society. 2006. pp 3549–52.
- Shin KS, Lee1 TS, and Kim HJ. An application of support vector machines in bankruptcy prediction model. *Expert Systems with Applications* 2005; 28: 127-35.
- Shyu KK, Lee PL, Lee MH, Lin MH, Lai RJ, and Chiu YJ. Development of a Low-Cost FPGA-Based SSVEP BCI Multimedia Control System *IEEE Transactions on Biomedical Circuits and Systems* 2010; 4: 125-32.
- Smola A J, and Scholkopf B. A tutorial on support vector regression. *Statistics and Computing* 2004; 14: 199–222.
- Soares A, Andrade A, Lamounier E, and Carrijo R. The development of a virtual Myoelectric prosthesis controlled by an EMG pattern recognition system based on neural networks. *Journal of Intelligent Information Systems* 2003; 21:127-41.
- Springer BA and Gill NW. Characterization of lateral abdominal muscle thickness in persons with lower extremity amputations. *Journal of Orthopaedic & Sports Physical Therapy* 2007; 37:635-43.
- Suzana D, Rodica T, Petrica B and Mircea D. Quantitative analysis of ultrasound data in assessment of muscle layer thickness of quadriceps muscle in young subject pre

- and post isometric contraction. In: 4th WSEAS International Conference on Cellular and Molecular Biology, Biophysics and Bioengineering/2nd WSEAS International Conference on Computational Chemistry, (Puerto de la Cruz, SPAIN: World Scientific and Engineering Acad and Soc) pp 33-7, 2008.
- Svoboda J, Sovka P, and Stancak A. Intra- and inter-hemispheric coupling of electroencephalographic 8-13 Hz rhythm in humans and force of static finger extension. *Neuroscience Letters* 2002; 334:191-95.
- Suryanarayanan S, Reddy N P, and Gupta V. Artificial neural networks for estimation of joint angle from EMG signals. In: *IEEE 17th Annual Conference of Engineering in Medicine and Biology Society*, Vol. 1, pp 823–24, 1995.
- Suykens J A K, Gestel T V, Brabanter J D, Moor B D, and Vandewalle J. *Least squares support vector machines*. Singapore: World Scientific Publishing. 2002.
- Talebinejad M, Chan AD, Miri A, and Dansereau RM. Fractal analysis of surface electromyography signals: a novel power spectrum-based method *Journal of Electromyography and Kinesiology* 2009; 19: 840-50.
- Tay FEH, and Cao L. Application of support vector machines in financial time series forecasting. *Omega* 2001; 29: 309–17.
- Taylor DM, Tillery SIH, and Schwartz AB. Direct cortical control of 3D neuroprosthetic device. *Science* 2002; 296:1829–32.
- Tonet O, Marinelli M, Citi L, Rossini PM, Rossini L, Megali G, and Dario P. Defining brain-machine interface applications by matching interface performance with device requirements. *Journal of Neuroscience Methods* 2008; 167: 91-104.
- Torres A, Fiz JA, Galdiz B, Gea J, Morera J and Jane R. A wavelet multiscale based method to separate the high and low frequency components of mechanomyographic

- signals. In: 27th Annual International Conference of the IEEE Engineering in Medicine and Biology Society, Vols 1-7 pp 7262-5, 2005.
- Van Bolhuis BM, Gielen C and van Ingen Schenau GJ. Activation patterns of mono- and bi-articular arm muscles as a function of force and movement direction of the wrist in humans. *The Journal of Physiology-London* 1998; 508:313-24.
- Van Gestel T, Suykens J A K, Baestaens D E, Lambrechts D, Lanckriet A, Lanckriet G, Vandaele B, De Moor B, and Vandewalle J. Financial time series prediction using least squares support vector machines within the evidence framework. *IEEE Transactions on Neural Networks* 2001; 12: 809–21.
- Vapnik V. *Estimation of Dependencies Based on Empirical Data.* , Berlin: Springer; 1982.
- Vonga CM, Wong PK, and Li YP. Prediction of automotive engine power and torque using least squares support vector machines and Bayesian inference. *Engineering Applications of Artificial Intelligence* 2006; 19: 277–87.
- Vredenburg J, and Rau G. Surface electromyography in relation to force, muscle length and endurance. In: *New Developments in Electromyography and Clinical Neurophysiology.* Basel: Karger, 1973, p 607–22.
- Waldert S, Preissl H, Demandt E, Braun C, Birbaumer N, Aertsen A, and Mehring C. Hand movement direction decoded from MEG and EEG. *Journal of Neuroscience* 2008; 28: 1000-8.
- Wang G, Yan ZG, Hu X, Xie HB, and Wang ZZ. Classification of surface EMG signals using harmonic wavelet packet transform. *Physiological Measurement* 2006; 27: 1255–67.

- Wang L, and Buchanan TS. Prediction of joint moments using a neural network model of muscle activations from EMG signals. *Transactions on Neural Systems and Rehabilitation Engineering* 2002; 10: 30–7.
- Weir JP, Ayers KM, Lacefield JF, and Walsh KL. Mechanomyographic and electromyographic responses during fatigue in humans: influence of muscle length. *European Journal of Applied Physiology* 2000; 81: 352-59.
- Wessberg J, Stambaugh CR, Kralik JD, Beck PD, Laubach M, Chapin JK, Kim J, Biggs SJ, Srinivasan MA, and Nicolelis MAL. Real-time prediction of hand trajectory by ensembles of cortical neurons in primates. *Nature* 2000; 408: 361-5.
- Wilson JA, Felton EA, Garell PC, Schalk G, and Williams JC. ECoG factors underlying multimodal control of a brain-computer interface. *IEEE Transactions on Neural Systems and Rehabilitation Engineering* 2006; 14: 246-50.
- Wininger M, Kim NH, and Craelius W. Pressure signature of forearm as predictor of grip force. *Journal of Rehabilitation Research and Development* 2008; 45:883-92.
- Wheeler KR, Chang MH, and Knuth KH. Gesture-based control and EMG decomposition. *IEEE Transactions on Systems, Man, and Cybernetics, Part C: Applications and Reviews* 2006; 36: 503-14.
- Whittaker J, Teyhen D, Elliott J, Cook K, Langevin H, Dahl H, and Stokes M. Rehabilitative Ultrasound Imaging: Understanding the Technology and its Applications. *Journal of Orthopaedic & Sports Physical Therapy* 2007; 37: 435-49.
- Worrell TW, Corey BJ, York SL, and Santiestaban J. An analysis of supraspinatus EMG activity and shoulder isometric force development. *Medicine & Science in Sports & Exercise* 1992; 24:744-8.

- Woods JJ and Biglandritch B. Linear and non-linear surface EMG/force relationships in human muscles. An anatomical/functional argument for the existence of both. *American Journal of Physical Medicine & Rehabilitation* 1983; 62:287-99.
- Xie HB, Wang ZH, Huang H, and Qin C. Support vector machine in computer aided clinical Electromyography. In: *Proceedings of the Second International Conference on Machine Learning and Cybernetics, Xi'an*, pp 1106–8, 2003.
- Xie HB, Zheng YP, Guo JY, Chen X and Shi J. Estimation of wrist angle from sonomyography using support vector machine and artificial neural network models. *Medical Engineering & Physics* 2009; 31:384-91.
- Xie HB, Zheng YP and Guo JY. Classification of the mechanomyogram signal using a wavelet packet transform and singular value decomposition for multifunction prosthesis control. *Physiological Measurement* 2009b; 30:441-57.
- Yoshitake Y, Ue H, Miyazaki M and Moritani T. Assessment of lower-back muscle fatigue using electromyography, mechanomyography, and near-infrared spectroscopy. *European Journal of Applied Physiology* 2001; 84:174-9.
- Yu X, and Liong SY. Forecasting of hydrologic time series with ridge regression in feature space. *Journal of Hydrology* 2007; 332: 290–302.
- Zecca M, Micera S, and Carrozza MC. Control of multifunctional prosthetic hands by processing the electromyographic signal. *Critical Reviews in Biomedical Engineering* 2002; 30:459-85.
- Zheng YP, Chan MMF, Shi J, Chen X and Huang QH. Sonomyography: Monitoring morphological changes of forearm muscles in actions with the feasibility for the control of powered prosthesis. *Medical Engineering & Physics* 2006; 28:405-15.

References

Zhou YJ and Zheng YP. Revoting Hough Transform (RVHT) and its application for muscle fiber orientation estimation in ultrasound images. *Ultrasound in Medicine and Biology* 2008; 34: 1474-81.

Zwarts MJ and Stegeman DF. Multichannel surface EMG: Basic aspects and clinical utility. *Muscle and Nerve* 2003; 28:1-17.

APPENDIX

I. Information Sheet

Project Title: Sonomyography

Principle Investigator: Prof. Yongping Zheng

Department of Health Technology and Informatics

The Hong Kong Polytechnic University

Contact number: (852) 27667664

This aim of this project is to develop a new method using ultrasound to evaluation muscle functions and to provide control signals for artificial arms. The development can help to provide better rehabilitation approaches for the problems related to muscles.

The contraction of forearm muscles of subjects will be monitored using ultrasound, electromyography, and wrist angle. An ultrasound sensor, three electrodes, and an electro-goniometer will be attached on the skin of the forearm. Ultrasound gel will be used between the ultrasound probe and the skin. The subject will feel no pain, and the attachment of the sensors will have no hurt to the body.

During the experiment, the subject will be asked to contract the forearm muscles and to flex and extend the wrist joint. The data will be collected for analysis. The subject can stop the experiment any time if they do not want to continue.

實驗指引

項目名稱： 超聲波肌肉的研究

項目負責人： 鄭永平教授

醫療科技及資訊學系

香港理工大學

聯絡電話： (852) 27667664

本實驗的目的是利用一維超聲波評估肌肉功能，為假肢控制提供一種新的信號。本實驗的開展可為肌肉康復提供更好的方法。

在前臂肌肉收縮的試驗中，超聲波圖像，肌電信號，手腕關節的角度信號都會被檢測到。超聲波探測器，3 個肌電電極，和角度測量器都會被固定在前臂。超聲波探測器和皮膚之間會被填滿超聲波耦合劑。受驗者將不會有任何的痛楚的感覺，所有固定在受驗者身上的儀器都是無害的。

在實驗中，受驗者會被要求做腕關節的彎屈和伸展運動已達到肌肉收縮的目的。實驗中的數據將會被用作以後的分析用。如果他們有任何不適，受驗者可以在任何時間提出終止實驗的要求。

II Consent Form

I, _____(name), hereby consent to participate in as a subject for the research project entitled “Sonomyography”. I understand the effect and details of the experimental procedures which have been explained to me.

I understand that I have the right to discontinue, with no reason given, my participation anytime, even during the experiment. I realize that any findings of the study will only be used for research purpose and will be properties of the Department of Health Technology and Informatics, The Hong Kong Polytechnic University.

Signed _____

Date _____

In Witness _____

Date _____

同意書

我_____（受試者姓名），在此同意作為受驗者參加“超聲波肌肉的研究”。我已經明白該測試的具體步驟以及可能造成的影響。

我已經知道我可以在任何時間，甚至是在測試中而終止測試，無需給予任何理由。我已經知道測試的結果只能用作科學研究，並且屬於香港理工大學，醫療科技及資訊學系。

受試者姓名 _____

日期 _____

作證人姓名 _____

日期 _____